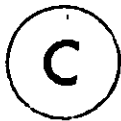SELF-TUNING AND ADAPTIVE CONTROL

OF A PILOT PLANT FLUIDIZED BED REACTOR

By

(C) SAU-MAN YANG, B.Eng.

A Thesis

Submitted to the School of Graduate Studies

In Partial Fulfilment of the Requirements

for the Degree

Master of Engineering

McMaster University

Hamilton, Ontario, Canada

January 1982

SELF-TUNING AND ADAPTIVE CONTROL

OF A PILOT PLANT FLUIDIZED BED REACTOR

MASTER OF ENGINEERING (1982)   McMASTER UNIVERSITY

(Chemical Engineering)   Hamilton, Ontario

TITLE   : Self-Tuning and Adaptive Control
               of a Pilot Plant Fluidized Bed Reactor

AUTHOR   : Sau-Man Yang, B.ENG. (McGill University)

SUPERVISOR·   : Professor J.F. MacGregor

NUMBER OF PAGES : xii, 156

ii

ABSTRACT

A pilot plant fluidized bed reactor in which complex and highly exothermic catalytic hydrogenolysis reactions are taking place, is being used to investigate the computer control of temperature, conversion and selectivities in such reactors. The process is highly nonlinear, characterized by asymmetric dynamics and considerable change in catalyst activity. Moreover, a deadtime of 360 s is introduced by an on-line process gas chromatograph employed to obtain the composition measurements. As a result, the cascade control system comprising a proportional-integral controller for reaction temperature in the inner loop and a Dahlin controller for propane selectivity in the outer loop was reported in previous works to have performed well in certain regions of operation at a given time but revealed very oscillatory and nearly unstable performance in other regions or at different times.

This nonlinear behaviour of the reactor is further investigated. It is found that by better matching the process response characteristics and by detuning the Dahlin controller, this unstable oscillatory behaviour of the cascade control system can be overcome and acceptable performance can be achieved over a wider range of operating conditions. Later, self-tuning adaptive controllers are tried in an attempt to better account for the changing gains and time constants of the nonlinear process, as well as for the time-varying catalyst activity. The cascade control scheme with Dahlin and Self-tuning regulator (STR) demonstrated excellent performance. Finally a double STR configuration for both the inner and outer loops is carried out. Problems associated with this implementation are discussed and possible improvements   suggested.

ACKNOWLEDGEMENTS

TABLE OF CONTENTS

LIST OF FIGURES

LIST OF TABLES

1. INTRODUCTION

With the breakthrough in mini and microcomputer technology, computer control applications have been widely adopted in many industries over the past ten to fifteen years. Reactor control represents one of the most important control problems in chemical processes. But it is most difficult to generalize reaction kinetics since almost every reaction is unique, characterized by a specific chemical model, involving one or more phases and taking place in one of a great variety of reactor configurations. It was pointed out by Shinskey [1] that

"In processes where transfer of mass or energy takes place, gain is a function of many factors, making generalization impossible. These processes are not only difficult to control because of dynamic behaviour, but are also difficult to understand. They are usually non-linear in more than one respect, and compensation improperly applied can aggravate the situation."

No doubt, the control of the pilot scale fluidized bed reactor in which highly exothermic hydrogenolysis reactions are carried out represents one of the most challenging control problems.

The pilot plant exhibits a number of very important characteristics:

(1) The highly exothermic nature of the reactions coupled with the large activation energies necessitates direct control of reaction temperature for stable and safe operation of the reactor.

(2) The process is highly nonlinear and exhibits asymmetric dynamics with the time constants and gains dependent very

1

much upon the operating levels of reactor temperature, the temperature of the oil entering the reactor heating/cooling coils and the hydrogen-to-butane feedrate ratio.

(3) The reactor is a "changing plant". The catalyst activity changes with time. It can be different from one reaction run to another.

(4) The compositions of the product gas are measured by an on-line gas chromatograph. It takes 360 s to analyze a sample and this constitutes a long measurement delay in the system. As a result, previous works on control [4] using conventional cascade proportional-integral (PI) controllers with dead-time compensation that performed well in certain regions of operation at a given time were seen to perform very poorly at slightly different conditions or at different times.

In this work this nonlinear behaviour of the reactor is further investigated and it is shown that by better matching the process response characteristics and by detuning the controller algorithm, acceptable performance can be achieved.

In order to overcome some of the inherent problems associated with controllers employing fixed parameters on a process which has variable dynamic characteristics, self-tuning adaptive controllers are considered in an attempt to better account for the changing gains and time constants of the nonlinear process, as well as for the time varying catalyst activity.

The structure of the thesis is outlined as follows:

Chapter 2: provides the background, the process description and the instrumentation of the pilot plant fluidized bed reactor system.

Chapter 3: reviews the fluidized bed reactor model and the application of the DYNSYS simulation executive for dynamic simulation on the reactor system.

Chapter 4:, discusses the different control methods to be used on the cascade control system for temperature and selectivity control.

Chapter 5: presents the simulation results for the reactor system including the effects of different choices of design parameters.

Chapter 6: describes the experimental application of both conventional multiloop and adaptive multiloop control on the real system.

Chapter 7: summarizes the general conclusions drawn from this work and provides recommendations for future work.

2. THE FLUIDIZED BED REACTOR SYSTEM

2.1 Introduction

2.1.1 Background

This process control study was conducted on a pilot-scale fluidized bed reactor (0.20 m diameter by 1.83 m high) in which butane hydrogenolysis reactions occur. The fluidized bed reactor was originally designed and constructed by Orlickas [2] and Shaw [3] and was used to study the phenomena occurring in fluidized bed reactors. Later McFarlane [4] carried out some preliminary control studies on this system; for this work, he upgraded the instrumentation, installed new control valves and interfaced a Nova 1200 minicomputer (Data General Corporation) with the control and instrumentation systems. The details of the reactor and the current control system are described in this chapter (Sections 2.2 and 2.4 respectively).

It is important to point out that the fluidized bed reactor was designed to be large enough to reduce wall effects and slugging but not so large as to entail excessive cost of chemicals over the long operating periods involved. At the same time, during operation, it exhibits many of the operating characteristics observed in industrial scale plants.

2.1.2 The Chemical Reaction System

The chemical reaction occurring in the fluidized bed is the hydrogenolysis of n-butane on a nickel-impregnated (10% by weight) silica-gel catalyst.

This reaction was extensively studied by Orlickas [2] and Shaw [3] . They showed that the following series-parallel reactions

4

occurred:

$$C_4H_{10} + H_2 \rightarrow C_3H_8 + CH_4 \tag{2.1.1}$$

$$C_4H_{10} + H_2 \rightarrow 2C_2H_6 \tag{2.1.2}$$

$$C_3H_8 + H_2 \rightarrow C_2H_6 + CH_4 \tag{2.1.3}$$

$$C_2H_6 + H_2 \rightarrow 2CH_4 \tag{2.1.4}$$
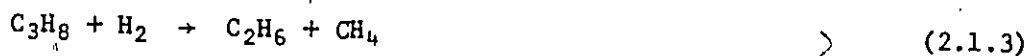
Although four hydrogenolysis reactions occur, only three are stoichiometrically independent. Not only are these reactions highly exothermic but also the kinetic studies of Orlikas and Shaw demonstrated that each of these reactions exhibit very high activation energies (ca. 210 kJ/mole). Their estimates of kinetic parameters and one of their fluidized bed reactor models are used in a simulation relating to this research program as described in Chapter 3.

2.2 Process Description

A simplified schematic diagram of the fluidized bed reactor system with its process control system along with the computer interfacing is shown in Figure 2.1. The cascade control scheme which is discussed in Chapter 4 is indicated on this diagram.
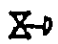
2.2.1 The Reactor

The reactor which is constructed from 16 gauge stainless steel consists of three sections: the bottom cone, the reactor barrel and the disengaging section. The reactor is 0.20 m diameter by 1.83 m high and the disengaging section, which is mounted on top, is 0.46 m diameter by 0.61 m high.

Figure 2.1   Schematic Diagram of the Fluidized Bed Reactor System
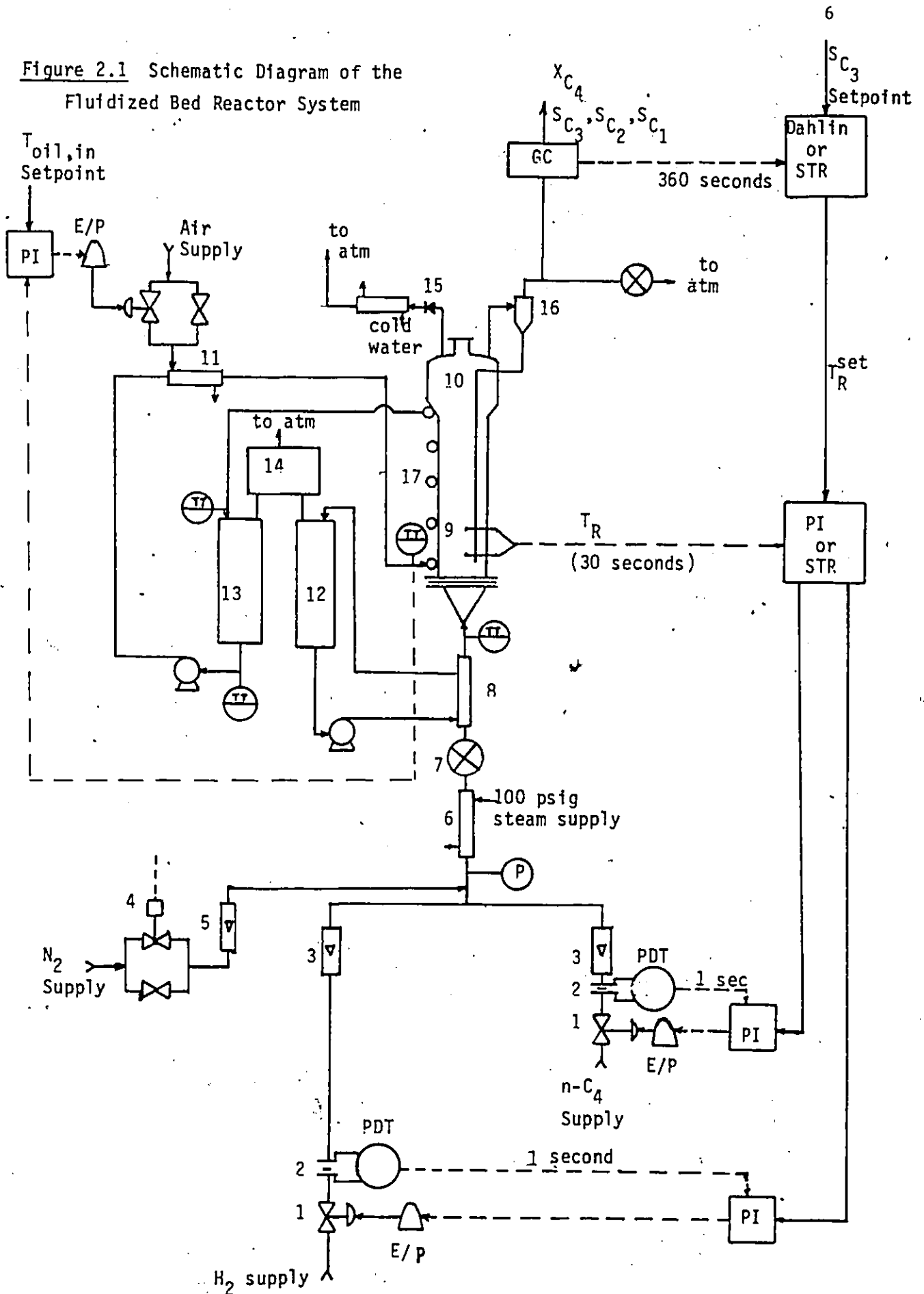
Legend for Figure 2.1 :

⌧	control valve
(TY)	multiplexed thermocouple
(PDT)	differential pressure transmitter
(P)	pressure gauge
⊗	back-pressure regulator
(E/P)	electro-pneumatic transducer
GC	Gas Chromatograph (Beckman Model 6700)
□	Controller — PI: proportional-integral controller
	STR: self-tuning regulator
	Dahlin: controller using Dahlin algorithm
T_R	temperature of catalyst bed in reaction chamber
T_R^{set}	setpoint of T_R
S	selectivity

Subscripts for S:

C_1	methane
C_2	ethane
C_3	propane
X_{C_4}	butane conversion

1. hydrogen and n-butane control valves

2. hydrogen and n-butane orifice plates

3. hydrogen and n-butane rotameters

4. nitrogen solenoid valve

Legend for Figure 2.1 (cont'd)

5. nitrogen flow indicator

6. feed preheater (steam)

7. backpressure regulator for feed system

8. feed preheater (circulating oil)

9. fluidized bed reactor, reaction chamber

10. fluidized bed reactor, disengaging section

11. air cooler (circulating oil system for heating/cooling coil)

12. heating tank, feed preheat circulating oil system

13. heating tank, heating/cooling coil circulating oil system

14. expansion chamber

15. reactor pressure relief valve

16. exit gas cyclone

17. heating/cooling coil

Feed gas enters the bottom cone of the reactor which is packed with 1.9 cm stainless steel Rasching rings to disperse the gas across the reactor cross-section. The gas then flows through a distribution/catalyst support plate, 0.0127 m thick drilled with 230, 1.4 mm-diameter holes. The 10% by weight nickel impregnated silica gel catalyst particles with diameters ranging from about 70 to 300 μm form a catalyst bed, the height of which is approximately 0.47 m under static conditions. A sheet of 200 mesh stainless steel screening placed over the distributor plate prevents the particles from falling through. The exit gas passes through a cyclone which returns any entrained catalyst particles to the catalyst bed. The reactor is maintained at constant positive pressure (ca. 115.1 kPa) by a back pressure valve (Brooks, model 66122BP) located after the cyclone and the exit gas sampling line. A 0.15 m flanged port on top of the disengaging section is used for charging catalyst and visual observation of bubbles when using nitrogen gas.

2.2.2 Heating-Cooling System

Two circulating oil systems are present; one in the feed-gas preheater system and the other in the heating-cooling coil system on the reactor. The circulating fluid is Sun 21 Heat Transfer Oil and electrical immersion heaters (4.5 kW for gas preheater system and 8.5 kW for reactor heating system) are used to heat the oil. The oil is circulated by Sihi centrifugal pumps.

(1) Gas Preheater: Feed gas is preheated to reaction temperature (∿225°C) by first heating it with 790.6 kPa steam in a brass shell-and-tube heat exchanger (single pass, 0.111 m^2) and then in two carbon steel heat exchangers (single pass, 0.185 m^2 each) by the circulating oil.

(ii) <u>Heating-Cooling System for the Reactor</u>: At start-up, the fluidized bed is heated to reaction temperature by circulating hot oil through 1.27 cm diameter stainless steel tubing which is spiralled on 5.1 cm centres around the reactor barrel and approximately one half the disengaging section. This heating coil is imbedded in heat transfer cement (Thermon Company) to improve the heat transfer to the reactor wall.

Once the reaction starts, heat must be removed by the circulating oil. This is accomplished by passing the oil through an air-cooled heat-exchanger (single pass, shell-and-tube exchanger, 0.111 m^2 area), referred to hereafter as the air cooler.

2.3 Minicomputer System

The pilot plant fluidized bed reactor is interfaced to the mini-computer system (NOVA 1200) in the department's computer control labora-tory. The computer system was used for all data logging programs and control algorithms that were implemented on the reactor. A layout of the computer facilities at the time of this study is given in Fig. 2.2.

The minicomputer system is a dual processor consisting of two Data General NOVA 1200, 16 bit minicomputers (A and B). They share an interprocessor bus (IPB), a 0.5 Mbyte fixed head disk and a Data Acquisi-tion and Control Interface (DGDAC). The minicomputers can access to 48 analog to digital (A/D) and 12 digital to analog (D/A) channels, 32 TTL inputs, 32 TTL outputs, 16 relay outputs and 32 contact sense lines in the DGDAC through FORTRAN callable software driver routines in the library file AIO.LB which was first developed by Harris [5] . During a computer run, either system A or system B can access to the DGDAC, but not both.
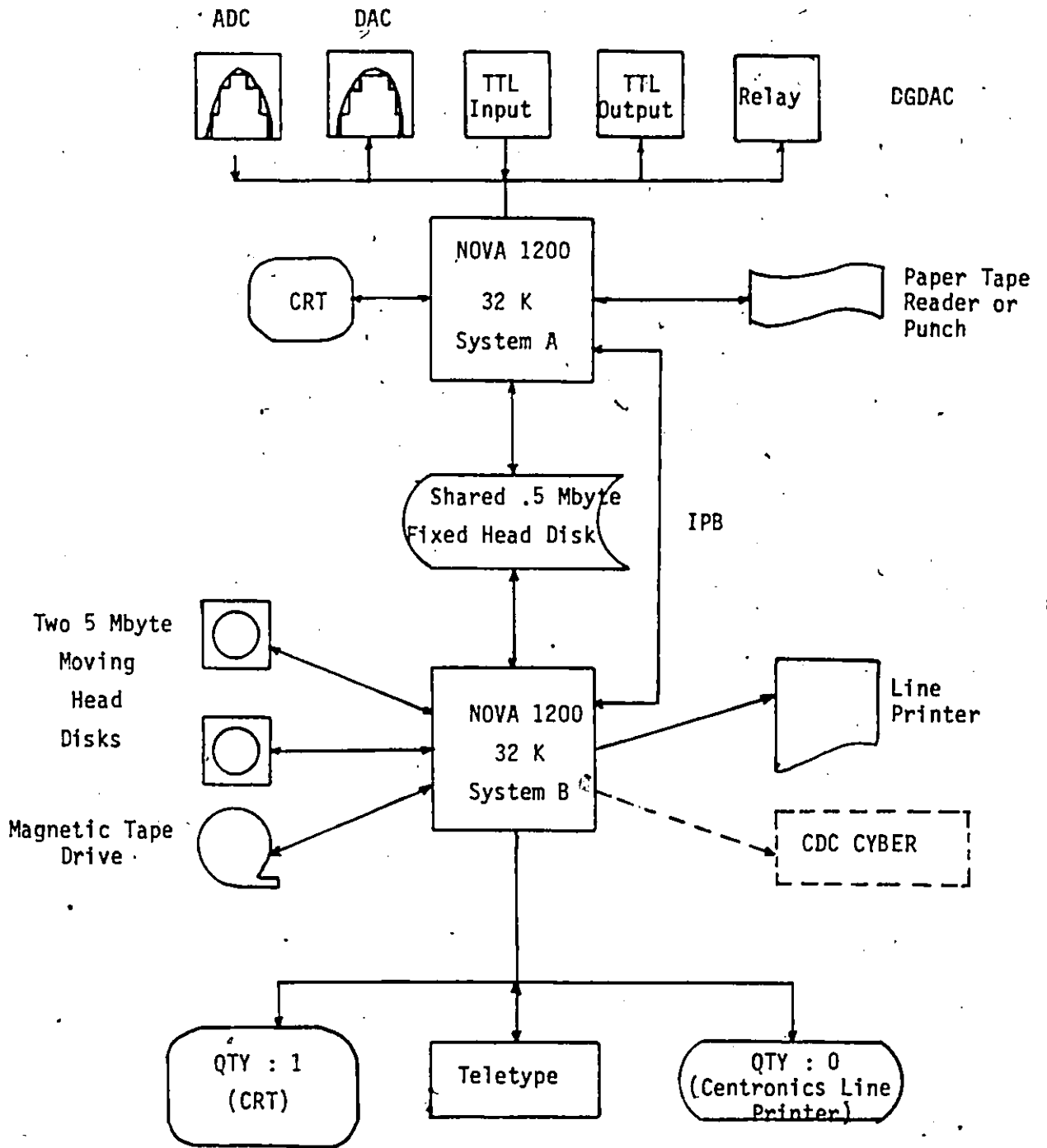
Figure 2.2 Layout of the Minicomputer System

The peripheral devices on Minicomputer A include a cathode ray tube (CRT), a paper tape punch and reader, hardware floating point processor, hardware multiply and divide and a real time clock. System A is used for the production runs and communicates with a video console and keyboard (CRT). Because of the reduced computation time, the hardware floating point and multiply/divide System A allows the accommodation of the big production program which has three major sampling and control tasks on the flow, temperature and gas chromatograph systems; while the parameter interrupts as well as detalogging and control results are passed from and to System B via the IPB.

System B is interfaced to two 5 Mbyte disks, one of which is removable and is used to store all the data. Any on-line parameter changes may also be communicated to System B via a teletype with a QTY port (QTY:1, is a CRT). The measurements and the setpoints introduced can be read from a hardcopy when the information has transferred from System A to System B and dumped out through another QTY port (QTY:0, a Centronics line pointer). After each experimental run, it is advisable to store all the data onto a magnetic tape using the magnetic tape drive. In addition, Minicomputer B is able to transfer data directly to the University's main Control Data Corporation (CDC) Cyber computer.

The computers use Data General's Real-Time Disk Operating System (RDOS) revision 6.62. All user software for this study was written using Real-Time FORTRAN in a multitasking environment.

2.4 Instrumentation and Process/Computer Interface

2.4.1 Instrumentation

2.4.1.1 Feed Flow System. The hydrogen and n-butane gases are fed to the reactor from cylinders. Six hydrogen cylinders (each containing 6.5 m^3 at S.T.P.) are connected to a common manifold; usual operation entails using one at a time and each can last for about one hour under normal reactor operating conditions (ca. 0.1 m^3/min). The butane originates from one large cylinder. Hot water is run over the cylinder as a film to maintain a reasonable operating pressure.

Two flowrate measuring systems are employed. Rotameters are used as a visual indication; that for hydrogen is a Fisher-Porter FP-$\frac{1}{2}$-21-G-10/80 and that for butane is Brooks BR-$\frac{1}{2}$-25G10. Originally there were two floats in the butane rotameter, but since only low flowrates were required only the light float was used. Orifice plates (2.50 mm diameter for n-butane and 2.00 mm diameter for hydrogen) along with pressure differential (ΔP) transmitters (Rosemount Alphaline: n-butane, model C1151DP4E22MBCE, hydrogen, model C115DP4C22MBCE, 4-20 ma output) were used to monitor (datalog) the flowrates by the computer. These were installed upstream of the rotameters. To ensure a constant calibration of these flow measuring devices, a constant pressure of 128.9 kPa was maintained on them by a back-pressure regulator (Fisher, type 38L) installed downstream of the rotameters.

The hydrogen and butane flowrates are controlled by pneumatically-activated valves (Badger Meter Inc. Research and Control Valves, air to open, type TY7SS; n-butane, Trim J; hydrogen, Trim G).

Interfacing the pressure transducers with the computer and the computer with the pneumatically controlled valves requires analog-to-digital (A/D) conversion and electro-pneumatic (E/P) converters respectively. The A/D converters are able to digitize input signals of 0 to 10 volts* and produce output voltages over a similar range. Thus, the milliamp signal from the pressure transducers was converted to a suitable voltage by installing dropping resistors across the outputs of the ΔP transmitters. The reverse procedure, that is producing the required pneumatic signal from the output voltage from the computer (D/A converters) requires conversion from voltage to current (1-9 V to 2-50 ma) and then an E/P converter (Fisher Controls Co.,Type 546) to linearly convert this current to pneumatic signals for actuation of the control valves. The calibration procedures and results for butane and hydrogen are given in Appendix A.2.1.

It is important to maintain the feed flowrate ratio (u_{H_2}/u_{C_4}) of the incoming gases above some critical ratio depending upon the reactor operating temperature, since it was observed on one occasion that severe coking of the catalyst occurred when the u_{H_2}/u_{C_4} ratio fell to around 3 for about 5 to 10 minutes. This coking led to severe catalyst deactivation. Since the catalyst could not be easily reactivated, complete replacement of catalyst was required. This experience led to the design and construction of an automatic device which caused the butane to be immediately shut off if the feed flowrate ratio was reduced to less than some specified value (usually 4.0). This safety device com-

* This is done in terms of computer units; 0-4095 computer units correspond to 0-10 V at the D/A output.

compares the ratio of the voltages which are transmitted to each flowrate control valve. In addition to this device, which was activated essentially all the time during reaction operation, computer software also ensured that the required ratio, as calculated by the control algorithms, was always above a specfied ratio. The physical device was used as back-up; however, it was essential during manual operation or in case of computer malfunctioning..

2.4.1.2 Cooling Oil Temperature Control. The air cooler is used to maintain a constant, preset oil temperature to the reactor cooling coils. In this way an attempt is made to maintain a constant heat load on the reactor. Cooling air from the 790 kPa lab system is used to control the outlet oil temperature. The air flowrate is con-trolled by a pneumatically operated valve (Badger Meter Inc., Research Control valve, air to open, Type TY7SS, Trim E) using similar auxiliary equipment as for the feed gas. A manually operated by-pass valve around the control valve can be used if a high rate of cooling is required.

During operation of the reactor, it was found advisable to have the electrical power on to the heaters in the oil hold tank (ca. 70% of maximum depending upon the conversion level and butane flowrate to the reactor).

2.4.1.3 Temperature Sensors. The temperatures throughout the reactor system (as indicated in Figure 2.1) are measured by Chromel-Alumel thermocouples (Thermo Electric (Canada) Ltd). These sensors are located at various vertical positions in the fluidized bed, on the outer wall of the reactor and in the oil and gas lines; exact locations are

given in Table 2.1. Radial traverses within the bed at various loca-
tions indicated essentially isothermal conditions, except in the
immediate vicinity of the wall, as long as the gas velocity was in
excess of about ten times that required for minimum fluidization.

Sixteen separate temperature measurements may be made at any
instant. A multiplexing system (internal design) transmits any two
signals at any given time. These relatively low level signals require
amplification and transmission to the A/D input channels.

The particular amplifier (ACROMAG, Model 314-WM-U) which was
used did create a problem in that it was somewhat incompatible with the
multiplexer chip since the existing combination gives rise to a rela-
tively long settling-out-time of 3 to 5 seconds, depending on the
difference in voltages between consecutive readings. Thus, this system
should require about 24 to 40 seconds to step through the eight channels
connected to each of the two amplifiers. This means that a "snapshot"
of all the temperatures cannot be taken at one time under a given opera-
ting condition. The problem was alleviated to some extent by judicious
choice of the consecutive temperatures which were multiplexed to the
amplifier. For example, the representative temperature of the bed was
assumed to be the average of these measured 0.15 m and 0.30 m from the
distributor plate. Thus these temperatures were measured consecutively.
The oil temperature to the cooling coils is also controlled. Since it

THERMOCOUPLE #   LOCATION

1	– Out of order
2	– Not in use
3	– Out of order
4	$T_{w,9"}$: Reactor wall, 0.23 m from distributor plate
5	T_{tank}: Oil line exiting circulating oil heating tank
6	$T_{R,2'}$: Reactor chamber, 0.61 m from distributor chamber
7	$T_{w,36"}$: Reactor wall, 0.91 m from distributor plate
8	$T_{oil,preheater}$: Oil line entering feed preheater
9	$T_{w,18"}$: Reactor wall, 0.46 m from distributor plate
10	$T_{oil,out}$: Oil line exiting heating/cooling coil
11	T_{feed}: Reactor feed line
12	$T_{R,3'}$: Reactor chamber, 0.91 m from distributor plate
13	$T_{R,4'}$: Reactor chamber, 0.22 m from distributor plate
14	$T_{oil,in}$: Oil line entering heating/cooling coil
15	$T_{R,1'}$: Reactor chamber, 0.30 m from distributor plate
16	$T_{R,\frac{1}{2}'}$: Reactor chamber, 0.15 m from distributor plate

Table 2.1 : Thermocouple Locations

is only slightly lower than the reactor temperature it, too, was measured immediately before the reactor temperatures. This measurement sequence also ensured that control procedures were executed under the same conditions.

Another problem which was encountered with the ACROMAG transmitter-amplifier was the continual slow drifting of the calibration of the amplified signals from the thermocouples. Moreover the calibration was non-linear so frequent recalibration (ca. every one or two hours) was necessary. Although a new multiplexing-amplifier system was designed, construction was not completed in time for the experimental program reported here.

2.4.1.4 <u>Gas Chromatograph System</u>. As Figure 2.1 indicates, a process gas chromatograph (Beckman Model 6700) was used to analyze the exit gas stream from the reactor. The chromatograph consists of an analyzer and programmer. The latter schedules the injection of samples to the columns and the transmission of data and pulses to and from the computer. Details of the gas chromatograph, its interface to the reactor and computer systems as well as its operation are not presented here. Both Tremblay [6] and McFarlane [4] have included comprehensive summaries of its operation in their theses. However some of the new settings of the component boards in the programmer, the procedure for preparing a calibration sample and the calibration curves for the different components are described in Appendix A.2.2.

For this chemical system, the time required by the chromatograph to process the complete analysis is 360 s. This introduces a considerable

dead-time between sampling and measurement which is very important in designing the control system for the reactor.

2.4.2 Process-Computer Interface

The reactor is started up under manual control. Thus variable voltage sources (0 to 10 volts D.C.) are required to allow manipulation of the control valves through the E/P converters. Four separate variable sources are available: one to manipulate hydrogen flow, one for butane and one for the air supply to the air cooler; the fourth is a spare.

A "Manual/Computer" switch at the reactor control station adjacent to the reactor allows the operator to select the manual or computer control mode. In the manual mode, manipulation of each of the valves is effected by a potentiometer on the voltage supplies. The start-up procedure recommended by Shaw [3] was easily carried out using this equipment.

In the computer mode, the voltage sources are manipulated by the computer via the D/A converter output channels. The voltages to be transmitted to the E/P converters are set or calculated within the user-generated software in terms of computer units (4095 units = 10 volts at the output of D/A unit).

Detailed schematics and information about some of the devices described above can be found in the technician's file in the Department. They are as follows :

- The circuit diagram and the details of the ratio comparitor device in Section 2.4.1.1.
- The block diagrams, input-output connection diagram of the multiplexing system and the multiplexer-cable connections in Section 2.4.1.3.

- The wiring of the Manual-Computer control box, a schematic of the process-computer interface and the pin connections for the interface cable in Section 2.4.2.

3. DYNAMIC SIMULATION MODEL OF THE REACTOR SYSTEM

3.1 Introduction

The simulation model used in this study for the fluidized bed reactor system was based on the previous work done by Orlikas [7] and Shaw [3]. Shaw tested a number of steady-state models which had been proposed for heterogeneous catalytic chemical reactions in fluidized beds and indicated that most models provided reasonable predictions (from a control point of view) as long as one parameter which related to the fluid-mechanical behaviour and also another parameter relating to catalyst activity were evaluated from reactor response data. It is the extension of these steady-state models to include the main dynamic effects which is described in this chapter. The essence of the chemical reaction kinetic model and the steady-state model is briefly reviewed prior to presentation of the dynamic model of the system.

3.2 Reaction Kinetics

The hydrogenolysis reactions which took place in the reactor were described in Section 2.1.2. The mechanistic kinetic model for the reaction system which was developed by Orlikas [2, 7] and further investigated by Shaw [3, 8] has been shown to describe the chemical kinetics for this reaction quite well. It was shown that this mechanistic model gave good predictions of conversion and selectivities over a wide range of conditions in the small packed bed integral reactor used for the study. A catalyst activity parameter (k/k_o) was included in the model since even the same catalyst exhibited differences in activity depending on the initial 'conditioning' treatment to which it was subjected. This parameter as included in the model was shown to account

for differences in catalyst activity during this experimental program.

The main characteristics of the reactions are that they are all highly exothermic ($\Delta H_R = -167.4$ kJ/mol), leading to a doubling of the reaction rates for about every 3°C increase in reaction temperature.

3.3 Fluidized Bed Reactor Model

Prior experimental and steady-state modelling studies conducted on this reactor by Shaw et al. [3, 8] found that the simple, two-phase model of Orcutt, Davidson and Pigford [9] described the conversion and product distribution (selectivity) with acceptable accuracy even though other models provided a better representation of the reactor under certain conditions. Therefore our dynamic model was based upon the Orcutt model because of its simplicity. The model assumes

(1) The reactor consists of two separate phases: a bubble phase in plug flow and a perfectly mixed emulsion phase.

(2) Spherical bubbles of constant size within which the gas is perfectly mixed but which contain no solid catalyst (hence no reaction occurs in bubble phase).

(3) Gas is perfectly mixed in emulsion phase; the gas flowrate into and out of the emulsion phase is that required to keep the solids in a fluidized rate (minimum superficial fluidization velocity, u_{mf}).

(4) The mass transfer coefficient for the transfer of gas between the bubble and emulsion phases is constant over the bed height.

(5) The system is isothermal throughout.

The mathematical model based on these assumptions is described below.

3.3.1 Material Balances

(1) __Bubble Phase:__ At any instant, for any component i in the bubble phase its concentration as a function of the height (h) through the bed is given by

$$u_b V_b \frac{dC_b^i}{dh} = Q(C_e^i - C_b^i) \qquad i = 1,2,3 \tag{3.3.1}$$

with initial conditions $C_b^i = C_o^i$ at $h = 0$. Q is the transfer or interchange rate for any component between a bubble of volume V_b and the emulsion. Since V_b, u_b, C_e and Q are assumed to be independent of height in the bed, the bubble material balance equations in (3.3.1) can be integrated from $h = 0$ to $h = H$ to give the exit bubble concentrations as

$$C_{b,H}^i = C_e^i + (C_o^i - C_e^i)\exp(-QH/u_b V_b) \quad (i = 1,2,3) \tag{3.3.2}$$

(ii) __Emulsion Phase:__ For any component i, a material balance over the entire perfectly mixed emulsion phase yields (with the use of Equation (3.3.2))

$$V_e \frac{dC_e^i}{dt} = S(C_o^i - C_e^i)\left\{u_{mf} + Nu_b V_b \left[1 - \exp\left(-\frac{QH}{u_b V_b}\right)\right]\right\} - r_i V_e \tag{3.3.3}$$

for $i = 1,2,3$

Simultaneous solution of this set of differential equations gives the emulsion phase concentrations through the reactor.

Using $V_e = V(1 - NV_b)$ and $H = V/S$, Equation (3.3.3) becomes

$$H(1 - NV_b) \frac{dC_e}{dt} = (C_o - C_e)\left\{u_{mf} + Nu_b V_b\left[1 - \exp\left(-\frac{QH}{u_b V_b}\right)\right]\right\} - H(1 - NV_b)r_i$$

$$\tag{3.3.4}$$

Since it has been found for this system that the time constant of Equation (3.3.4) is small compared to the time constant of the Equation describing the enthalpy or temperature change of the reactor contents (Equation (3.3.12)) the concentration of the various reacting species was assumed to be at their pseudo steady-state values throughout. Therefore change of concentration with respect to time is assumed to be zero; thus, there results:

$$(C_o - C_e)\{ u_{mf} + Nu_bV_b[1 - \exp(- \frac{QH}{u_bV_b})]\} = H(1 - NV_b)r_i \qquad (3.3.5)$$

Knowing the division of flow into each phase, the bed exit concentration can then be solved simultaneously from the set of Equations (3.3.2) and (3.3.5). Note that the calculation of concentration involves only algebraic equations.

(iii) <u>Disengaging Section</u>: Since the concentrations are measured by a process chromatograph at the exit of the reactor, the dynamics of the disengaging section may also be important under some operating conditions at least. Here, this section is modelled as a perfectly mixed vessel. Thus, the transient mass balance for each component i may be written:

$$\frac{dM_i}{dt} = F_{i,in} - F_{i,out} \qquad (3.3.6a)$$

$$= F_{i,in} - Q_{out} \frac{M_i}{V} \qquad (3.3.6b)$$

where M_i = mass of component i in the vessel (Kg)

$F_{i,in}$ = inlet mass flowrate of component i (Kg/s)

$F_{i,out}$ = outlet mass flowrate of component i (Kg/s)

Q = volumetric flowrate of the stream (L/S)

V = volume of the vessel (L)

Since

$$Q_{out} = Q_{in} \frac{T_{out} P_{in}}{T_{in} P_{out}}$$ (3.3.7)

where   T = absolute temperature of the stream (K)

P = total pressure in the stream (kPa)

Note that both $F_{i,in}$ and Q_{in} are required and these may be obtained from the calculation of the product exit stream from the reactor. Thus Equation (3.3.6) can be integrated to give the mass hold up of the component i, M_i, in the vessel.

The mass flowrate of each component i in the outlet stream may be obtained from:

$$F_{i,out} = Q_{out} \cdot \frac{M_i}{V}$$ (3.3.8)

Empirical Correlations: Several empirical correlations available from literature were used for predicting certain physical phenomena in the bed:

(1) Bubble diameter, d_b, as a function of bed height was given by Kato and Wen [10]:

$$d_b = 0.14 \rho_p d_p h \left(\frac{u_b}{u_{mf}}\right) + [6 \left(\frac{u_b - u_{mf}}{n_o \pi}\right)]^{0.4} g^{-0.2}$$ (3.3.9)

Since the Orcutt model assumes a constant bubble diameter with respect to height, an integrated average value of d_b was calculated by Shaw et al. [8] .

(2) The interchange rate Q between the bubble and the emulsion

phases was calculated from the correlation [11] :

$$Q = 0.11 \frac{V_b}{d_b}$$
(3.3.10)

It was assumed that the form of the correlation applied but an

additional multiplying factor (interchange parameter) was

required to compensate for difference in the reactor system

employed here. A sensitivity analysis [3] demonstrated

that this was by far the most important parameter in the fluid

mechanical part of the model.

(3) The bubble rise velocity u_b was predicted by Shaw et al. [8]

$$u_b = 0.711 (g\ d_b)^{1/2} + (u - u_{mf})$$
(3.3.11)

3.3.2 Enthalpy Balances

(1) Reactor Contents: Assuming that the gas and the catalyst

particles are at the same uniform temperature in the bed, then an

enthalpy balance on the chemical gas/solid phases yields:

$$(WC_{pB} + \epsilon V \overline{\rho_g}\ \overline{C_{pg}})\ \frac{dT_R}{dt}$$

$$= V_o \overline{C_{pg}}\ \overline{\rho_g}(T_o - T_R) + h_W A_W(T_W - T_R) + \sum_{j=1}^{r} R_j \overline{\Delta H_j} W$$
(3.3.12)

Since the second term on the left hand side of this equation is small

compared to the first term, it can be neglected. Thus, the final form

of the enthalpy balance on the reactor contents is

$$WC_{pB}\ \frac{dT_R}{dt} = V_o \overline{C_{pg}}\ \overline{\rho_g}(T_o - T_R) + h_W A_W(T_W - T_R) + \sum_{j=1}^{r} R_j \overline{\Delta H_j} W$$
(3.3.13)

where r = number of reactions where heat is generated (equal to 3 as explained in Section 3.3.3.)

(ii) <u>Reactor Wall</u>: The reactor wall, cooling coils, and supporting structure in contact with the wall was judged to have a mass sufficient to make their dynamic effect an important consideration in the temperature dynamics of the overall system. If these elements are lumped into a single mass (M_w) at a uniform temperature (T_w), an enthalpy balance yields

$$M_W C_{pw} \frac{dT_w}{dt} = h_W A_W (T_R - T_W) + h_c A_c (T_{oil} - T_W) - Q_{loss} \qquad (3.3.14)$$

(iii) <u>Reactor Heating/Cooling Coils</u>: The temperature response of both heat exchanger units was assumed to be rapid in relation to the rest of the system; therefore the instantaneous outlet temperature from the cooling coils was calculated from the steady-state relationship for a heat exchanger with a constant source temperature using the effectiveness factor relationship as follows:

$$\varepsilon = \frac{1 - \exp[-(NTU)(1-R)]}{1 - R\exp[-NTU(1-R)]} \qquad (3.3.15)$$

where $R = \frac{(WC_p)_{oil}}{M_w C_{pw}} \simeq 0$

$$NTU = \frac{h_c A_c}{(WC_p)_{oil}}$$

Also,

$$\varepsilon = \frac{T_{oil,out} - T_{oil,in}}{T_w - T_{oil,in}} \qquad (3.3.16)$$

Knowing T_w and $T_{oil,in}$, Equation (3.3.15) and (3.3.16) are combined to eliminate ε and to calculate $T_{oil,out}$.

The mean bulk temperature of oil in the heating/cooling coils is taken as the arithmetic average of the oil inlet and outlet temperature:

$$T_{oil} = T_{oil,in} + \frac{(T_{oil,out} - T_{oil,in})}{2} \tag{3.3.17}$$

3.3.3 Reaction Rates and Heats of Reaction

If F is the fraction of n-butane that reacts to form propane and methane, Equations (2.1.1) and (2.1.2) are rewritten respectively, as

$$FC_4H_{10} + FH_2 \rightarrow FC_3H_8 + FCH_4 \tag{3.3.18}$$

$$(1-F)C_4H_{10} + (1-F)H_2 \rightarrow 2(1-F)C_2H_6 \tag{3.3.19}$$

These are added to give

$$C_4H_{10} + H_2 \rightarrow FC_3H_8 + 2(1-F)C_2H_6 + FCH_4 \tag{3.3.20}$$
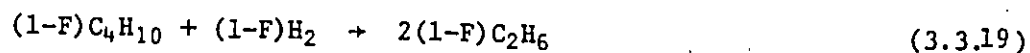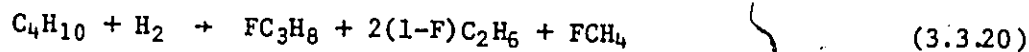
Equations (2.1.3), (2.1.4) and (3.3.20) are three heat-producing reactions for which heats of reaction may be calculated; thus r is equal to three in Equation (3.3.13). Their rates of reaction are given by RP, RE and RB respectively as follows:

Let RB = net rate of reaction of n-butane

RP2 = net rate of reaction of propane

RE2 = net rate of reaction of ethane

with units = mol/(unit volume emulsion phase-sec).

It is easy to show that the rates of reactions can be expressed in terms of the rate of hydrocarbon reacting as examplified by the rate of reaction of propane in the following illustration:

C_4H_{10}

$\downarrow$ rate = RB.F

C_3H_8 [net rate of production of C_3H_8 = RP2]

$\downarrow$ rate of reaction, Equation (2.1.3)

C_2H_6
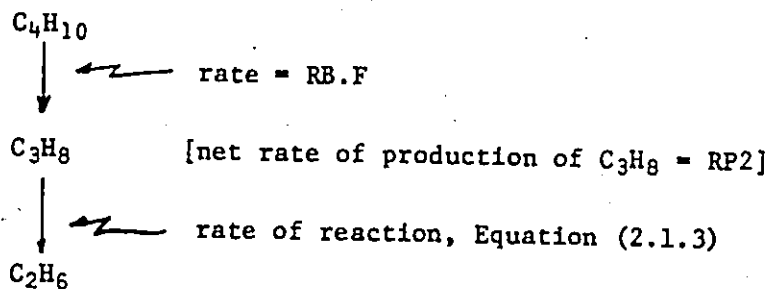
Define the rate of reaction of Equation (2.1.3), RP (g moles propane reacted/unit volume emulsion phase-sec)

$$RP = (RB.F) - RP2 \qquad (3.3.21)$$

Similarly, for ethane, the rate of reaction of Equation (2.1.4), RE is given by

$$RE = RP + 2(1 - F)RB - RE2 \qquad (3.3.22)$$

Heats of reaction for Equations (2.1.3), (2.1.4) and (3.3.20) are calculated using heats of formation of the product and reactant species, evaluated from polynomial expressions in temperature as given by Kjaer [12].

3.4   The DYNSYS Simulation

3.4.1 Introduction

A computer simulation program called DASTFF2 was modified from an existing program written by McFarlane [4] , for use on the CDC Cyber Computer System in the University's Computer Centre. The program was written using a modular dynamic simulation approach utilizing the DYNSYS simulation executive which was developed by Bobrow [13, 14] to allow convenient dynamic simulation of chemical processes. A DYNSYS module consists of a steady state or a dynamic model to be written in terms of first ordinary differential equations, which are solved simultaneously in all modules by an Adams-Morton-Shell formulated third order predictor corrector routine.

The original DYNSYS executive main program was restructured by McFarlane [4] into a Subroutine Model 1 and a program external to

DYNSYS was created to define all inputs, setpoint changes, load distur-
bances, etc. in performing the control function. Through this modifi-
cation, Model 1 can conveniently integrate the appropriate modules over
one time interval when provided with updated inputs and returns the pre-
diction of the system outputs at one time step ahead to the calling
program.

3.4.2 Application of DYNSYS on Fluidized Bed Reactor System

Since the temperature response of the air cooler was assumed to
be rapid in relation to the rest of the system, the instantaneous outlet
oil temperature from the air cooler, which is the temperature of the
oil entering the reactor heating/cooling coils, $T_{oil,in}$, was taken to be
freely adjustable as an input to the reactor. Therefore the DYNSYS
simulation does not include the air cooler. The fluidized bed reactor
has been simulated by two processing units:
REACO1, the reactor, including the wall and heating/cooling coil and
HOLDO1, the disengaging section, modelled as a well mixed vessel with a
mass hold up.

With the modification of the DYNSYS executive main program into
a subroutine, Model 1 and a calling program to be created, the computer
program has the following structure:

Program DASTFF2 – the calling program provided by the user to
fulfill the desired (control) function

Subroutines: MODEL 1, TYPE 1 (REACO1), TYPE 8 (HOLDO1), ORCMIX,
HREACT.

The DYNSYS subprograms:

Subroutines: DYN1, DYN2, GET, FETCH, FETCHR, OUTPUT

Functions: Y1, PROPS.

The relationship between the calling program, the subroutines and function subprograms are illustrated by Figure 3.1. For the detailed functions and descriptions of the DYNSYS subprograms, the reader is referred to the DYNSYS manual by Bobrow et al. [13].

An information flow diagram for the system is shown in Figure 3.2 and each unit is described separately in the sections REAC01 and HOLD01.

The main features of the DYNSYS program are outlined here so that the reader obtains some impression of what is involved. All the details of the DYNSYS executive program are available in the manual.

There are four main storage arrays for DYNSYS and the general flow of information between them is indicated in Figure 3.3. The numbers shown in the figure are representative of the fluidized bed reactor and are the initial values read into the computer program.

The process matrix MP(I,J),dimensioned as 20 x 8, contains the ordered list of unit numbers, module type and the associated streams (input streams shown positive, followed by output streams shown negative). There are two processing units involved: REAC01 and HOLD01 with their corresponding type number 1 and 8. Their related streams are shown in Figure 3.2. It should be noted that the last element in each row is used for the storage of a pointer for locating extra parameter in the EX(100) vector to be described below. All the unfilled locations in the storage arrays are initialized to be zero.

The equipment parameter storage array EP(20,5) contains up to five equipment parameters for each unit. If more than five parameters are
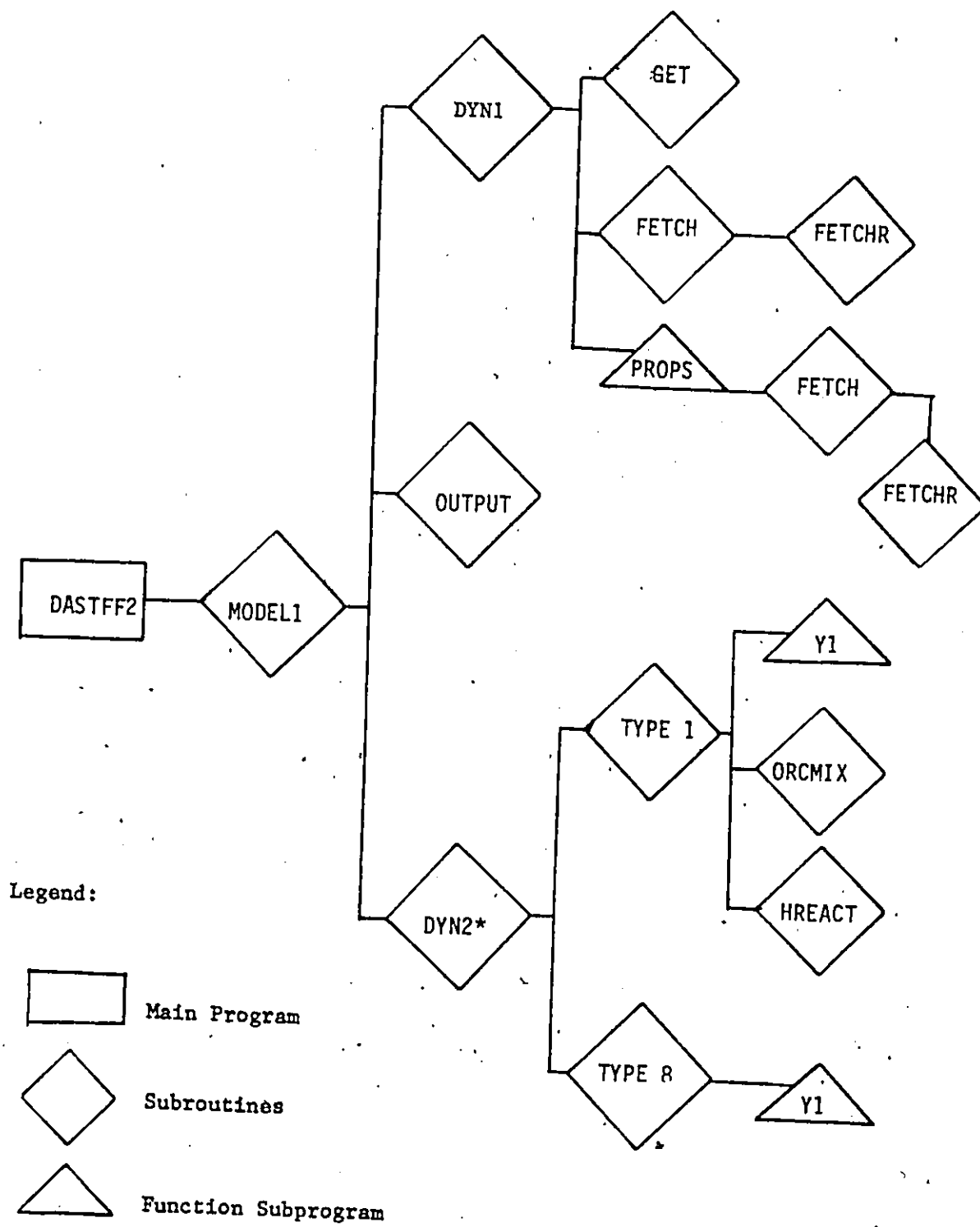
Figure 3.1 Structure of the DYNSYS Simulation Program in Its
Application to the Fluidized Bed Reactor
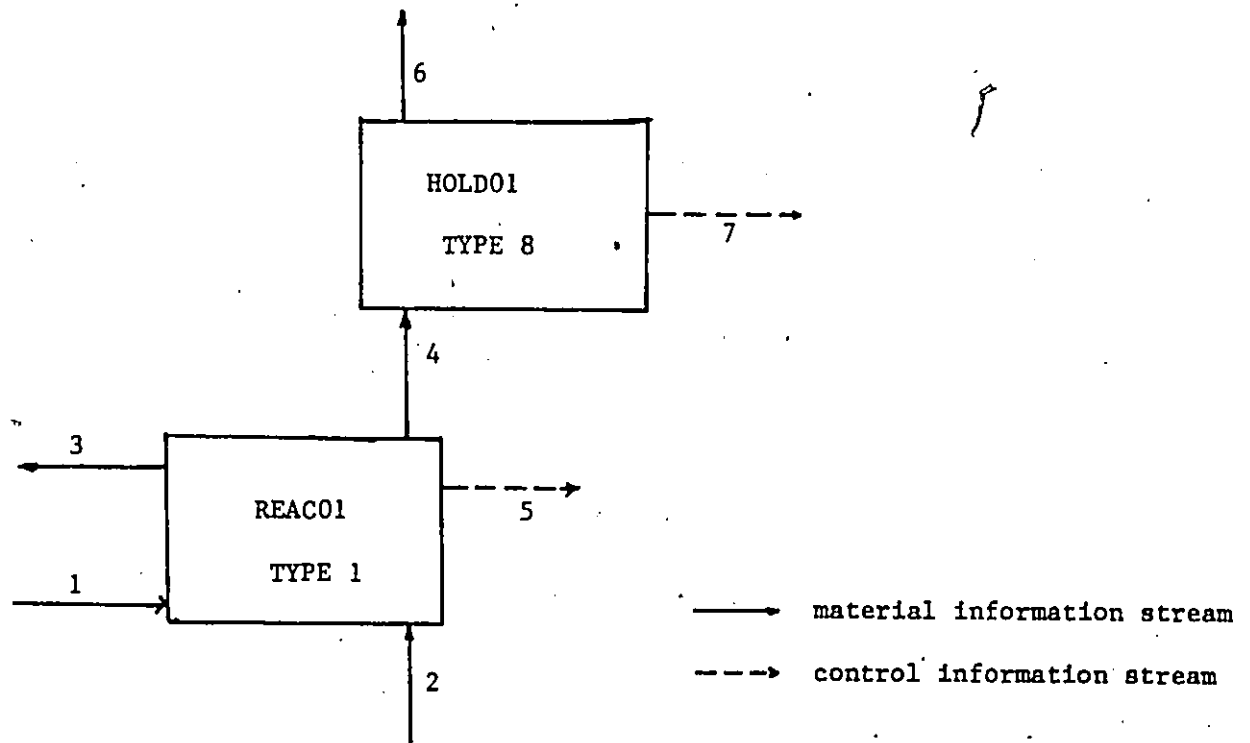
Stream 1 oil inlet to reactor heating/cooling coil

2 reactor feed

3 oil exiting reactor heating/cooling coil

4 product gas exiting from reactor to disengaging section

5 reactor information stream

6 exit gas from disengaging section

7 disengaging section information stream

Figure 3.2 Information Flow Diagram for DYNSYS Simulation

MP(20,8)

Unit No.	Type	Streams					
1	2	3	4	5	6	7	8
1	1.	1.	2.	-3.	-4.	-5.	1
2	8.	4.	-6.	-7.	-	-	6
.							
.							
.							

EP(20,5)

Parameters				
1	2	3	4	5
7000.0	1.87	21.4	17.36	0.0165
124.6	10.	-	-	-

EX(100)

Additional Parameters				
3000.	0.64	0.25	0.	1.
0.	0.	0.	0.	0.
26.22	4.	5.3	39.35	8.65

S(2,50,20)

No.	Flag	Flow	Temp	Pressure								
1	2	3	4	5	6	7	8	9	10	11	12	...
1	5.	565.7	247.	1.1	0.	0.	0.	0.	0.	565.7	0.	
2	5.	0.	260.	1.1	0.	0.	0.	0.	0.	0.	0.	
3	5.	565.7	0.	0.	0.	0.	0.	0.	0.	565.7	0.	
4	5.	0.	0.	1.1	0.	0.	0.	0.	0.	0.	0.	
5	11.	247.4	253.	260.	0.	0.	0.	0.	0.	0.	0.	
6	5.	0.	0.	1.	0.	0.	0.	0.	0.	0.	0.	
7	11.	0.	0.	1.	0.	0.	0.	0.	0.	0.	0.	
.												
.												
.												
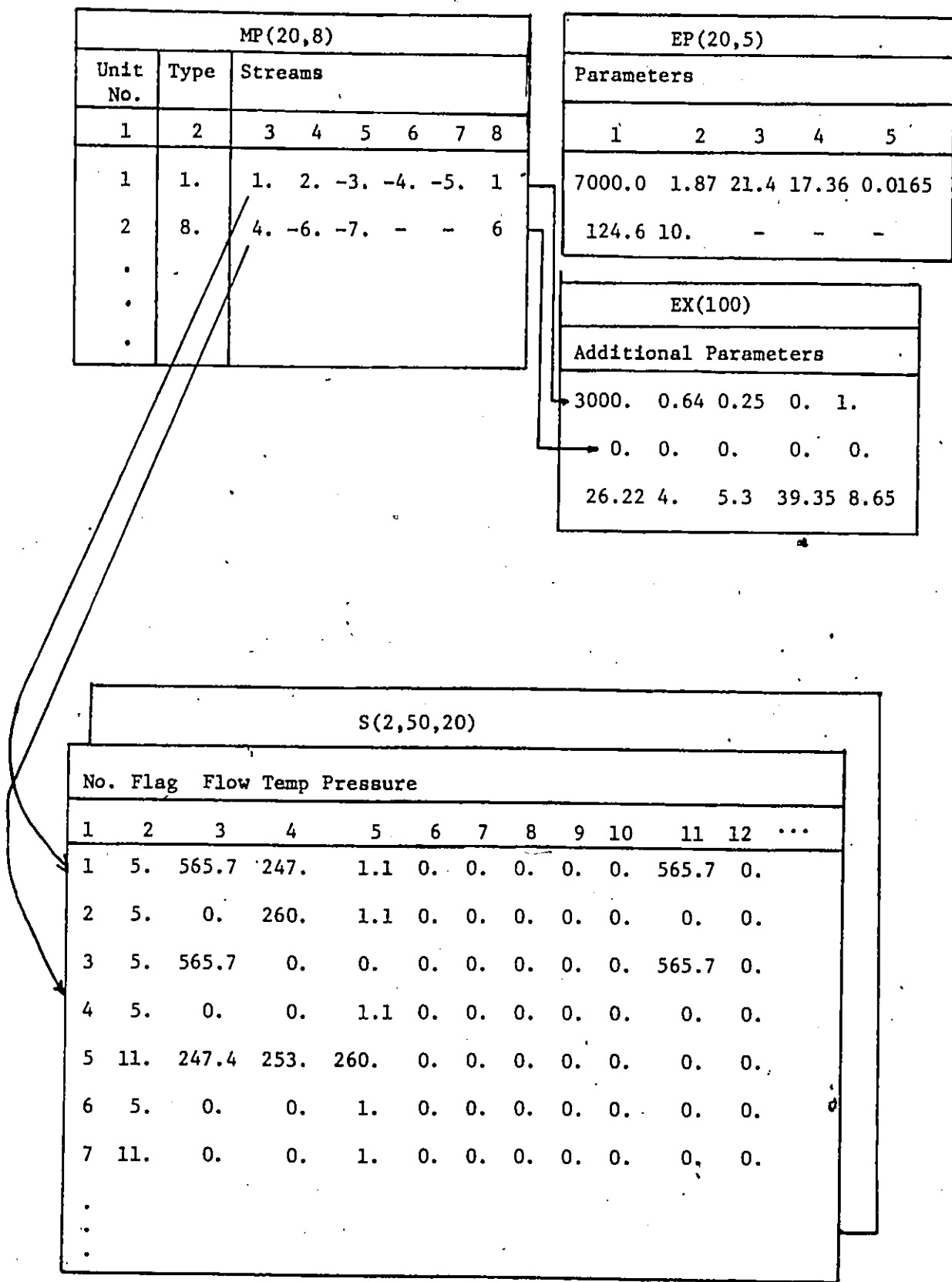
Figure 3.3 · Main Storage Units for DYNSYS and Information Flow Between Them

required for a unit computation, these parameters are stored in the extra equipment parameter vector EX(100). The executive sets up the last column in the process matrix MP( ) as a pointer to this table. This feature allows storage of an indefinite amount of information for the EX vector in the data set. The physical significance of these parameters are to be described in the modules.

The stream information array S(I,J,K), dimensioned as 2 x 50 x 20, is used to store the stream information for the present time step, I = 1 and for the previous time step, I = 2. Each row (J) is allocated for each stream number (J) as defined in the process matrix MP( ). The stream number is stored in K = 1 location.

For K = 2, the stream flag serves the dual purpose of identifying the stream type and, if negative, suppresses printing of the stream variables in the output. In general, there are two types of streams:

(1) material information stream (flags with absolute value ≤10); these are indicated by solid connecting lines on the information flow diagram in Figure 3.2 and may include total flow, temperature, pressure and the flows or concentrations of the components. For this simulation, the stream list has been defined as:

   K = 1 – stream number, (1,2,3,4,6).

      2 – stream flag, = 5

      3 – total mass flow (g/sec)

      4 – temperature (°C)

      5 – pressure (atm)

      6 – CH_4 flowrate

      7 – C_2H_6 flowrate

8 - C_3H_8 flowrate

9 - C_4H_{10} flowrate

10 - H_2 flowrate

11 - circulating oil flowrate

12 - air flowrate

flowrates in g/sec

(2) control information streams (flags with absolute value >10) represented by dashed lines indicate that the information flow is concerned with control variables (such as the pressure used to activate a valve) or sensed variables (such as temperature in a tank). The stream list for stream 7 which is a control information stream is the same as that for material infromation stream because the sampled stream coming out from the disengaging section requires the same information whereas the control information stream 5 has the following stream list:

K = 1 - stream number, = 5

2 - stream flag, = 11

3 - T_{oil}, mean bulk temperature of oil in cooling coil (°C)

4 - T_w, average wall temperature over bed height (°C)

5 - T_R, reaction temperature (°C)

6 - S_1, selectivity of methane (moles methane produced/moles butane reacted)

7 - S_2, selectivity of ethane

8 - S_3, selectivity of propane

9 - CONV, conversion of butane

REAC01: Type 1

The reactor module REAC01 (TYPE 1) consists of the following equations which were described in Section 3.3:

1. algebraic equation describing the pseudo-steady state reactor mass balances: Equation (3.3.5).

2. differential equation describing temperature dynamics of reactor contents: Equation (3.3.13).

3. differential equation describing temperature dynamics of reactor wall: Equation (3.3.14).

4. algebraic equation describing enthalpy balance on oil in heating/ cooling coil: Equations(3.3.15) to (3.3.17)

A solution to the steady state mass balance was provided by Shaw [3] as the Subroutine ORCMIX It incorporates the reaction rate expressions Equations (3.3.1) to (3.3.3) and solves the (pseudo) steady state mass balance Equation (3.3.5) for each component. While the heats of reaction Equations (2.1.3), (2.1.4) and (3.3.20) are calculated in subroutine HREACT.

The calculation flowcharts and listings, together with the argument list, for subroutines ORCMIX, and HREACT may be found in Section 3.3.1 and Appendix A3.1 of McFarlane's thesis [4].

HOLD01: TYPE 8

The dynamic effects of the open volume above the fluidized bed and constituting the disengaging section are also important. The mixing patterns within this free space are unknown. In fact, a mixing model (for example, part of the volume could be considered perfectly mixed ,another part in plug flow) should be formulated perhaps on the basis of pulse testing experiments, which would account for the mixing process which occurs there. In the absence of this experiment, the volume above the fluidized

bed was considered to be perfectly mixed. Thus, module HOLD01 is based on the differential equation describing the unsteady state mass balance for each component in the incoming stream, i.e. Equation (3.3.6).

The information flow diagram showing the associated streams with this module is given in Figure 3.2. A program listing of TYPE 8 is included in Appendix C.3.1. The equipment and extra parameter list defined for this unit on Figure 3.3 are given below:

Equipment List:

$EP(2,1)$: V

$EP(2,2)$: $T_{in} - T_{out}$

Extra List:

$EX(1)$: $M_{C_1}^*$ (corrector step) $EX(6)$: $M_{C_1}^\#$ (predictor step)

$EX(2)$: $M_{C_2}^*$ ("   ") $EX(7)$: $M_{C_2}^\#$ ("   ")

$EX(3)$: $M_{C_3}^*$ ("   ") $EX(8)$: $M_{C_3}^\#$ ("   ")

$EX(4)$: $M_{C_4}^*$ ("   ") $EX(9)$: $M_{C_4}^\#$ ("   ")

$EX(5)$: $M_{H_2}^*$ ("   ") $EX(10)$: $M_{H_2}^\#$ ("   ")

3.4.3 Parameter Estimation

Many of the parameter values in the foregoing model were readily available in the literature, or had been previously well estimated from statistically designed kinetic experiments [2, 8]. There still remained, however, a number of unknown parameters, which related to the dynamics of the reactor system, that had to be estimated by least-squares methods from data collected on the fluidized bed reactor itself by McFarlane [4].

* initial values, to be replaced by values calculated in corrector step using the computer program.

initial values, estimated from the mass flowrate of each component exiting the reactor bed.

At the time of data collection for this parameter estimation program, the Beckman Gas Chromatograph was not in service and so exit stream selectivities were not available. In this work, the catalyst activity was re-estimated by non-linear least squares optimization algorithm for multiresponse parameter using the exit stream selectivities from reaction run data. The subroutine UWHAUS, based on Marquardt's algorithm [16], is used to estimate the parameter in a model (Subroutine ORCMIX) given experimental data. A listing of the calling program KACT1 with the modified subroutines is given in Appendix C.3.2.

4. CONTROL METHODS USED ON THE PILOT PLANT FLUIDIZED BED REACTOR

4.1 Introduction

The highly exothermic nature of the reactions coupled with the large activation energies meant that direct control of the reaction temperature was a necessity for safe and stable operation. This was accomplished by manipulating the ratio of hydrogen to n-butane feedrates. The other manipulatable variables, oil temperature and inlet feed temperature, could not be used for this purpose since their effect on T_R was slow due to heat transfer limitations. However, maintaining stable reaction temperature is not the ultimate goal of control for this system. The primary control objective is propane selectivity control.

Propane selectivity is defined as the number of moles of propane produced per mole of butane reacted. Propane is one of the intermediate products of the reactions described by Equations (2.1.1) to (2.1.4), and it was chosen for two reasons: the control scheme reported here is univariate and so independent control of only one product is possible; and of all the products, propane is the most sensitive to changes in the operating conditions.

A cascade control configuration resulted and Figure 2.1 shows how the cascade control system interfaced to the process equipment. At the lowest level, the individual feedrates of hydrogen and n-butane were controlled at one second intervals; at the next level the feedrate ratio was controlled by the reaction temperature controller every 30 seconds; and at the highest level the reaction temperature setpoint was controlled by the selectivity controller when the product selectivities became available from the chromatograph every 360 seconds. An independent

40

controller, manipulating the air flowrate through an air-cooled heat exchanger, was used to maintain the oil temperature at any preselected value.

The dominant feature in the selectivity control loop is that the effluent gas is sampled every 360 s and analyzed with an on-line Beckman process gas chromatograph. The complete chromatographic analysis cycle requires 360 s for completion thereby introducing a considerable dead-time in obtaining the concentration measurements. This was known to cause problems for proportional-integral (PI) controllers [1] and some controller with inherent dead time compensation was required. This was an important consideration in the control studies.

4.2 Temperature and Selectivity Control, Base Case: Dahlin + PI

The cascade control configuration using PI algorithm to control the reaction temperature in the inner loop and Dahlin algorithm [17] to control the propane selectivity in the outer loop was used as a base case for comparison to the other control schemes tested in this thesis.

A dynamic simulation model was developed for the system and control of the reactor temperature was simulated using a discrete PI controller in the velocity form

$$\left. \frac{u_{H_2}}{u_{C_4}} \right|_t = \left. \frac{u_{H_2}}{u_{C_4}} \right|_{t-1} + K_P [\epsilon_{T_{R,t}} - \epsilon_{T_{R,t-1}} + K_I \epsilon_{T_{R,t}}] \qquad (4.2.1)$$

where $\epsilon_{T_{R,t}} = T_{R,t}^{measured} - T_{R,t}^{set}$

K_P = proportional gain

K_I = integral gain

The tuning of this PI controller [4] was accomplished by minimizing a weighted sum of squares criterion with respect to the controller parameters, K_p and K_I. Four consecutive setpoint changes were made while the following criterion was evaluated:

$$\underset{K_p, K_I}{\text{Min}} \left\{ \sum_{i=1}^{N} \left[\frac{T_{R,i} - T_{R,i}^{set}}{T_{R,i}^{set}}\right]^2 + w \sum_{j=1}^{N} \left[\frac{S_{3,j} - S_{3,j}^{set}}{S_{3,j}^{set}}\right]^2 \right\} \qquad (4.2.2)$$

where N = 200 control intervals

w = relative weighting of S_3 deviations with respect to T_R deviations

A measurement error $\sim N(0., 0.35^2)$ was added to the predicted response of T_R, and to the response S_3 was added an error $\sim N(0., 0.008^2)$. The PI parameter estimates under different weightings are summarized in Table 4.1.

The open loop behaviour of the reactor was examined by step-testing using the simulation model [4]. It was found that the heating and cooling responses vary widely depending upon the reactor operating temperature, the catalyst activity, the hydrogen-to-butane feed ratio, and the cooling-oil temperature. This means that there are significant differences in the system gains and time constants for the heating and cooling responses.

Table 4.1

PI Parmeter Estimates

w		K_p	K_I
0.	(minimize squared variation in T_R)	1.508	0.268
0.000125	(equal weighting of S_3 and T_R)	1.030	0.340
1.	(minimize squared variation in S_3)	0.573	0.073

Because a 360 s dead-time was introduced by the chromatograph
analysis time in the selectivity control loop, the Dahlin algorithm [17]
was used for selectivity control. This controller algorithm has been
shown to be most useful when it is desired that the closed-loop
response (here the selectivity loop) resembles a first-order plus dead-
time process. Here the dead-time was specified as 360 s and the
desired closed-loop time constant, λ, could be adjusted on-line. The
response of the propane selectivity to a set-point change in reactor
temperatures may be further approximated as a first order plus dead-time
response (time constant τ and gain K). The resulting Dahlin controller
was simply a discrete-time PI controller with one period of dead-time
compensation, that is

$$\nabla T_{R,t}^{set} = - a_1 \nabla T_{R,t-1}^{set} + \frac{a_1}{a_3} [\epsilon_{S_{3,t}} - a_2 \epsilon_{S_{3,t-1}}] \qquad (4.2.3)$$

where $\quad a_1 = 1 - e^{-360/\lambda}$

$\qquad a_2 = e^{-360/\tau}$

$\qquad a_3 = K(1 - a_2)$

$\qquad \epsilon_{S_3} = S_3^{set} - S_3^{measured}$

At one set of nominal operating conditions, step tests on the
simulation model were used to estimate an approximate inner loop gain
(K = -0.0173) and time constant (τ = 180 s). Since the up and down
responses of the system were substantially different, these average
values were a compromise. Upon implementing this control system on the
pilot plant reactor at conditions close to that used in the simulation
model, the controller performance for small set-point changes was quite

acceptable and in accordance with what was expected. [4]. However, after a few days when the catalyst activity had increased (from 1.87 to 2.50 estimated by the procedure described in Section 3.4.3) and a substantial set-point change (about .10 change) in selectivity was called for, the controllers led to the oscillatory and unstable behaviour. This very poor controller performance was attributed to the fact that the Dahlin algorithm was tuned very tightly (a desired closed-loop time constant of $\lambda = 150$ s was called for). Then when the process response (represented by K and τ) changed substantially due to the time varying catalyst activity and due to the very nonlinear behaviour of the process over the selectivity change requested, the Dahlin controller exhibited this nearly unstable behaviour.

This nonlinear behaviour of the reactor system was investigated further and the results are reported in this work. It will be shown in Section 5.3.2 that by better matching the process response characteristics and by detuning the Dahlin algorithm, this unstable oscillatory behaviour of the cascade control system can be overcome and acceptable performance can be achieved over a wider range of operating conditions.

In order to overcome some of the inherent problems associated with controllers employing fixed parameters on a process which has variable dynamic characteristics, it is logical to consider the use of self-tuning and adaptive controllers. These control schemes should be able to retune the controller as the catalyst activity changes with time, or as the process gain and time constants change when moving into a different region of operation. Self-tuning and adaptive control is discussed in the following section.

4.3 Self-Tuning and Adaptive Control

4.3.1 Introduction

The design of automatic control systems normally requires an accurate model of the system to be controlled before a suitable controller can be designed. However, for many industrial processes, it is very difficult to get an accurate model because of changing process conditions and disturbances in the system. Furthermore, even though identification schemes can be used to determine models for stationary processes, they may involve excessive plant experimentation and off-line analysis. It also demands a level of expertise sometimes not available in the industry. Thus an adaptive control system in which the parameters of a simple model are estimated on-line and subsequently used in the controller is very attractive for practical applications.

In developing a self-tuning regulator (STR), the parameters of a single-input, single-output stochastic model are estimated on-line using a linear least square recursive technique. The updated parameter estimates are then used in a minimum variance controller to calculate the control signal at each sampling instant. Very little a priori information about the process is required and the regulator can be easily implemented. This approach takes into account system time delays and can be used to control processes with slowly time varying parameters.

This section presents the basic equations for the self-tuning regulators (STR) as well as constrained STR. Their application to the fluidized bed reactor is also discussed.

4.3.2 Review on Theory of STR

The principal theoretical developments of self-tuning regulators, as discussed in Astrom et al. [18] and Clarke et al. [20], presumes that the process may be described by a model of the form

$$Y_{t+b} = \frac{\bar{B}(z^{-1})}{A(z^{-1})} U_t + \frac{C(z^{-1})}{A(z^{-1})} a_{t+b} \qquad (4.3.1)$$

whereas Box and Jenkins [21] use the notation

$$Y_{t+b} = \frac{\omega(z^{-1})}{\delta(z^{-1})} U_t + \frac{\theta(z^{-1})}{\nabla^d \phi(z^{-1})} a_{t+b} \qquad (4.3.2)$$

Both forms are capable of providing an adequate representation of a dynamic-stochastic system. However it is felt that the Box and Jenkins notation provides more insight into the nature of the process dynamics and stochastic disturbances by separating them into two terms. The common denominator in Astrom's representation mixes up the dynamic and stochastic models and it is no more than a mathematical representation of the output. The Box-Jenkins notation is to be adopted in this thesis because it clearly indicates the form of the estimation model in an adaptive environment.

The definitions of the symbols are given in the Nomenclature. It should be noted that in the Auto-regressive-integrated-moving-average (ARIMA) model for the white noise, all the roots in the numerator and denominator polynomials should lie inside the unit circle in the z-plane for stable operation. Furthermore, the allowance for d roots equal to unity (usually d = 0 or 1) enables integral action in the controller.

The next two sections summarize all the important equations to be used in the self-tuning and adaptive control on the reactor. For details of the derivation, the reader is referred to Harris [22,23].

4.3.2.1 Minimum Variance (M.V.) Control with Recursive Least

Squares Estimation

Assume that the single-input, single-output plant can be represented by Equation (4.3.2) or

$$Y_{t+b} = \frac{\omega(z^{-1})}{\delta(z^{-1})} U_t + N_{t+b} \qquad (4.3.3)$$

where $\quad N_{t+b} = \frac{\theta(z^{-1})}{\nabla^d \phi(z^{-1})} a_{t+b}$

The disturbance model can be reexpressed as

$$N_{t+b} = \frac{\theta(z^{-1})}{\nabla^d \phi(z^{-1})} a_{t+b} = \psi_1(z^{-1}) a_{t+b} + \frac{T(z^{-1})}{\phi(z^{-1})\nabla^d} a_t \qquad (4.3.4)$$

where $\psi_1(z^{-1}) a_{t+b}$ = the forecast error; and $\psi_1(z^{-1})$ is a polynomial of

order b-1

$$\frac{T(z^{-1})}{\phi(z^{-1}) \nabla^d} a_t = \text{ the b step ahead forecast.}$$

The minimum variance controller u_t in terms of Y_t is given by

$$U_t = -\frac{\delta(z^{-1})}{\omega(z^{-1})} \frac{1}{\psi_1(z^{-1})} \frac{T(z^{-1})}{\phi(z^{-1})\nabla^d} Y_t \qquad (4.3.5)$$

Expressing the process output Y_{t+b} explicitly in terms of the M.V. controller parameters : α_1, β_1

$$Y_{t+b} = \alpha(z^{-1}) Y_t + \beta(z^{-1}) \nabla^d u_t + \varepsilon_{t+b} \qquad (4.3.6)$$

where $\quad \alpha(z^{-1}) = \alpha_0 + \alpha_1 z^{-1} + \ldots + \alpha_m z^{-m}$

$$\beta(z^{-1}) = \beta_0 + \beta_1 z^{-1} + \ldots + \beta_\ell z^{-\ell}$$

and ε_{t+b} is the b step ahead forecast error $\psi_1(z^{-1}) a_{t+b}$.

The orders of m and ℓ are

$$m = \hat{r} + \max(q - b, p + d - 1) \tag{4.3.7}$$

$$\ell = s + p + b - 1 \tag{4.3.8}$$

Define $\underline{\phi}_t = [-Y_t, -Y_{t-1} \cdots - Y_{t-m+1}, \nabla U_{t-1} \cdots \nabla U_{t-\ell}]^T$

$$\underline{\theta} = [\alpha_0 \cdots \alpha_m, \beta_0, \beta_1 \cdots \beta_\ell]^T$$

Equation (4.3.6) can be rewritten as

$$Y_{t+b} = \underline{\phi}_t \underline{\theta} + \varepsilon_{t+b} \tag{4.3.9}$$

Equation (4.3.9) admits linear least squares estimation which may be expressed recursively

$$\underline{\hat{\theta}}_t = \underline{\hat{\theta}}_{t-1} + \underline{K}_t (Y_t - \underline{\phi}_{t-b} \underline{\hat{\theta}}_{t-1}) \tag{4.3.10}$$

where $\underline{K}_t = \dfrac{\underline{P}_t \underline{\phi}_{t-b}^T}{1 + \underline{\phi}_{t-b} \underline{P} \underline{\phi}_{t-b}^T}$

The parameters after being updated at every sampling interval can be used in the control law

$$\nabla^d U_t = - \frac{\hat{\alpha}(z^{-1})'}{\hat{\beta}(z^{-1})} Y_t \tag{4.3.11}$$

4.3.2.2 Constrained STR

M.V. controller sometimes calls for excessively large variation in the manipulated variable. In situations where this manipulation is too severe, it is common practice to calculate control laws which minimize the variance of Y subject to a constraint on the variance of ∇U_t, that is to minimize

$$I_1 = E\{Y_t^2 + \xi''(\nabla^d U_t)^2\} \qquad (4.3.12)$$

However the solution required to solve this linear quadratic control problem needs spectral factorization [24], or the steady-state solution of a matrix Riccati equation [25].

An alternative and much simpler approach to constraining the variations in the manipulated variable has been proposed by Clarke and Hastrys-James [26] and Clarke and Gawthrop [26]. Rather than minimizing Equation (4.3.12), they treat the simpler problem of minimizing an instantaneous performance index

$$I_2 = \{\hat{Y}_{t+b/t}^2 + \xi' (\nabla^d U_t)^2\} \qquad (4.3.13)$$

where $\hat{Y}_{t+b/t}^2$ is the minimum variance forecast of Y_{t+b} made at time t.

Clarke and Gawthrop [20] proved that minimizing (4.3.13) is equivalent to minimizing

$$I_3 = E\{Y_{t+b} + \xi \nabla^d U_t\}^2 = E\{\phi_{t+b}\}^2 . \qquad (4.3.14)$$

where $\xi = \xi'/\omega_0$

The resulting controller can be shown [22] to be

$$\nabla^d U_t = \frac{-\alpha(z^{-1})}{\beta(z^{-1}) + \xi \delta(z^{-1})\theta(z^{-1})} Y_t$$

$$= -\frac{\delta(z^{-1}) T(z^{-1})}{\omega(z^{-1})\psi_1(z^{-1})\phi(z^{-1}) + \xi \delta(z^{-1})\theta(z^{-1})} Y_t \qquad (4.3.15)$$

ξ is a tuning parameter. If $\xi = 0$, a M.V. controller without constraint is obtained. Note that $\xi = \xi'/\omega_0$ and since ξ' is positive, the sign of ξ must be that of ω_0.

4.3.3 Application to the Fluidized Bed Reactor

4.3.3.1 Control of the Reaction Temperature

In the fluidized bed reactor a self-tuning regulator was first implemented on the inner temperature loop since the performance of this loop was observed to change with time and with process conditions, and it also strongly affects the selectivity controller. The performance index upon which the controller was based was the constrained one-step ahead criterion [20].

$$\underset{U_t}{\text{Min}} \quad E \sum_{j=t}^{t} [(T_R - T_R^{set})^2_{j+1} + \xi \, \nabla U_j^2] \qquad (4.3.16)$$

where U_t is the hydrogen-to-butane feedrate ratio and ∇U_t is the change in the ratio.

In developing a control model for the reaction temperature, the following reasonable assumptions may be made:

    (i) a first-order transfer function with no delay is a reasonable approximation for the reactor temperature dynamics,

    (ii) the major disturbances to the inner (temperature-control) loop were white measurement noise, and

    (iii) step disturbances in the temperature setpoint were called

        for every 6 minutes by the outer loop selectivity controller.

Using these assumptions, the process described by Equation (4.3.2) can be represented by:

$$Y_{t+1} = \frac{\omega_0}{1 - \delta z^{-1}} U_t + \frac{1 - \theta z^{-1}}{1 - z^{-1}} a_{t+1} \qquad (4.3.17)$$

As illustrated in Appendix B.4.1, the orders ℓ, m, b and d were determined to be $\ell = m = 1$, $b = d = 1$. This means that the optimal (in

the sense that the output variance is minimized) constrained controller structure would be of the form:

$$\beta_0 \nabla U_t = \beta_1 \nabla U_{t-1} + \alpha_0 (T_R - T_R^{set})_t + \alpha_1 (T_R - T_R^{set})_{t-1} \quad . \qquad (4.3.18)$$

where u_t is the hydrogen-to-butane feedrate ratio and ∇u_t is the change in this ratio from the previous control time to the present one.

Furthermore, the reactor temperature can be expressed in terms of the input as in Equation (4.3.9)

$$(T_R - T_R^{set})_t = -\alpha_0 (T_R - T_R^{set})_{t-1} - \alpha_1 (T_R - T_R^{set})_{t-2} + \beta_0 \nabla U_{t-1}$$

$$- \beta \nabla U_{t-2} + e_t \qquad (4.3.19)$$

The controller parameter vector $\underline{\theta}$ was estimated using the exponentially discounted recursive least squares algorithm [18]

$$\hat{\underline{\theta}}_t = \hat{\underline{\theta}}_{t-1} + \underline{K}_t (Y_t - \underline{\phi}_{t-1} \cdot \hat{\underline{\theta}}_{t-1}) \qquad (4.3.20)$$

where
$$\underline{K}_t = \frac{\underline{P}_t \, \underline{\phi}_{t-1}^T}{FLAM + \underline{\phi}_{t-1} \, \underline{P}_{t-1} \, \underline{\phi}_{t-1}^T} \qquad (4.3.21)$$

and
$$\underline{P}_t = \frac{1}{FLAM} \left(\underline{P}_{t-1} - \frac{\underline{P}_{t-1} \, \underline{\phi}_{t-1}^T \, \underline{\phi}_{t-1} \, \underline{P}_{t-1}}{FLAM + \underline{\phi}_{t-1} \, \underline{P}_{t-1} \, \underline{\phi}_{t-1}^T} \right) \qquad (4.3.22)$$

$FLAM \leq 1.0$, is the exponential discounting factor in the recursive least squares algorithm to allow the controller to track changing parameters.

4.3.3.2 Control of the Propane Selectivity

As mentioned earlier in Section 4.1, the primary control objective is propane selectivity control. Again the Clarke and Gawthrop[20] method is used to minimize the instantaneous performance index:

$$\text{Min}_{T_R^{set}} \quad E \sum_{j=t}^{t} [(S_3 - S_3^{set})_{j+1}^2 + \xi \, \nabla(T_R^{set})_j^2 \,] \qquad (4.3.23)$$

As explained previously in Section 4.2, the closed-loop response of the selectivity loop can be specified to resemble a first-order plus dead-time process, where the dead-time was 360 s. By a similar derivation, as in that presented in Section 4.3.3.1, the optimal controller structure of the outer STR would be of the form

$$\beta_0 \nabla(T_R^{set})_t = \beta_1 \nabla(T_R^{set})_{t-1} + \alpha_0(S_3 - S_3^{set})_t$$
$$+ \alpha_1(S_3 - S_3^{set})_{t-1} \qquad (4.3.24)$$

The selectivity expressed in terms of the reactor temperature setpoint is

$$(S_3 - S_3^{set})_t = -\alpha_0(S_3 - S_3^{set})_{t-1} - \alpha_1(S_3 - S_3^{set})_{t-2}$$
$$+ \beta_0 \nabla(T_R^{set})_{t-1} - \beta_1 (T_R^{set})_{t-2} + e_t \qquad (4.3.25)$$

Again, the estimates of the parameters α_0, α_1, β_0 and β_1 can be updated at each time instant by a recursive least squares algorithm using equation (4.3.25) and then used in euqation (4.3.24) to calculate the current control action. An exponential discounting factor used in the recursive least squares algorithm will further allow the controller to track changing parameters.

5. SIMULATION STUDIES ON THE REACTOR SYSTEM

5.1 Introduction

In this pilot scale fluidized bed reactor system, complex and highly exothermic hydrogenolysis reactions are taking place. For this reason, the dynamic simulation model for the reactor system, as described in Chapter 3, was used to study the system before the experimental studies were performed.

The objective of this simulation study was to investigate:

(1) the sensitivity of the system response to the parameter values in the Dahlin controller on propane selectivity, given a proportional-integral (PI) controller on the reactor temperature in the inner loop of the cascade control system,

(2) the behaviour of the system when a self-tuning regulator (STR) is substituted for the PI controller in the inner loop, and

(3) the behaviour of the system when a STR was substituted for the Dahlin controller in the outer loop.

5.2 Computer Software for the Simulation

In order to accommodate the simulations indicated above, a calling program (DASTFF2) was written to call those subroutines (as discussed in Section 3.4.2) which are appropriate for the study of a given control scheme. The characteristic feature is that the program could be run interactively to allow the following options:

53

(a) Measurement noise could be included if desired.

(b) The inner and/or outer loop could be opened or closed.

(c) Any desired controller could be implemented in the inner and outer loop. This option provided flexibility in the choice of a PI or STR controller on the inner loop and a Dahlin or STR controller on the outer loop.

As shown in the flow chart in Figure 5.1, the program begins with the initialization of constants/parameters and definition of the input variables to subroutine MODEL1 which, in turn, integrates the reactor variable equations from t_n to t_{n+1}. It then enters into the various control option specifications. Process measurement noise can be added. Inner control loop options include no control, using PI controller or the STR for the temperature control while the outer loop can have the option of no control, implementing Dahlin algorithm or STR to control propane selectivity. For all closed loop runs, the control signals are contrained to conform to the physical limitations of the reactor system.

After each integration step, the reactor and controller (if any) variables of interest are stored in a data file to be used in a plotting routine. At the end of the desired number of integration steps, the variables of interest for each run are printed. A plotting program STPLT2 is used to plot the variables. Listings of the calling program DASTFF2 and the plotting program STPLT2 are included in Appendices C.5.1 and C.5.2 respectively.

5.3 Results of the Simulation Runs

5.3.1 Introduction

The cascade control configuration used in this study is shown in

START

INITIALIZE
CONSTANTS

DEFINE NUMBER OF
INTEGRATION STEPS

DEFINE INPUTS, DESIRED
CONTROLLER SETPOINTS

A

CALCULATE OUTPUTS
FROM MODEL1

MEASUREMENT NOISE TO BE
ADDED ?

YES

NO

INNER
CONTROL LOOP
OPTION

OUTER
CONTROL LOOP
OPTION

ITI=0   NO CONTROL

ITI=1   PI

IST=1   STR

IOP=0   NO CONTROL

IOP=1   PI

IOP=2   STR

B
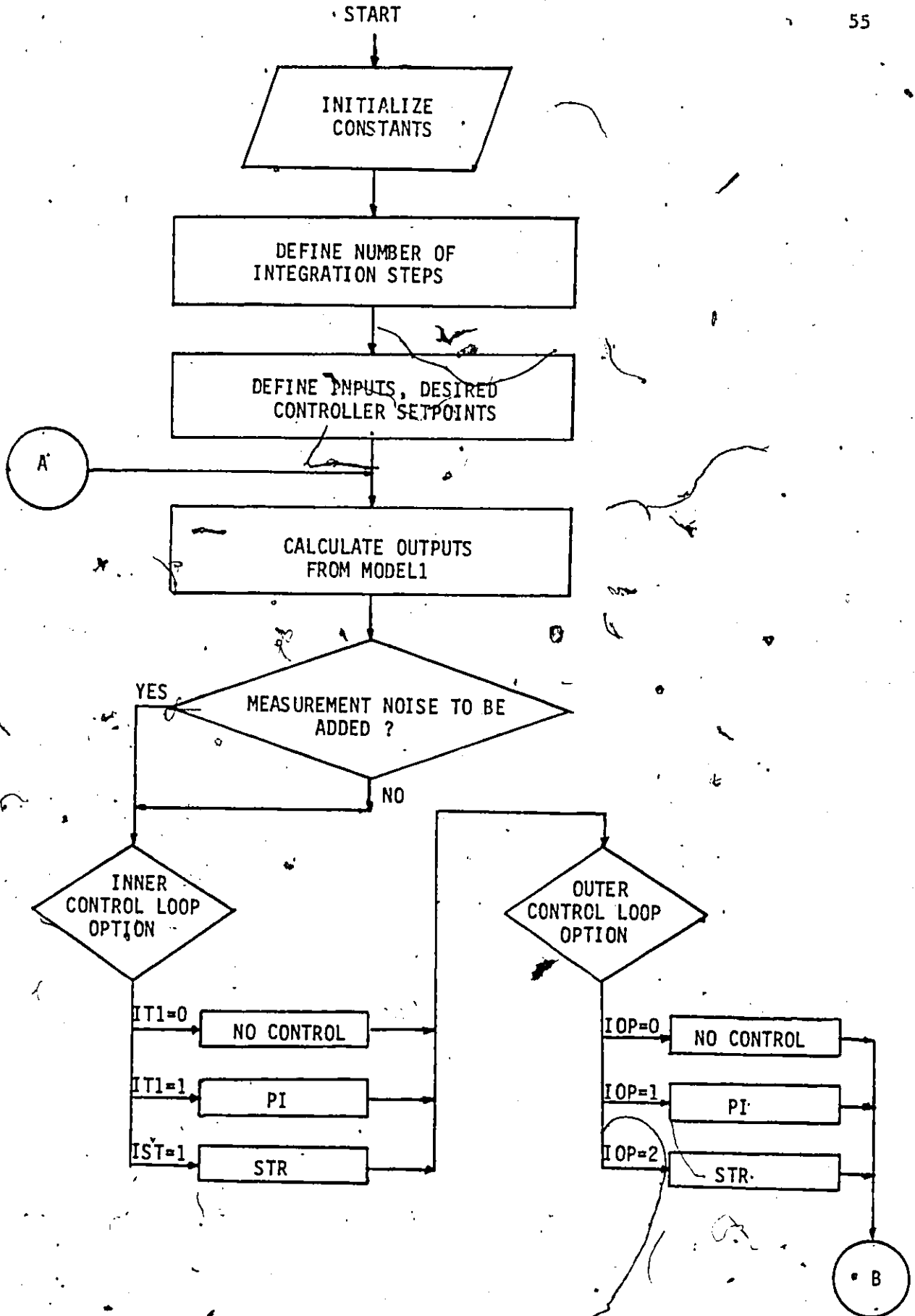
Figure 5.1 Flow Chart for Computer Calling Program DASTFF2

Figure 5.1 (cont'd)
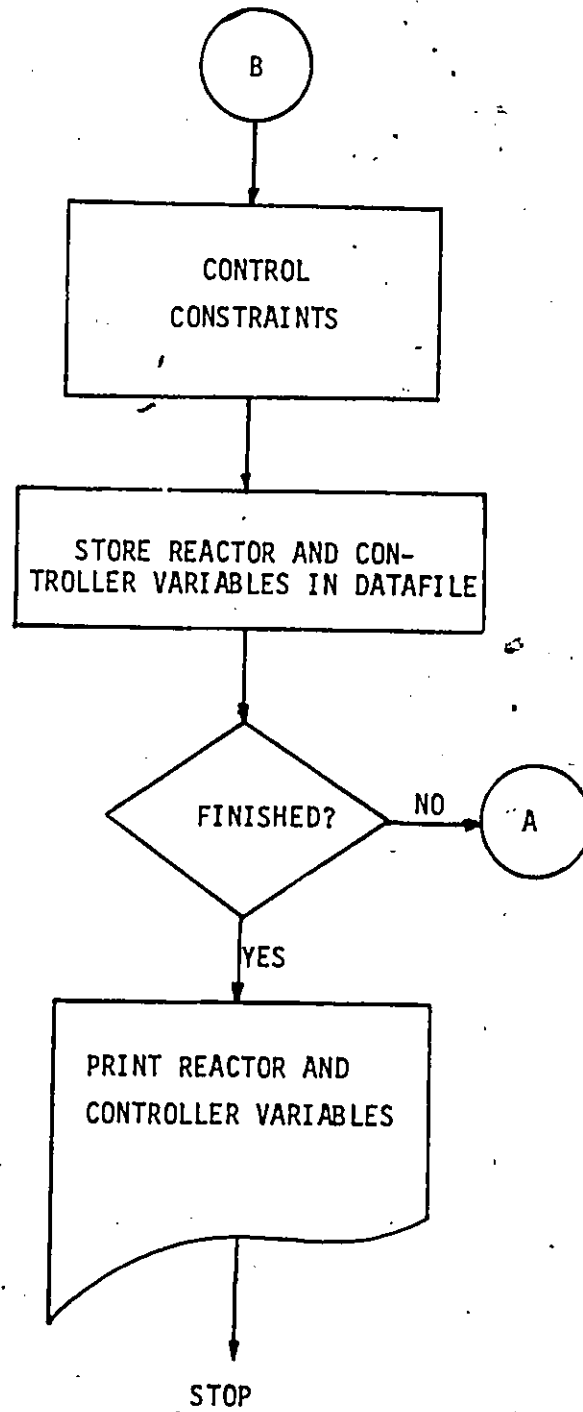
Figure 2.1 and different control methods have been discussed in Chapter 4. This section presents the results of the dynamic simulation described in Chapter 3 using the various controllers. In all the simulation runs, a measurement error $\sim N(0, .1^2)$ was added to the predicted response of reactor temperature, and to the response of propane selectivity was added an error $\sim N(0, .002^2)$.

5.3.2 Dahlin + PI

Throughout all the reported simulations, total volumetric feed-rate of hydrogen and butane combined and oil inlet temperature were constant at $0.1 \text{ m}^3/\text{min}$ (S.T.P.) and 247°C respectively. The tuning parameters of the PI algorithm, $K_p = 1.03$ and $K_I = 0.34$ were used for the inner temperature loop. As for the Dahlin controller implemented in the outer selectivity loop, the gain $K = -0.022$ was used and τ and λ were allowed to vary to determine the sensitivity of the system to these parameter values.

Three sets of τ and λ values were chosen to further investigate the performance of the cascaded Dahlin and PI controllers. They were $\tau = 250$, $\lambda = 350$; $\tau = 250$, $\lambda = 500$ and $\tau = 450$, $\lambda = 500$ as shown in Figures 5.2, 5.3 and 5.4 respectively. The choice of these three sets of values originated from the fact that τ and λ were thought to be under-specified in previous work [4]. It should be noted that all the graphs which are to be presented in this thesis will have the same format with the different variables of interest plotted versus the number of control intervals. This control interval refers to the time interval between control action on the reactor temperature (inner loop) which, for the experimental system, was 30 s. Thus, 240 control intervals represent a

time elapse of two hours. In the temperature plot, the top solid curve

gives the reactor temperature response T_R; the dotted lines represent

the setpoints T_R^{set} which are the outputs from the outer loop controller

(Dahlin or STR); and the bottom curve is the inlet temperature ($T_{oil,in}$)

of the cooling oil for the reactor. The second and third plot responses

of the butane conversion and propane selectivity (S_3), respectively.

Propane selectivity was the controlled variable; its desired value

(S_3^{set}) is indicated by dotted lines on the third plot and was preset at

any desired value by the operator. The last plot shows the response of

the manipulated variable, the ratio of hydrogen-to-butane feedrates

u_{H_2}/u_{C_4}.

In the set of graphs shown in Figure 5.2, the selectivity setpoint

was changed in a series of steps in the order: 0.32, 0.25, 0.32, 0.36

and 0.40. This was the range of selectivities expected during the

actual experimental runs.

It should be noted that only during simulation studies can the

S_3 response be predicted using the model in between the sampling interval

(6 minutes) of the selectivity loop. And the heavy dots on the graphs

of T_R, S_3 and u_{H_2}/u_{C_4} indicate the time when a chromatographic sample is

taken.

Figures 5.2, 5.3 and 5.4 indicate the responses of the system for

the same S_3 setpoint changes but with different values of the Dahlin

parameters τ and λ. Looking at these results, it is obvious that the

results in Figure 5.3 ($\tau = 250$, $\lambda = 500$) give the best response to

changes in S_3 setpoint. Using $\lambda = 350$ as in Figure 5.2 gave a similar

S_3 response but required greater variations in u_{H_2}/u_{H_4}. These responses

for $\lambda \geq 350$ appear to represent a considerable improvement over that
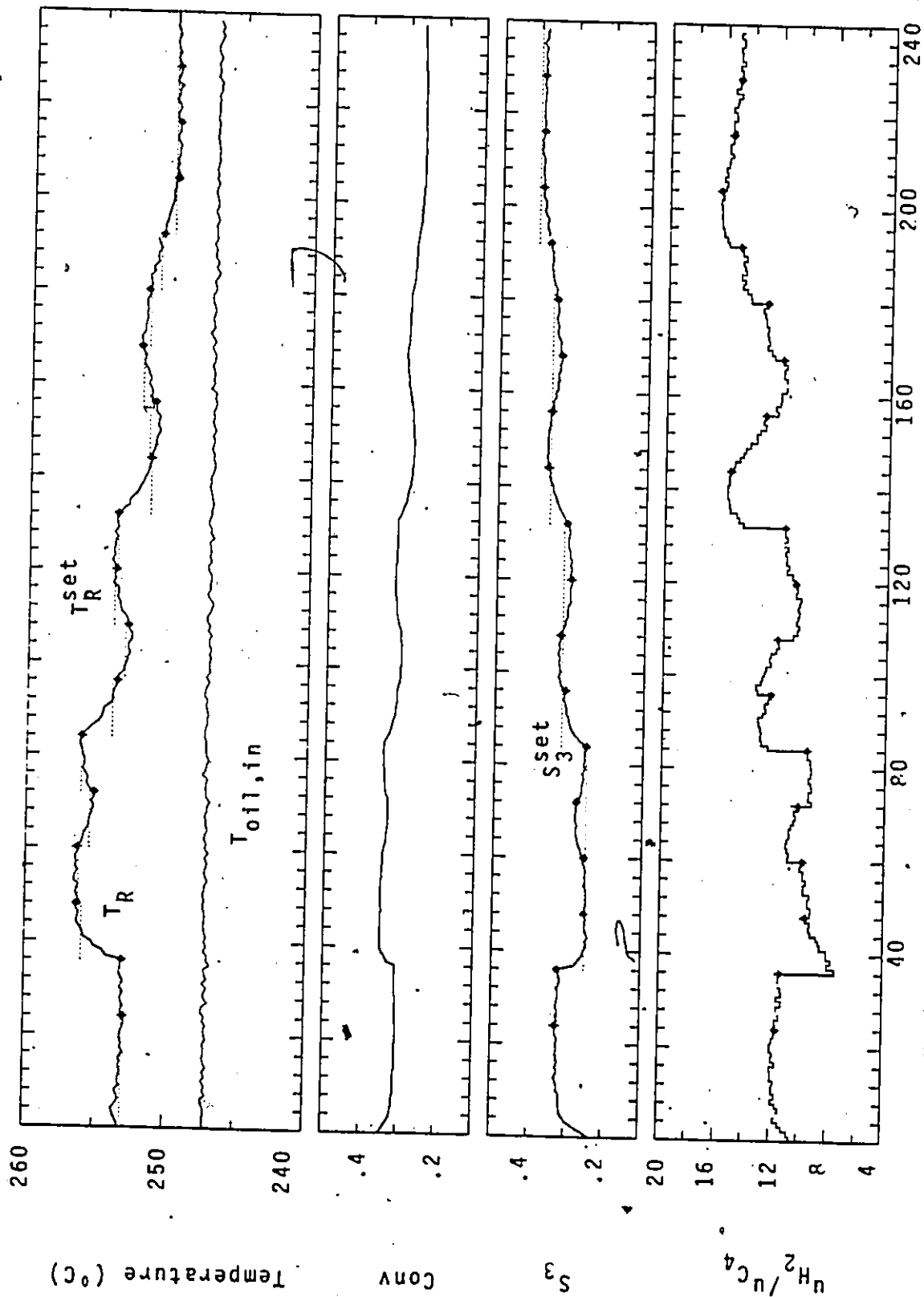
Figure 5.2 Dahlin($\tau=250,\lambda=350$) + PI cascade controller performance responding to a series of selectivity setpoint changes (Simulation)
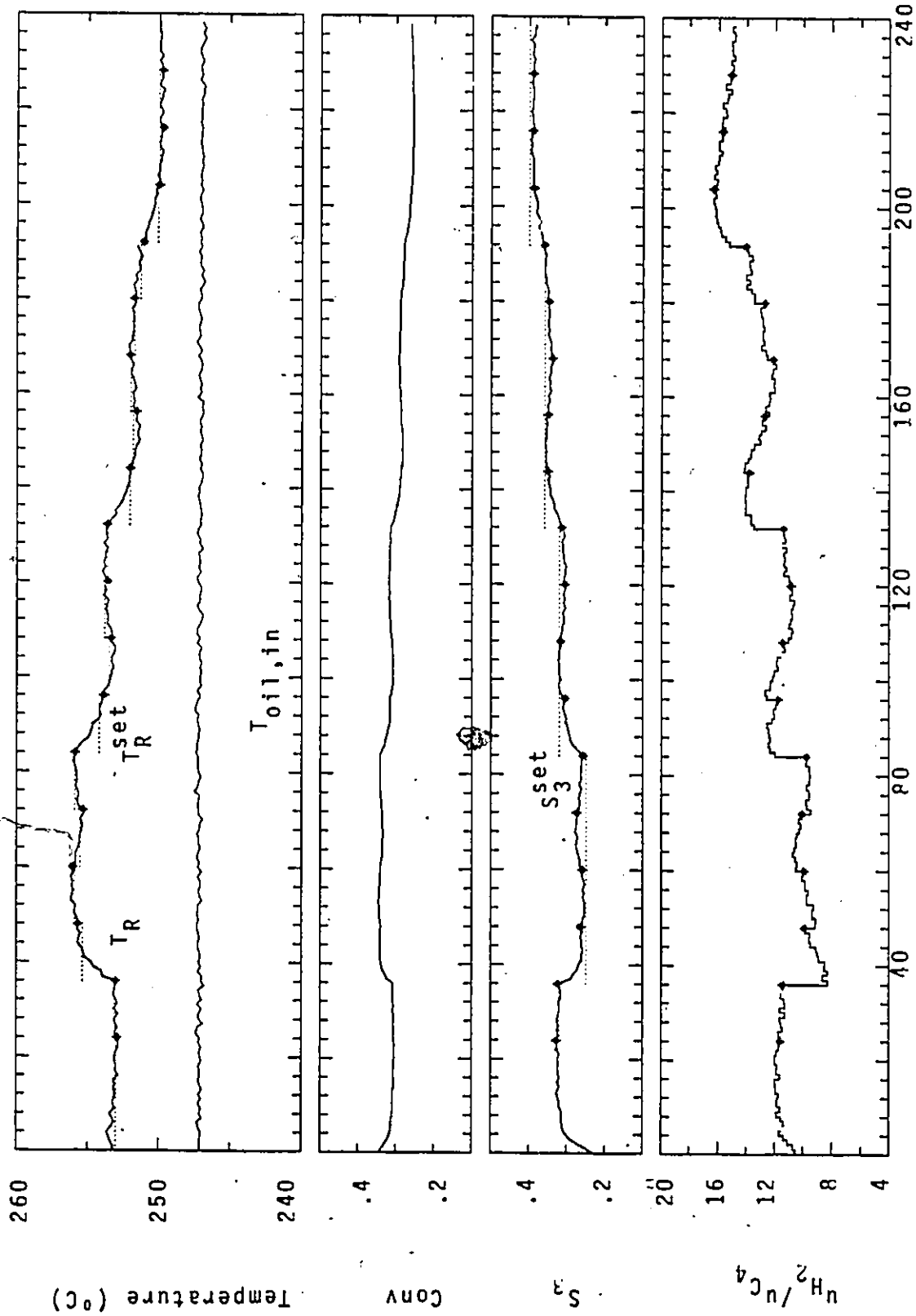
Figure 5.3 Dahlin($\tau=250,\lambda=500$) + PI cascade controller performance responding to a series of selectivity setpoint changes (Simulation)

61
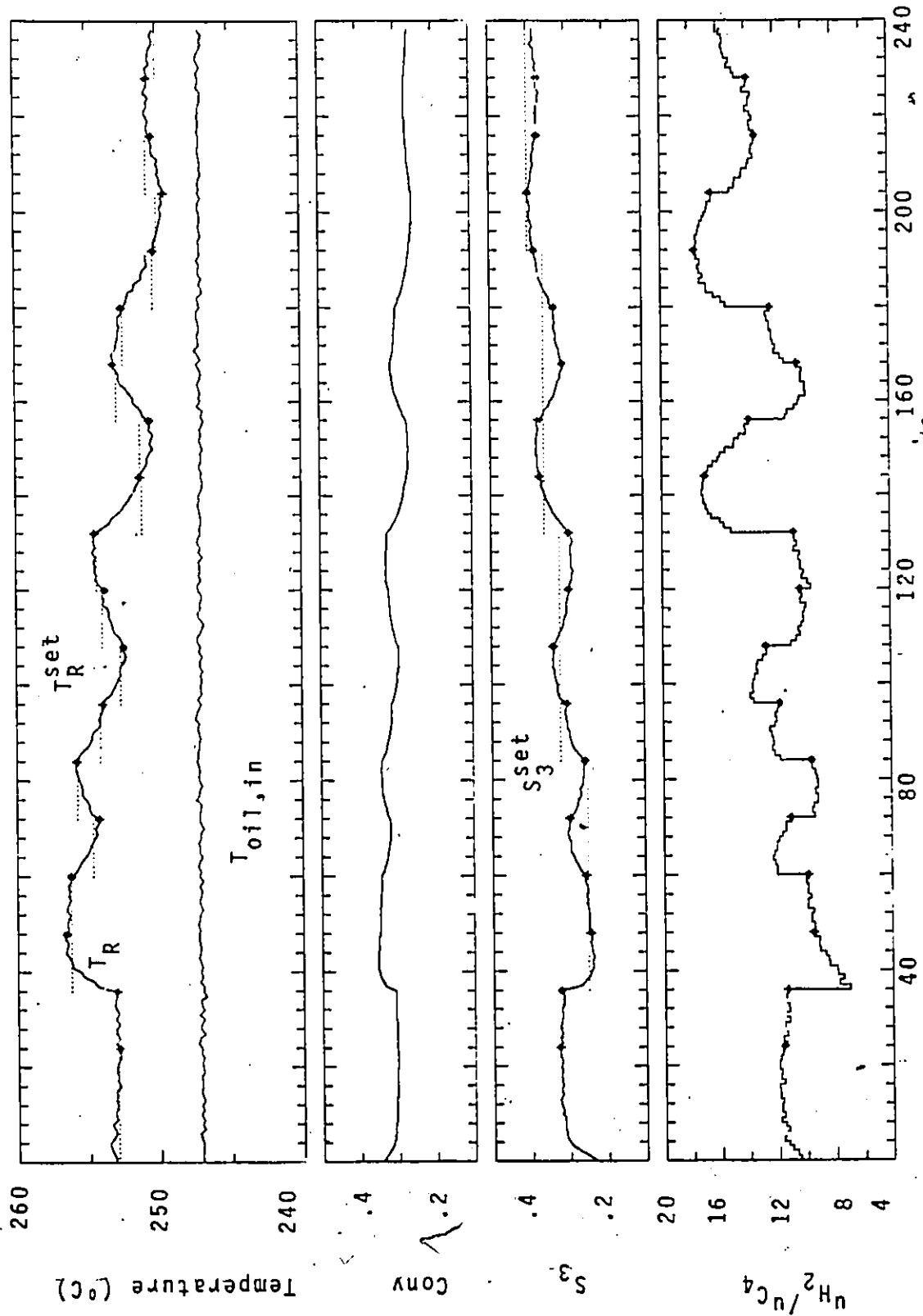
Figure 5.4 Dahlin(τ=450,λ=500) + PI cascade controller performance responding to a series of selectivity setpoint changes (Simulation)

obtained in previous work [4] with smaller λ's. This implies that the model mismatch was probably too great to demand reasonable responses from the system. This is further illustrated in Figure 5.4 when τ was increased to 450 ($\tau = 250$ being more realistic). There even with $\lambda = 500$ the model mismatch had become severe enough that oscillations had set in.

The simulation results in Figure 5.5 show the performance of the detuned Dahlin ($\tau = 250$ and $\lambda = 500$) plus PI cascade controller responding to a change in S_3^{set} from .32 to .27 and a load disturbance on the reactor wall by lowering the $T_{oil,in}$ from 247 to 242°C. The control system was well behaved.

As a setpoint change in S_3 was introduced, the Dahlin controller computed a new T_R^{set} for the reactor temperature controller which in turn calculated a new setpoint by the PI algorithm for the hydrogen-to-butane feed ratio. The u_{H_2}/u_{C_4} decreased instantaneously in order to raise the T_R. The S_3 stepped down smoothly to the new desired level.

Later on when the load disturbance occurred at A, the reactor temperature decreased in response to the decreased oil inlet temperature because the rate of heat transfer to the wall from the catalyst bed increased. A greater heat generation by the reaction was required to maintain reaction temperature; the temperature controller called for decreasing u_{H_2}/u_{C_4} which in turn, fell very quickly. This action caused the selectivity to drift off the target. On the other hand, a decrease in T_R^{set} was called for when the Dahlin controller realized the deviation of S_3 from its target and brought the S_3 back to the desired level after two sampling intervals. Note that the decrease in T_R^{set} was requested by
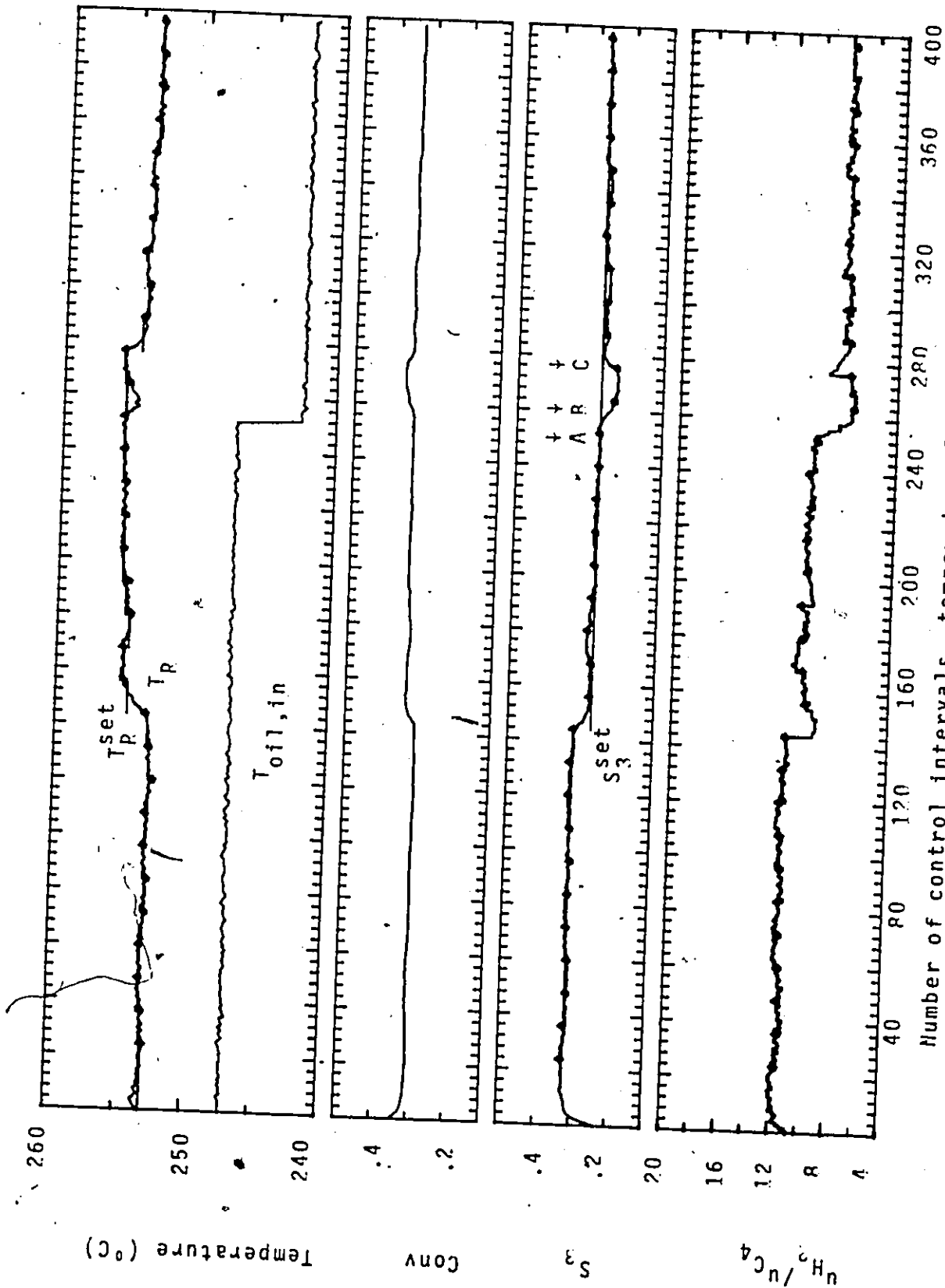
Figure 5.5 Dahlin(τ=250,λ=500) + PI cascade controller performance responding to a selectivity setpoint change and a load disturbance in $T_{oil,in}$ (Simulation)

the Dahlin algorithm at point C, two sampling intervals after the load disturbance had taken place. The reason for this becomes apparent when one realizes that the selectivity data on the graphs is plotted against the time at which the sample was taken; those data are not really available to the computer until six minutes later. Thus at the subsequent sampling point B, the Dahlin controller was comparing S_3^{set} with S_3 at point A and, finding no error, the controller did not take any action. It was not until the next sampling interval at C, that the Dahlin controller did detect an error and act accordingly.

In summary, this simulation suggests that the performance of the cascade control system with the tuning parameters $\tau = 250$, $\lambda = 500$, $K_p = 1.03$ and $K_I = 0.34$ is satisfactory.

5.3.3 Dahlin + STR

A self-tuning algorithm has been developed for the fluidized bed reactor as described in Section 4.3. Basically the algorithm can be divided into two parts at every sampling instant: (1) estimation of the new parameters in the control models and (2) implementation of appropriate control action. Before the self-tuning algorithm can be used, the constants and initial values listed below must be specified:

Model order	m, ℓ
Discounting factor	FLAM
Constraining factor	ξ
Initial parameter estimates	$\underline{\theta}_0$
Initial covariance matrix	$\underline{P}_0$
Scaling factor	β_0

The model structure of the controller was taken to be $m = \ell = 1$ as explained in Section 4.3.3.1. When the discounting factor, FLAM, in the recursive least squares (RLS) algorithm is less than 1.0, passed data is discounted exponentially as

$$\sum_{s=1}^{t} FLAM^{t-s} \epsilon_s^2$$

The effective time span (window length) over which data plays a role in the evaluation of the least squares is given by $1/(1-FLAM)$. Thus, decreasing FLAM from .99 to .95 decreases the effective number of obser- vations used in estimating the parameters from 100 to 20. The adaptation of the parameters although faster will then also be less smooth. There is no discounting of past data when FLAM = 1. Figures 5.6 (FLAM = 1.), 5.7b (FLAM = .98) and 5.8 (FLAM = .95) demonstrate the effects of varying FLAM on the controller parameters. The first two plots give the varia- tions in the STR parameter estimates and the last plot shows the behaviour of the pole of the controller when the system was subject to the same sequence of setpoint changes in S_3 as in Figure 5.2. Despite the signi- ficant differences in the three sets of parameters, the system responses in each case are nearly identical as shown in Figure 5.7a.

After initialization of the parameter estimating procedure (first four sampling periods), the controller parameters started adapting. The first setpoint change in S_3 at the 31st sampling instant led to the most severe changes in the parameters for FLAM = .95 (Figure 5.8). The parameters for FLAM = 1. (Figure 5.6) seemed to change hardly despite the fact that a series of setpoint changes in S_3 were later introduced. On the other hand, changes in parameter values were observed in the case
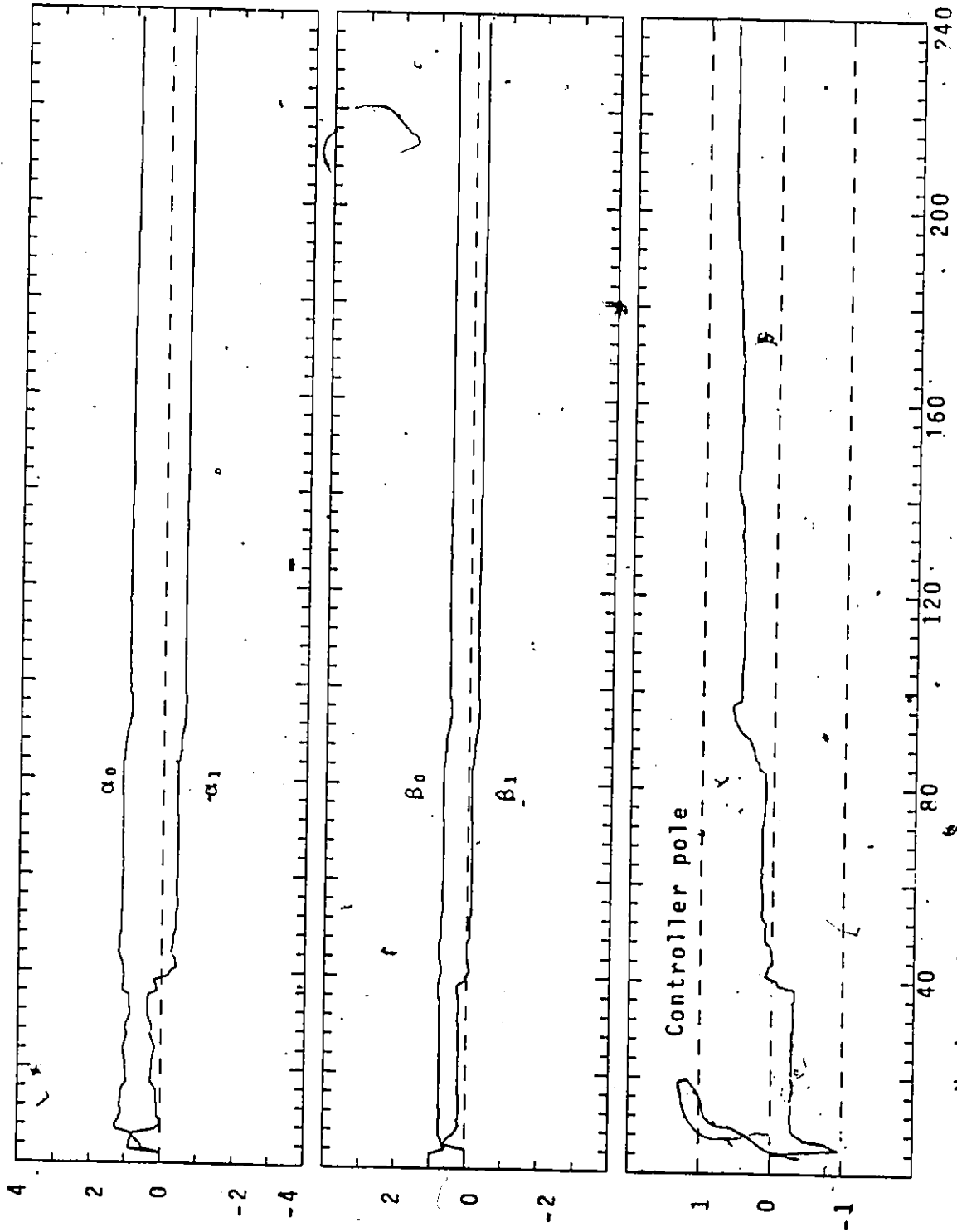
Figure 5.6   Parameter estimates and pole of the Inner STR when FLAM=1.0 (Simulation)

66
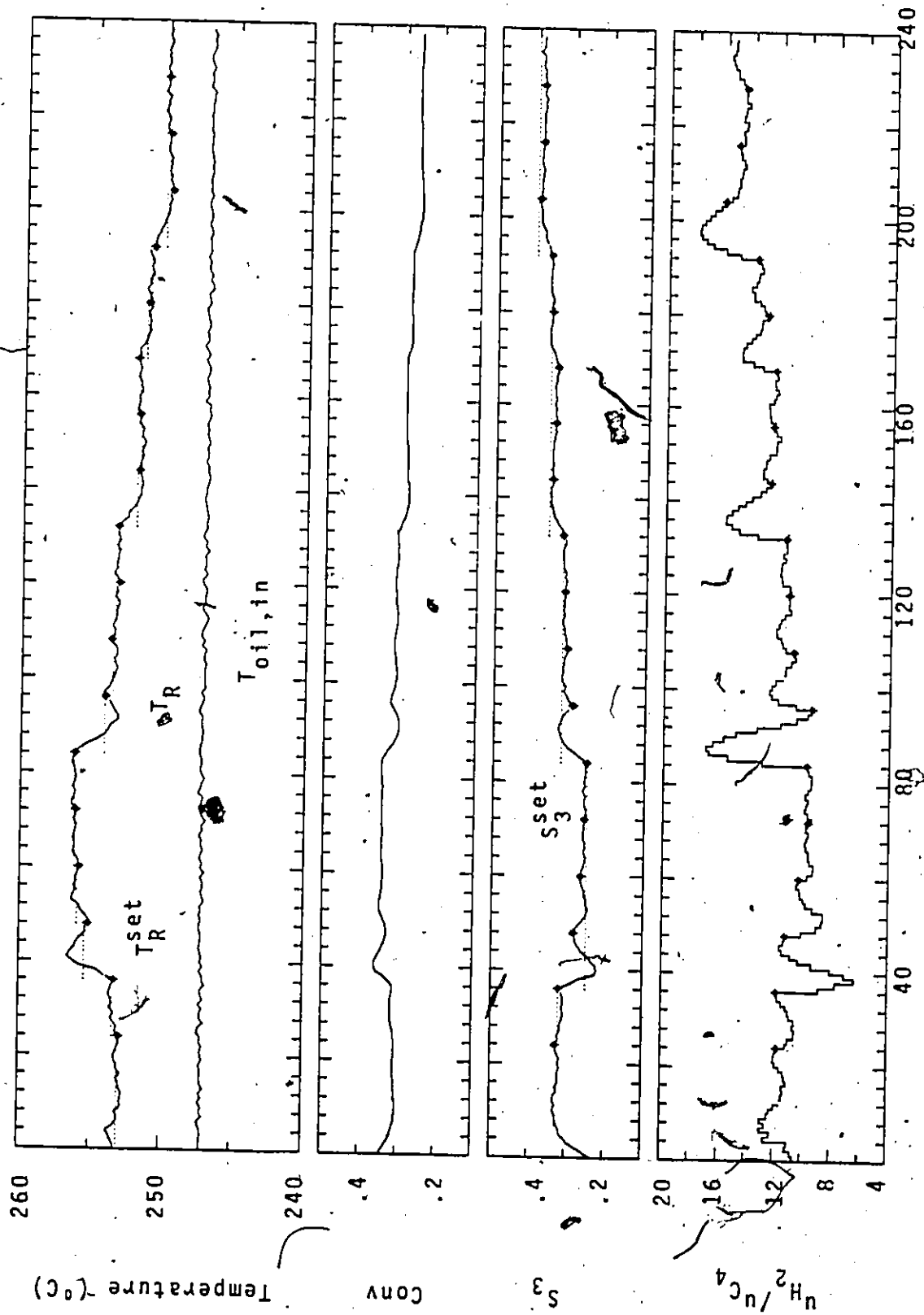
Figure 5.7a Dahlin + STR(FLAM=.98,ξ=.5) cascade controller performance (Simulation)
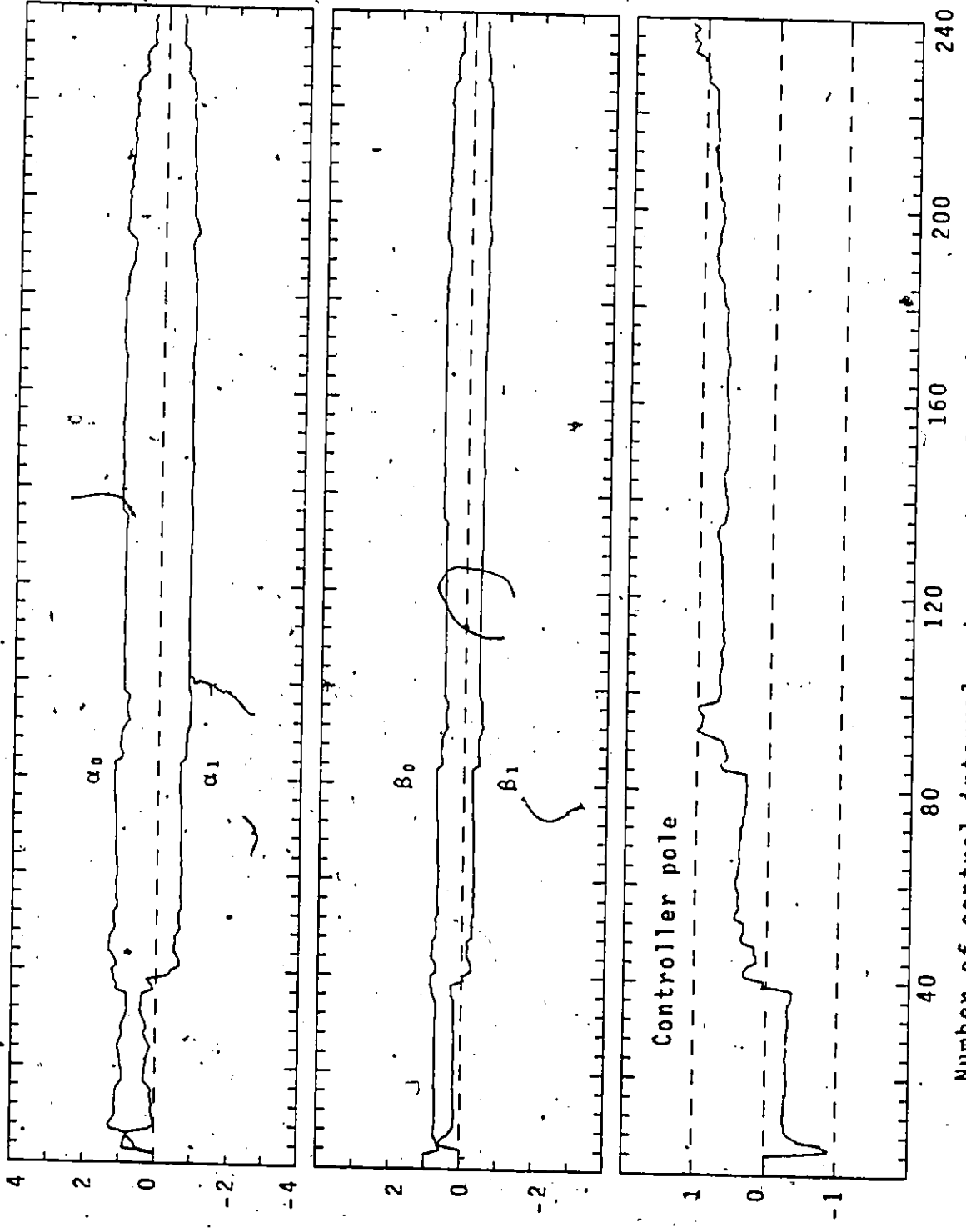
Number of control intervals, temperature loop (30 s)

Figure 5.7b Parameter estimates and pole of the inner STR when FLAH=.98,ξ=.5
(Simulation)

Figure 5.8 Parameter estimates and pole of the inner STR when FLAM=.95 (Simulation)
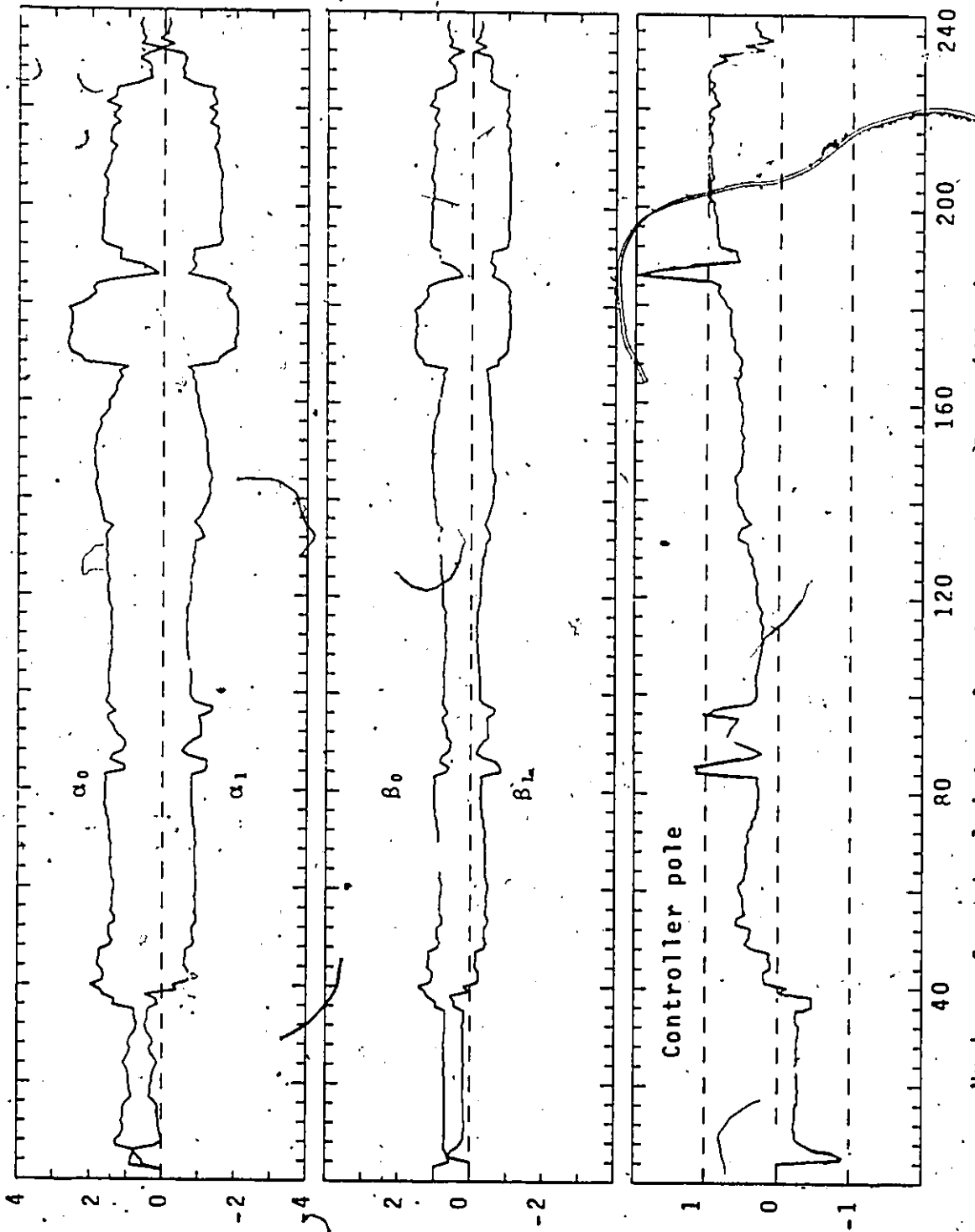
Number of control intervals, temperature loop (30 s)

of FLAM = .95. At some particular instants, the pole of the controller lay outside the unit circle but stability was achieved as these values moved quickly back into the unit circle (see lower plot of Figure 5.8). The behaviour of the parameters for FLAM = .98 gave intermediate responses between the two extreme cases. Since the performance of the system was basically insensitive to the values of FLAM in the simulation study, FLAM = .98 was used for the rest of the simulation runs.

The ξ in Equation (4.3.14) is a constraining factor used to weigh the past control actions. For $\xi = 0$, a minimum variance controller without constraint is obtained. The constraining factor is generally very effective in reducing the variance of the manipulated variable without significantly increasing the variance of the controller variable.

Figures 5.9 and 5.10 show the two cases of $\xi = .2$ and $\xi = 2$. respectively. These results are to be compared to Figure 5.7 with $\xi = .5$. The relatively unconstrained controller with $\xi = .2$ gave rise to large step changes in the manipulated variable u_{H_2}/u_{C_4} (Figure 5.9a). In effect tighter control was implemented on the reactor temperature. These excessive variations in the feedrate ratio upset the production rate of the desired products of reaction giving the oscillating behaviour of S_3. This response can be improved by increasing the ξ value to .5 as shown in Figure 5.7a. The consecutive changes in the feedrate ratio decreased in magnitude and the behaviour of the S_3 is more acceptable. However, further increasing the constraining factor to 2.0, the results as shown in Figure 5.10a indicate that the manipulated variable was so heavily constrained that it could not bring T_R to the appropriate setpoint in a reasonable time. In this case, the dynamics of the reactor temperature

71
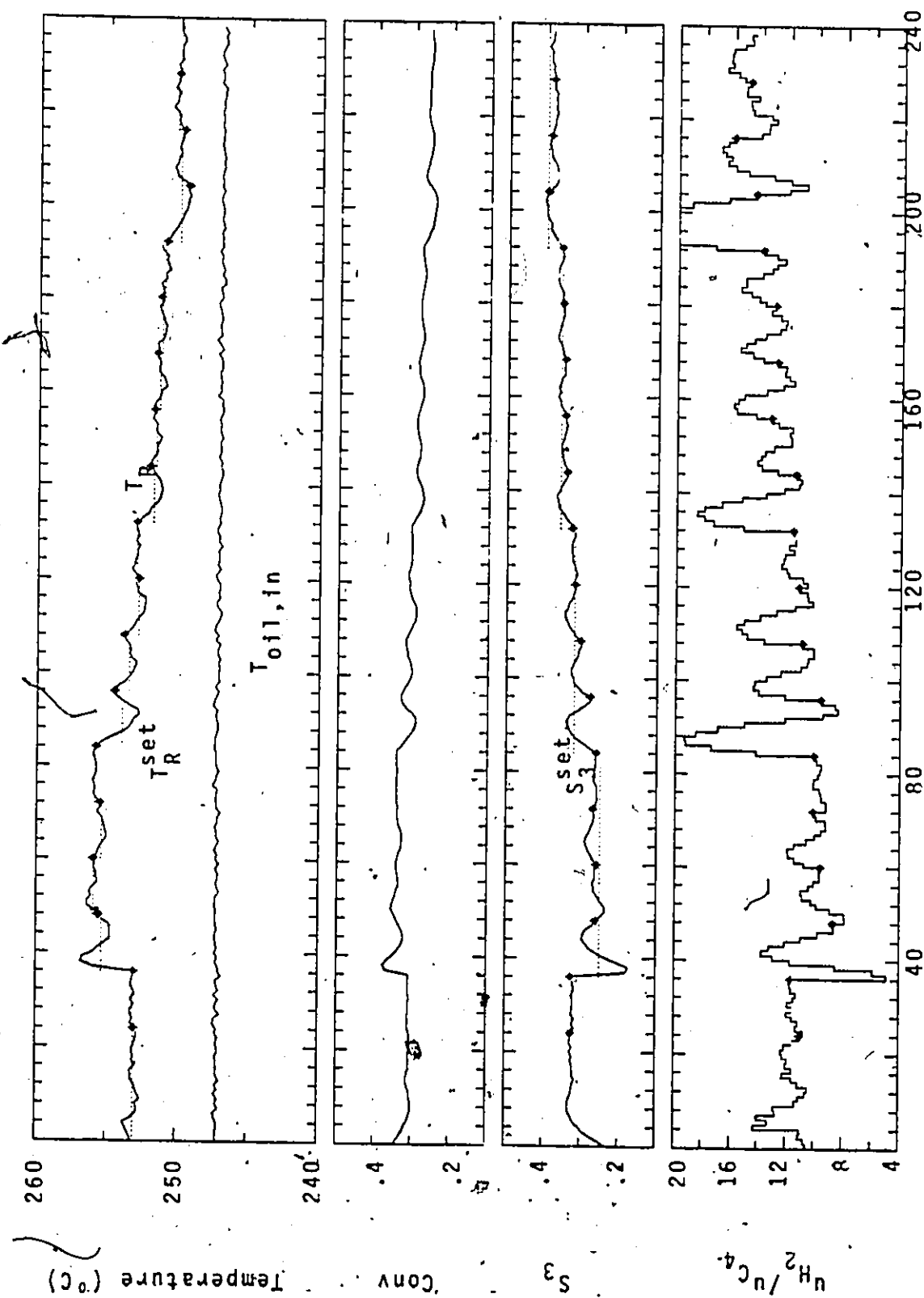
Figure 5.9a Dahlin + STR(FLAM=.98,ξ=.2) cascade controller performance
(Simulation)
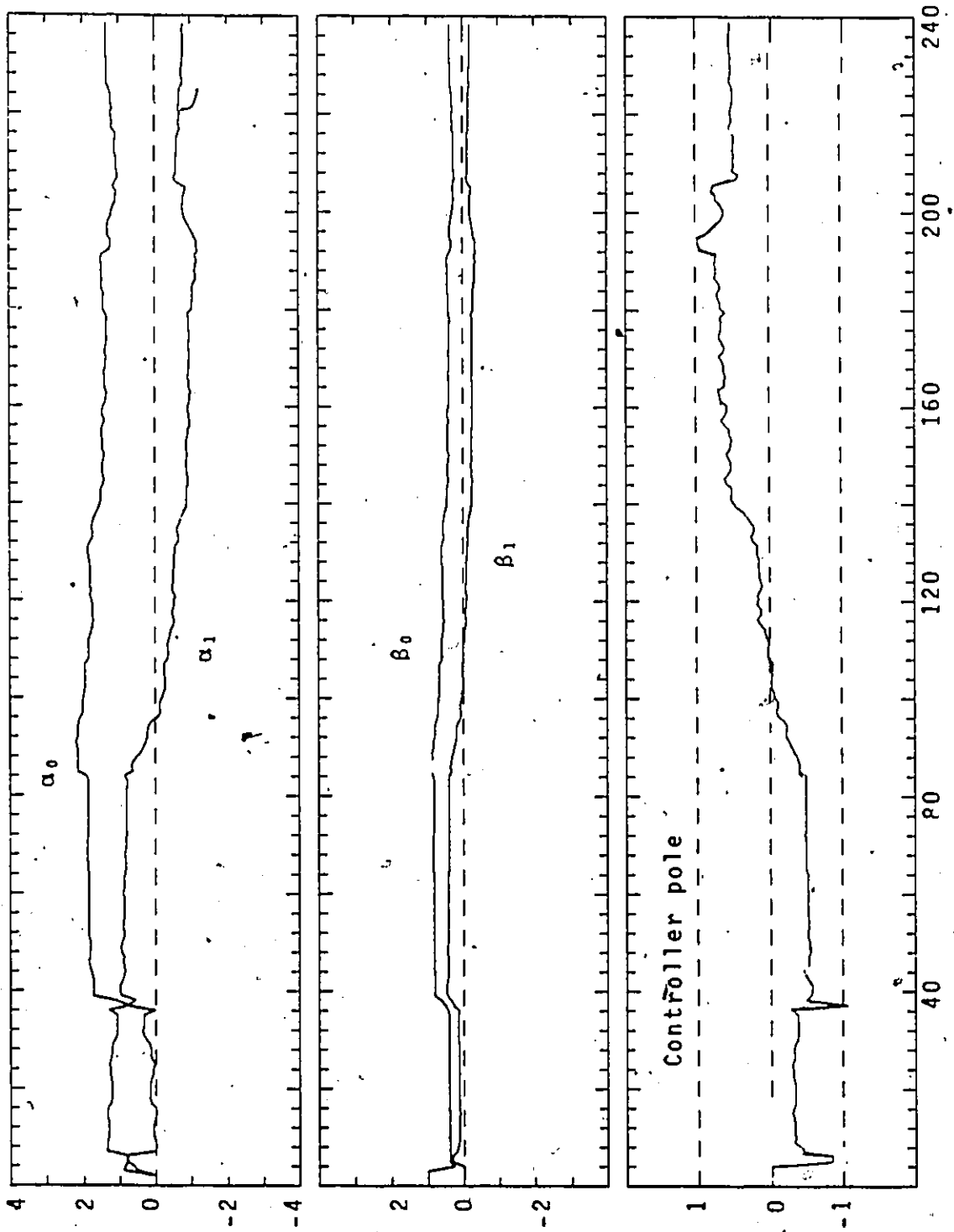
Figure 5.9b Parameter estimates and pole of the inner STR when $\xi = .2$ (Simulation)
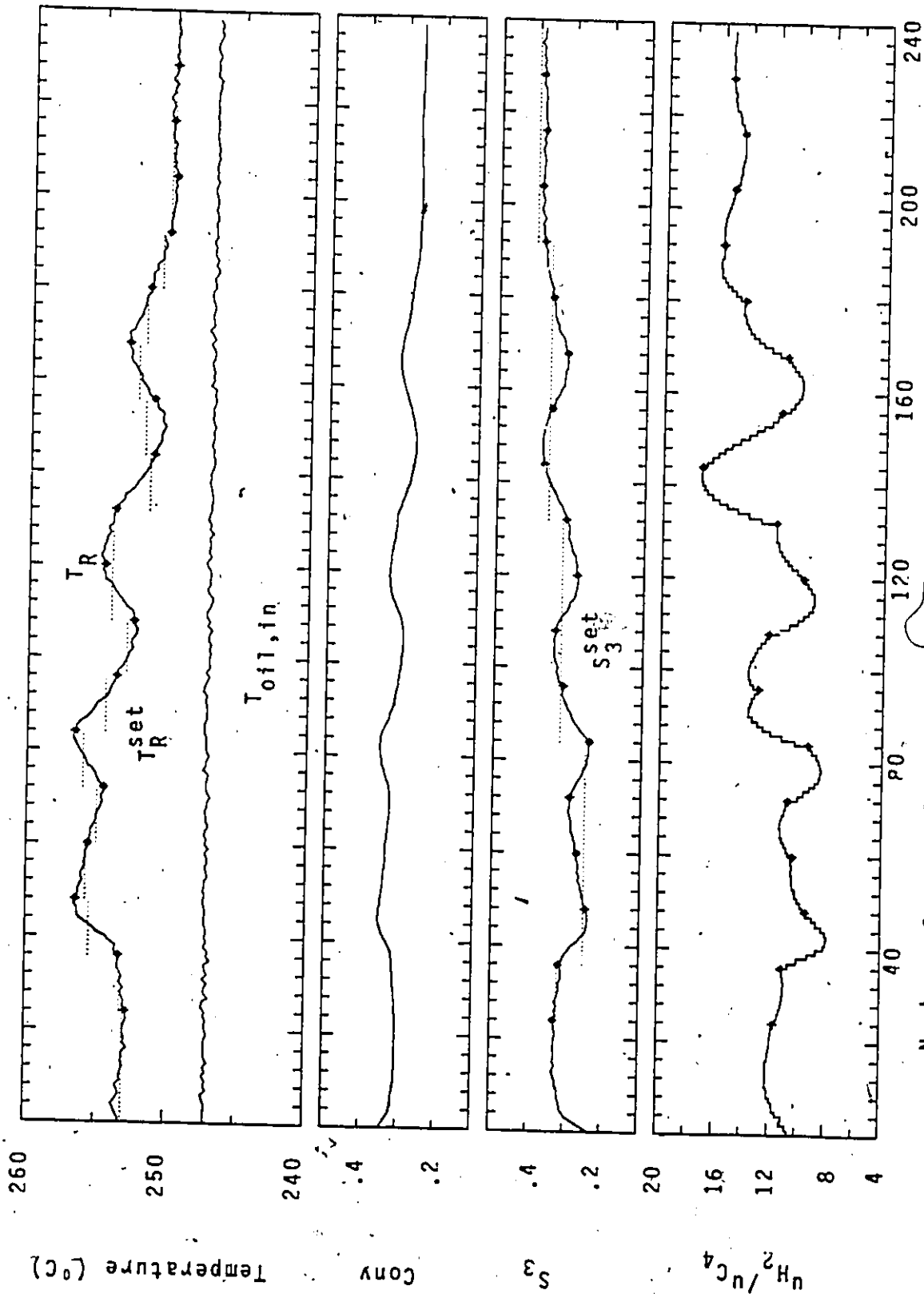
Figure 5.10a Dahlin + STR(FLAM=.98,ξ=2) cascade controller performance(Simulation)
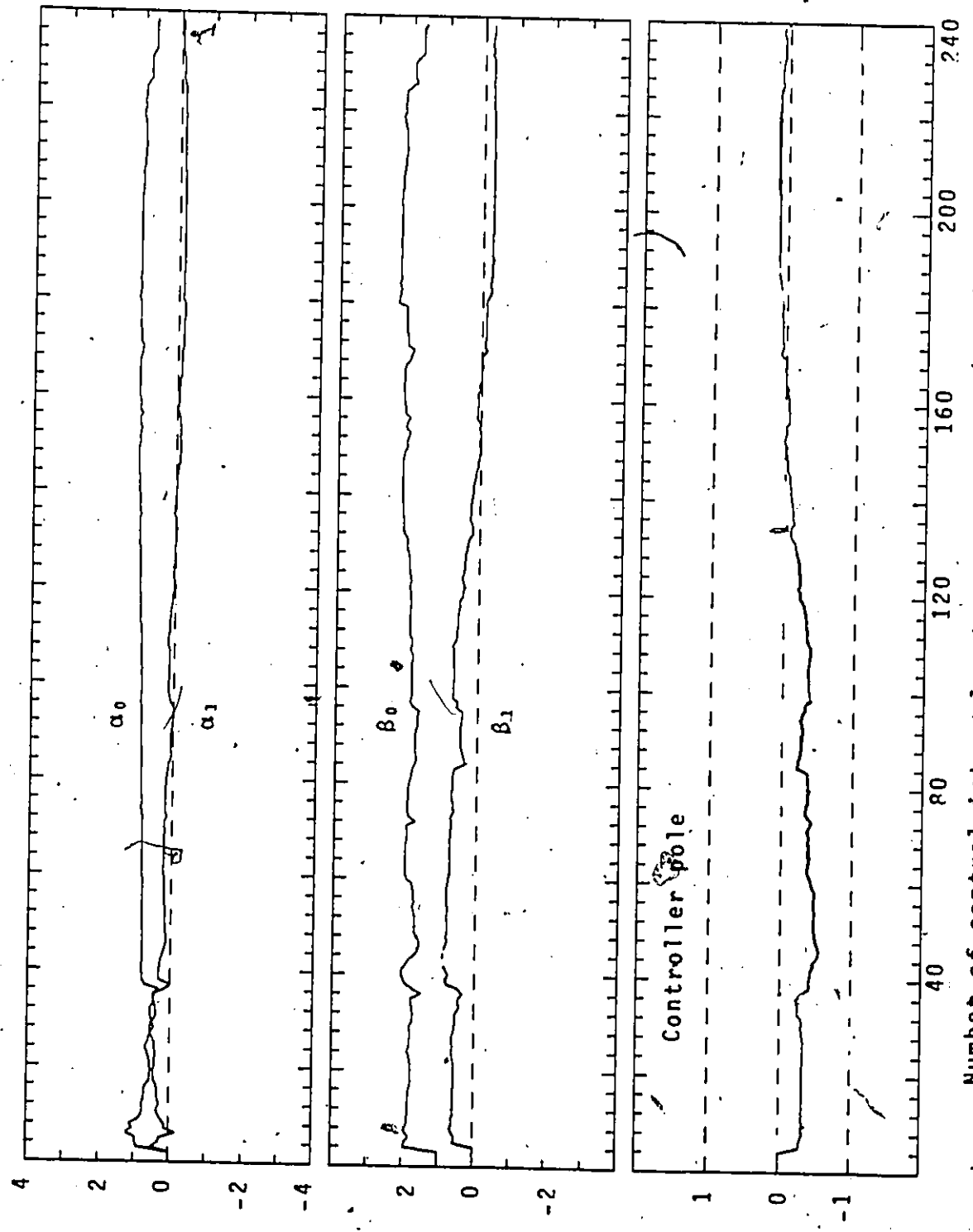
Number of control intervals, temperature loop (30 s)

Figure 5.10b Parameter estimates and pole of the inner STR when $\xi=2$. (Simulation)

were slowed to a great extent; consequently, oscillatory behaviour in S_3 was observed.

Initial choices of the parameters $\underline{\theta}_0$ and $\underline{P}_0$:

The initial parameter estimates $\underline{\theta}_0$ (except β_0), were chosen to be zero based on the assumption that prior information about the reactor system was unknown. However better initial guesses are possible by using the tuning parameters from the PI algorithm. The behaviour of the system and the responses of the controller parameters were found to be the same whether the initial value for the parameters were assumed to be zero (except $\beta_0 = 1$) or were taken as the PI tuning parameters.

At the same time initial estimates for $\underline{P}_0$ are needed to start the recursive estimation scheme. Since $\underline{\theta}_0$ represents the prior expectation of $\underline{\theta}$ and $\underline{P}_0$ represents a matrix proportional to the covariance matrix of the prior distribution of $\underline{\theta}$, one can either achieve very rapid updating under the situation of little prior knowledge using large values for $\underline{P}_0$ or very slow but smooth updating under the situation of substantial prior knowledge ($\underline{P}_0$ small). The choice of $100\underline{I}$ for $\underline{P}_0$ seems to be appropriate in this case (with no prior information).

For the scaling factor β_0, there is some controversy as to whether it should be constant. Poor guesses of a fixed β_0 can cause problems of system stability and poor convergence. However if β_0 is being estimated, poor behaviour can occur when the parameter converges to a wrong value or a singular estimation situation can arise when all the parameters converge. Here in the simulation runs β_0 was allowed to adapt in order to observe possible changes which might occur over the range of operation. Later, during the actual reaction runs as discussed in Chapter 6, β_0 is fixed because the initial parameter estimates are calcu-

lated from the operating PI tuning parameters and β_0 in that case can be considered as a good estimate. This procedure should avoid any problems of stability or convergence.

The results in Figure 5.11a show an identical simulation run as in Figure 5.5. In this case the difference is that the PI controller on the inner temperature loop was replaced by a self-tuning regulator (STR) while the previously described detuned Dahlin algorithm ($\lambda = 500$, $\tau = 250$) was used on the outer loop for selectivity control. For the STR, the constraining factor, ξ, and the least squares discounting factor FLAM were set equal to 0.5 and 0.98 respectively.

On a setpoint change in S_3, the controller gave an initial over-shoot in T_R but kept close to the target until a load disturbance on the reactor occurred. The STR had tuned itself in to provide comparable control as in the PI case in Figure 5.5a. Starting off with initial parameter estimates of zero for all parameters except for β_0 which was taken as unity, the variations in the controller parameter estimates are shown in Figure 5.11b.

5.3.4 STR + STR

Figure 5.12a shows the same simulation run using a double STR configuration for both the inner and outer loops. The inner STR had the same tuning parameters as the one referred to in Figure 5.11 under Section 5.3.3. The structure of the outer STR was taken to be $m = \ell = 1$ as described in Section 4.3.3.2. The constraining factor $\xi = .5$ and least square discounting factor FLAM = .98 were the same as those used in inner STR. The initial parameters were based on the values calculated from the Dahlin algorithm ($\alpha_0 = 6.$, $\alpha_1 = 1.4$, $\beta_0 = .2$, $\beta_1 = .1$). Since these
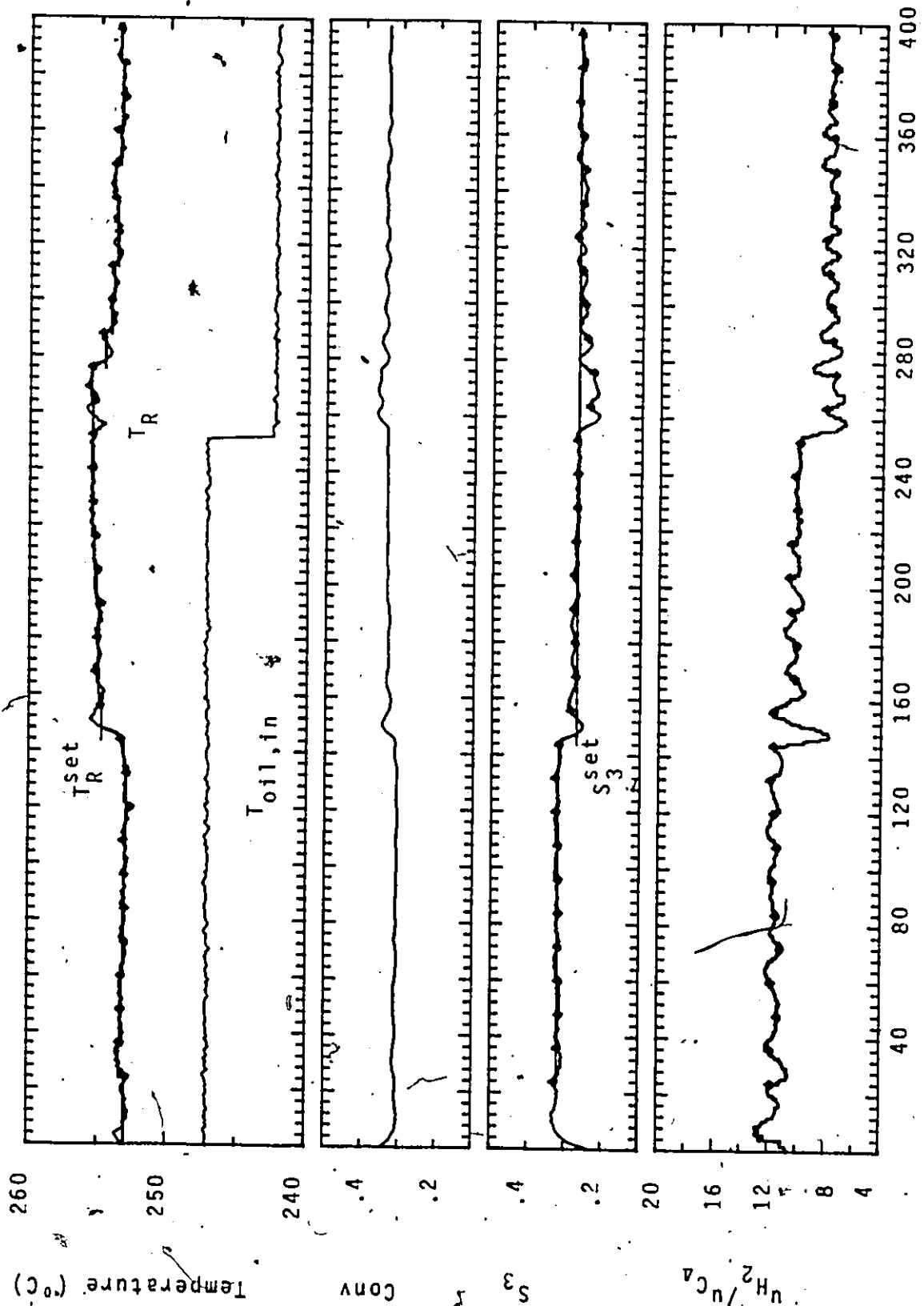
Figure 5.1ïa Dahlin + STR(FLAM=.98,ξ=.5) cascade controller performance responding to a selectivity setpoint change and a load disturbance in $T_{oil,in}$ (Simulation)
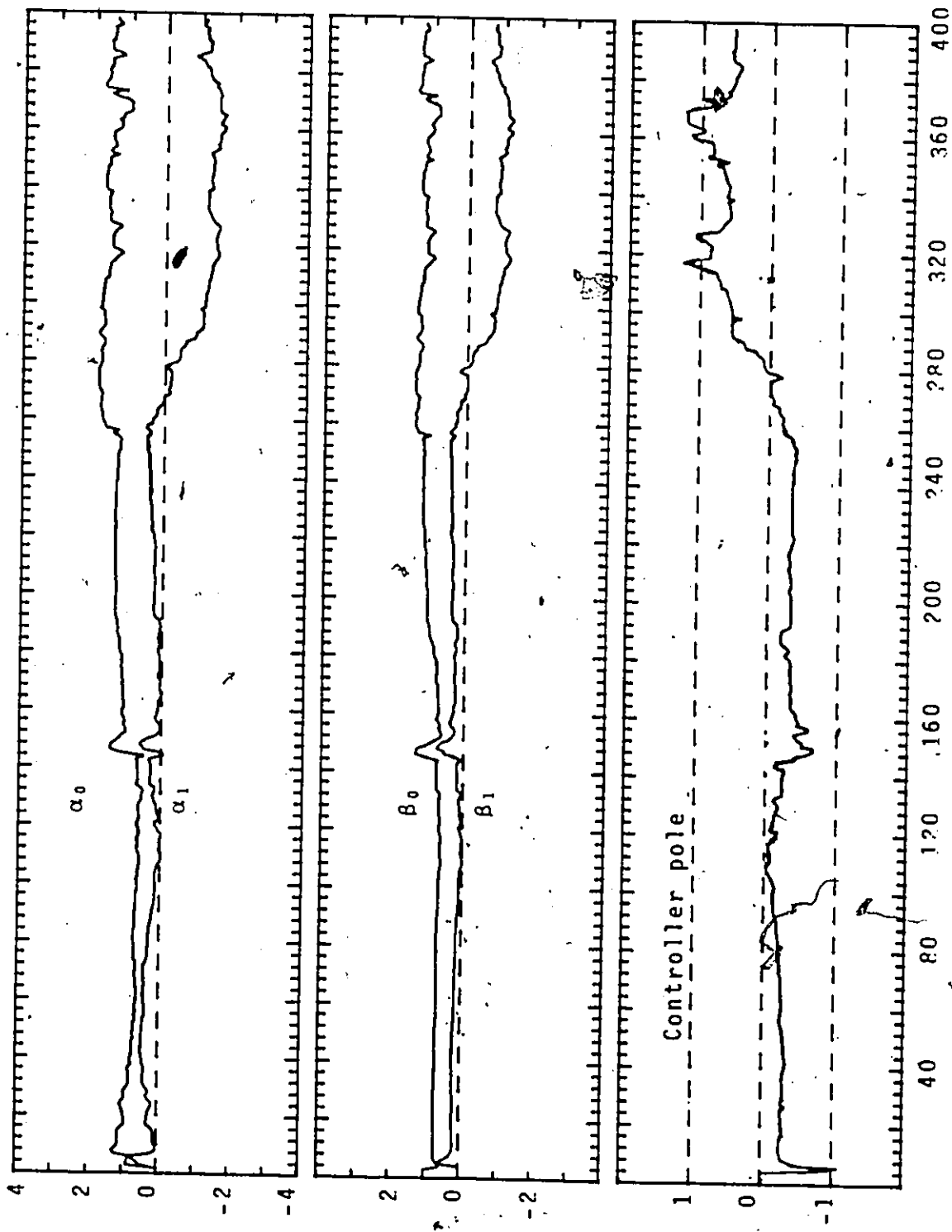
Figure 5.11b Parameter estimates and pole of the inner STR (Simulation)
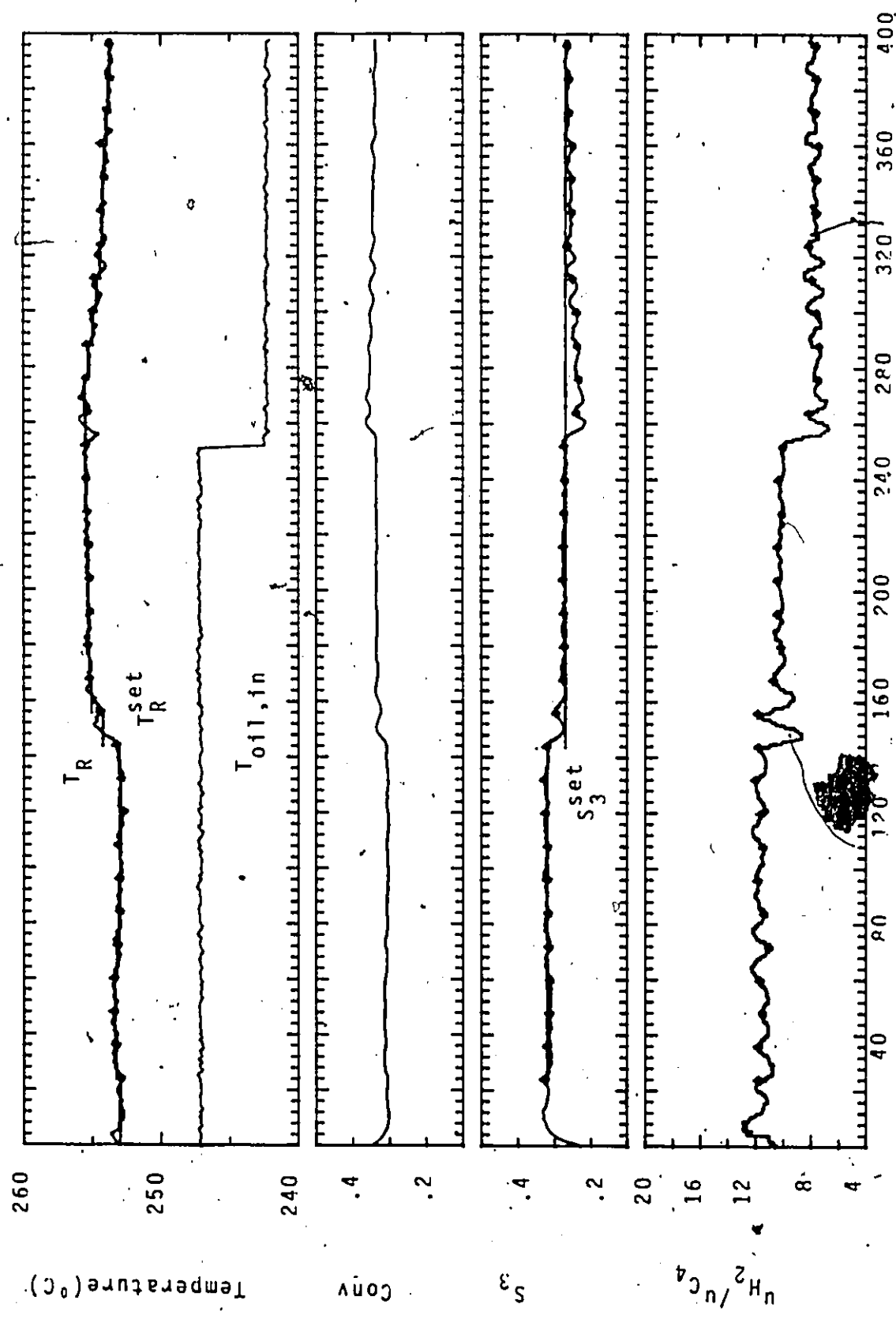
Figure 5.12a   Double STR cascade controller performance responding to a selectivity setpoint change and a load disturbance in $T_{oil,in}$ (Simulation)
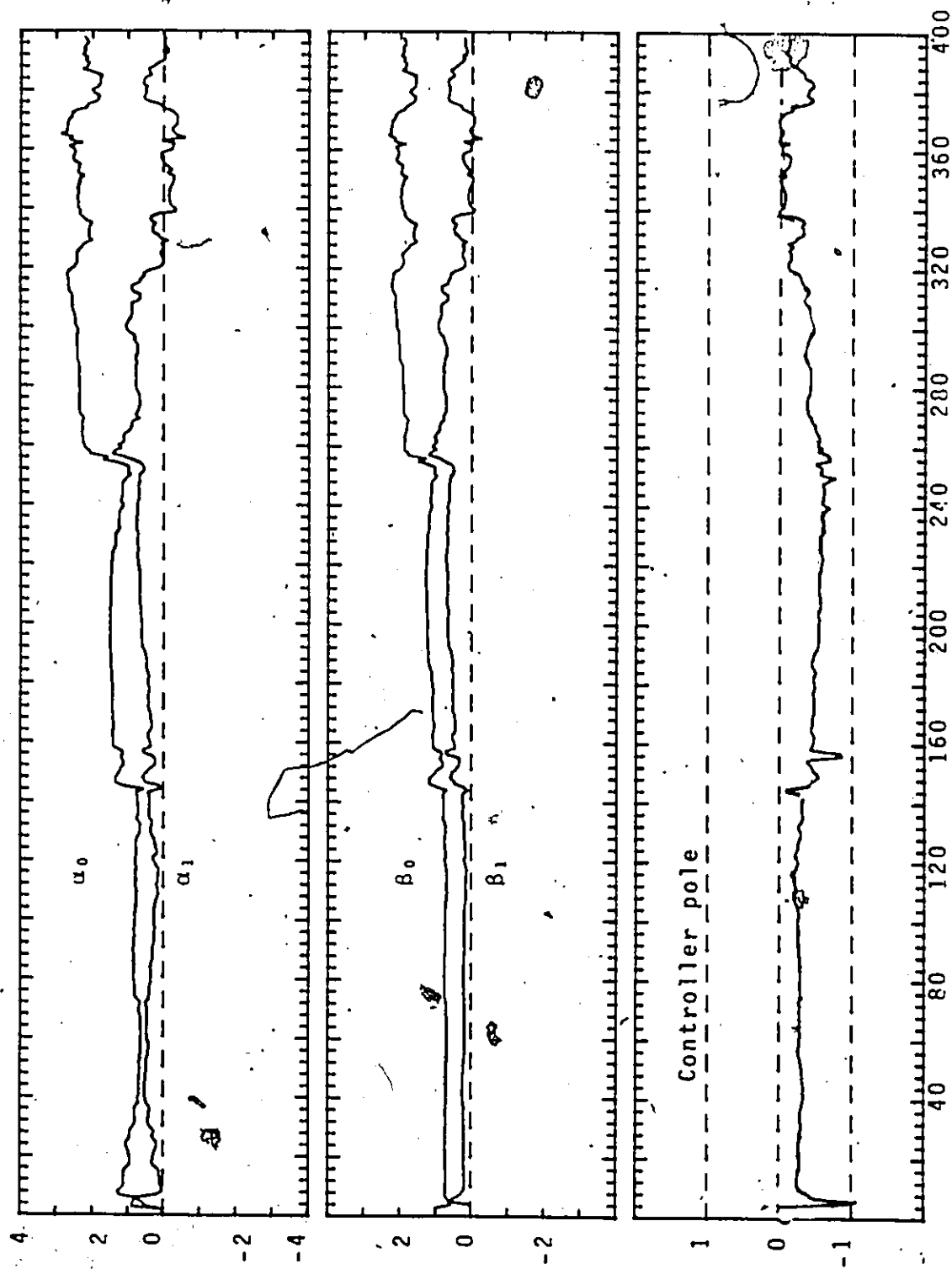
Number of control intervals, temperature loop (30 s)

Figure 5.12b Parameter estimates and pole of the Inner STR (Simulation)
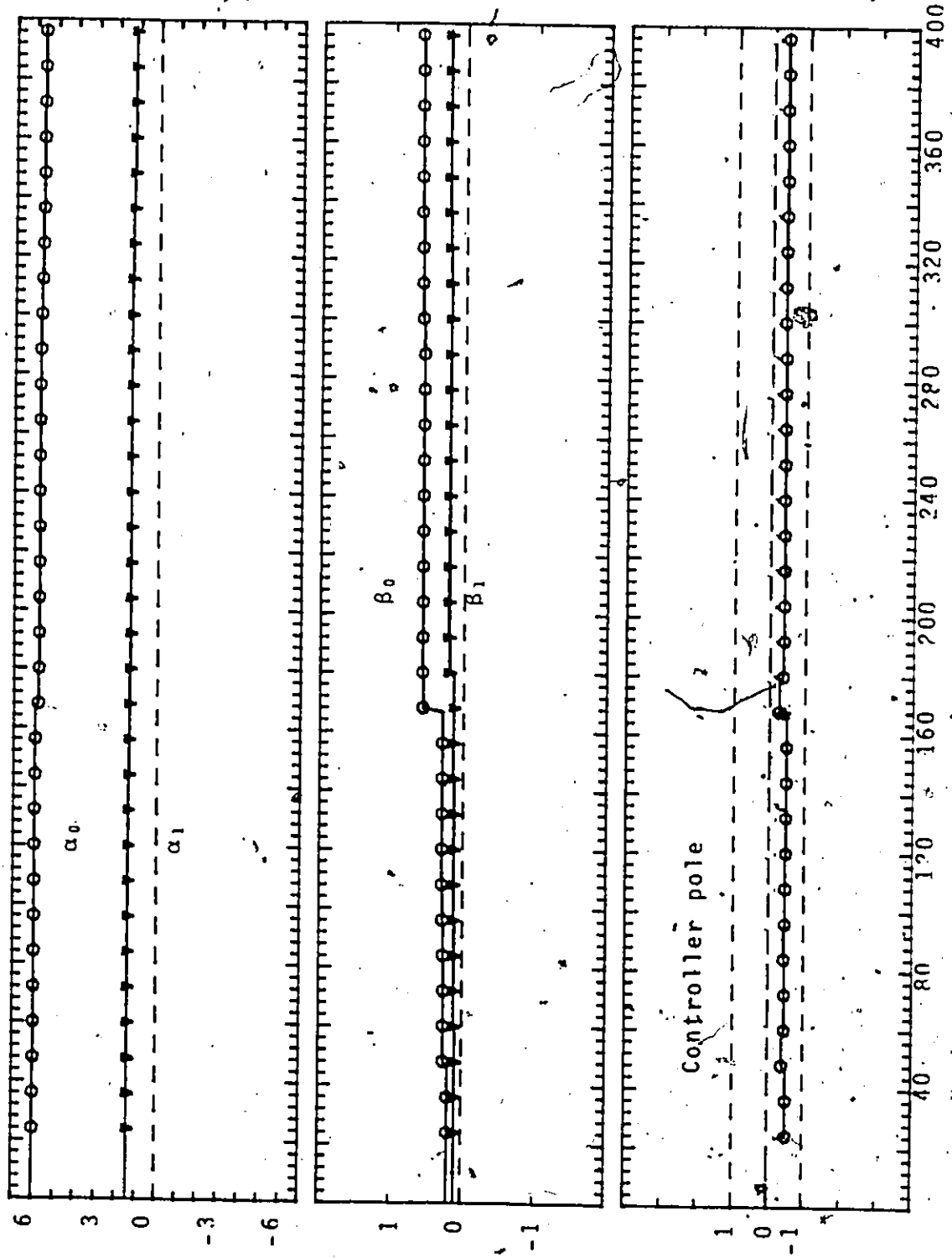
Figure 5.12c Parameter estimates and pole of the outer STR (Simulation)

Number of control intervals, temperature loop (30 s)

could be regarded as good estimates, the initial $\underline{P}_0$ was chosen to be $10\underline{I}$.

On the setpoint change in S_3, the outer STR called for a big adjustment in T_R^{set} and this was followed by a smaller second adjustment in T_R^{set} to bring the S_3 right onto the target. When the load disturbance on the reactor occurred, the adjustments in T_R^{set} were so gradual that the S_3 could not recover until after four sampling intervals, one sampling period later than the Dahlin case. The variations in the inner STR parameter estimates are shown in Figure 5.12b and those for outer STR are shown in Figure 5.12c. There are little variations in the tuning parameters α_0 and α_1 of the outer STR. As for β_0 and β_1, the only change occurred at the setpoint change of S_3. It was recognized later (after the reactor control runs to be described in Section 6.4.4) that these little variations in α_0 and α_1 were due to the fact that the starting covariance values in $\underline{P}_0$ for α_0 and α_1 were not properly scaled according to their magnitudes as compared to the magnitudes of β_0 and β_1. Later on, load disturbance occurring in the reactor wall caused the deviation of S_3 from its target. However the magnitude of this deviation value was small and the outer STR regarded S_3 essentially as nearly always on target and therefore did not carry out any adjustment in the controller parameters.

6. EXPERIMENTAL STUDIES ON THE REACTOR SYSTEM

6.1 Introduction

This chapter reports the experimental observations associated with the cascade control strategies which were applied to the pilot plant fluidized bed reactor. The details associated with these strategies were developed through the dynamic simulation program which was presented in Chapters 4 and 5.

6.2 Experimental Procedure

Because the chemical system is potentially quite dangerous and considerable quantities of highly flammable gases are involved in the reactor at a relatively high temperature level, it is important to implement safe operating procedures from start-up to shut-down. This procedure also entails a thorough check of the reactor system prior to starting it up. Detailed instructions for experimental check-out, catalyst conditioning and reactor operation were described in previous work [3]. These procedures were followed throughout but an improvement was made here by upgrading the flow control system to enable much closer control of the operation than was previously achieved.

The entire reactor system can be operated either manually at the site or remotely under computer control using the Nova 1200 minicomputer. It was found to be more convenient to allow computer-controlled operation at the reactor site rather than in the computer room. This not only reduced the operator travel from computer to reactor, but also meant that fewer operating personnel were required. This was important since, the experimental runs extended over long operating periods (16-18 hours).

The computer program can be initiated at the start up of the reactor for datalogging only. The reactor data is collected and stored on disk files at each sampling interval of the three major loops:

(1) the flow loop sampled at every second

(2) the temperature loop sampled at every 30 s

(3) the gas chromatograph loop sampled at every 360 s.

Prior to the initiation of any of the controllers, satisfactory operating conditions must be obtained under manual operation. As soon as the flow control loop has been activated, the whole system can be switched over to computer-control. The different control loops are then initiated one at a time:

(1) the air cooler controller to control the inlet oil tempera-
    ture to the reactor heating/cooling coil

(2) the temperature controller to control the average temperature
    as measured in the reaction chamber at 0.15 and 0.30 m from
    the distributor plate

(3) the selectivity controller to maintain the propane selec-
    tivity at a desired operating level.

Control action for each loop is taken at every sampling interval. The control signals calculated from the control algorithms were set as set-points to the individual DDC control loops, that is, at every 360 s the controller for propane selectivity computes according to the control algorithm a setpoint to the reaction temperature whose controller in turn calculates a setpoint for the u_{H_2}/u_{C_4} ratio to the two flow con-trollers giving rise to different setpoints for hydrogen and n-butane flows based on a constant total flowrate of the mixture.

At the end of each run, all the collected data were printed and also stored on magnetic tapes. They were then transferred to the computer system (Control Data Corporation) in the University's computer centre to have the results plotted.

6.3 Minicomputer Program Setup for the Experimental Study

The real-time multitasking computer programs that were used in the experimental study of the fluidized bed reactor system were modified and extended so that they could take care of the following aspects:

(1) All values were echoed to the CRT screen and checked before final entry into the computer. This is very important in on-line implementation because a mistakenly entered number may result in disastrous consequences for the reacting system.

(2) Many different control strategies can be used. This means that:

a. step changes in the $u_{H_2}./u_{C_4}$ ratio may be introduced with open reaction temperature and propane selectivity loops.

b. either a PI or STR controller may be used in inner loop for temperature control.

c. either a Dahlin or STR controller may be implemented in the outer loop for propane selectivity control.

(3) Transition from manual manipulation to computer control must be smooth.

Since the computer programs have been extended to the extent that the entire program is more than double its original size, the previous

arrangement of the computer system did not provide enough memory to allow the programs to be executed. The configuration of the existing facilities had to be modified as described in Section 2.3. However, with this configuration the computer is more susceptible to I/O runtime error; as a result these errors occurred more frequently.

A list of the various tasks and subroutines of the user software developed for these data acquisition and control studies is included in Figure 6.1. The arrows indicate their interactions. The main task, MSBA, in system A receives any parameter changes from system B. It activates the other three tasks:

(1) FSBA: flow sampling and control task

(2) TSBA: temperature sampling and control task

(3) GCSBA: gas chromatograph sampling and control task

and coordinates their sampling and controlling as indicated by the user through parameter interrupts. The flow task which is sampled at the fastest rate of 1 s is responsible for the transfer of all the update measurements of the different loops to system B through the inter-processor bus (IPB). In system B, the main task XPBP receives any interrupt from the console and facilitates the parameter changes as requested by the user. It then passes the parameters to system A to effect the changes via IPB. It also activates a printing task PRBA which prints out the different measurements and setpoints when appropriate flags are set.

This computer program has the option of filtering the flow and temperature measurements if they are found to be too noisy but it was not used in the reaction runs to be presented.

SYSTEM B

XPBR

- facilitates parameter changes
  and transfers information to
  System A
- activates printing task PRBA

PRBA

- reads data from $DPI
- writes data to files to be
  stored on disc
- prints data on line printer

IPB

SYSTEM A   IPB

FSBA

- writes data to $DPO
- samples H_2 and C_4 flows
- filters flows(if necessary)
- calculates and takes control
  action

MSBA

- opens channels
  for information
  transference
- receives in-
  formation from
  System B
- activates tasks
  FSBA, TSBA
  and GCSBA

TSBA

- calls AIOFLIP and samples 16
  temperatures
- filters measurements (if ne-
  cessary)
- chooses desired control
  scheme
- calculates control action and
  provides setpoints to H_2 and
  C_4 flows

AIOFLIP

FORM

UYINCR

RLS

GCSBA

- calls GCIBA to initiate a
  gas chromatograph cycle
- waits 360 s
- calls GCCBA to calculate C_4
  conversion and selectivities
- chooses desired control
- calculates control action and
  provides setpoint for T_R

GCIBA

GCCBA

Figure 6.1   Structure of Minicomputer Software for the Fluidized Bed Reactor
             System .

6.4 Results of the Experiments on the Reactor

To verify the main results of the simulation study, a similar set of experimental runs were performed except under somewhat different operating conditions as described in the next paragraph. The cascade control using PI and Dahlin for the inner temperature and outer propane selectivity control respectively was applied first. Then the STR was used for temperature control only. It was allowed to tune itself before the propane selectivity control by the Dahlin algorithm was turned on. Finally a double STR cascade control strategy was implemented. Under most conditions the parameter values obtained from the simulation were used. When the outer STR was used, the actual system demonstrated quite large deviations from simulation results. The effects of various design decisions and parameter values were investigated.

There were some differences in the operating conditions between the actual reaction and simulation runs. The actual reaction depends very much on the activity of the catalyst and the initial starting conditions such as inlet oil temperature to attain steady state operation. These differences in operating conditions should be kept in mind when the simulation results are compared with the experimental results.

The ratio of the hydrogen-to-butane flowrates was constrained between 4 and 20 throughout all the runs; similarly a constant total volumetric flow rate of .081 m^3/min (S.T.P.) was used. The oil inlet temperature was held constant around 264°C by the air cooler controller.

The testing sequence of the proposed control strategies is as follows. The cascade scheme with PI and Dahlin for temperature and propane selectivity control respectively was evaluated first (Figure 6.2)

by first turning on the PI controller for temperature control and a set-point change for T_R was introduced to test whether the PI tuning parameters were appropriate or not. The S_3 loop was then activated and the control system was evaluated for step changes in S_3.

6.4.1 Dahlin + PI

As a basis of comparison for the different control schemes on the fluidized bed reactor, the cascade control system was chosen with a PI controller on the inner loop for reactor temperature and the Dahlin algorithm for control of propane selectivity on the outer loop. The control intervals on temperature and propane selectivity were 30 s and 360 s, respectively. The response under the control scheme is shown in Figure 6.2. Testing of the temperature loop was first performed using a step increase of T_R^{set} from 265 to 267°C with the PI tuning parameters $K_p = 1.03$ and $K_I = 0.34$ (which were used in the simulation runs and found to be adequate). Note that the PI controller for the feedratio responds instantaneously to the change resulting in large initial decrease in u_{H_2}/u_{C_4}. The reactor temperature achieves its setpoint temperature within five sampling periods (1 sampling period = 30 s); note initially there is an overshoot of about 1°C but this is quickly damped. The set-points for the $T_{oil,in}$ were introduced according to the reactor tempera-ture so as to maintain a temperature difference of about 3 to 5°C between oil inlet temperature and T_R. It was found that this difference serves as a reasonable driving force for heat transfer from the reactor.

The Dahlin controller for propane selectivity was then activated and tested for setpoint changes in S_3: a step up from .3 to .33 and a step down from .33 to .28. Since a dead time of 360 s is introduced by
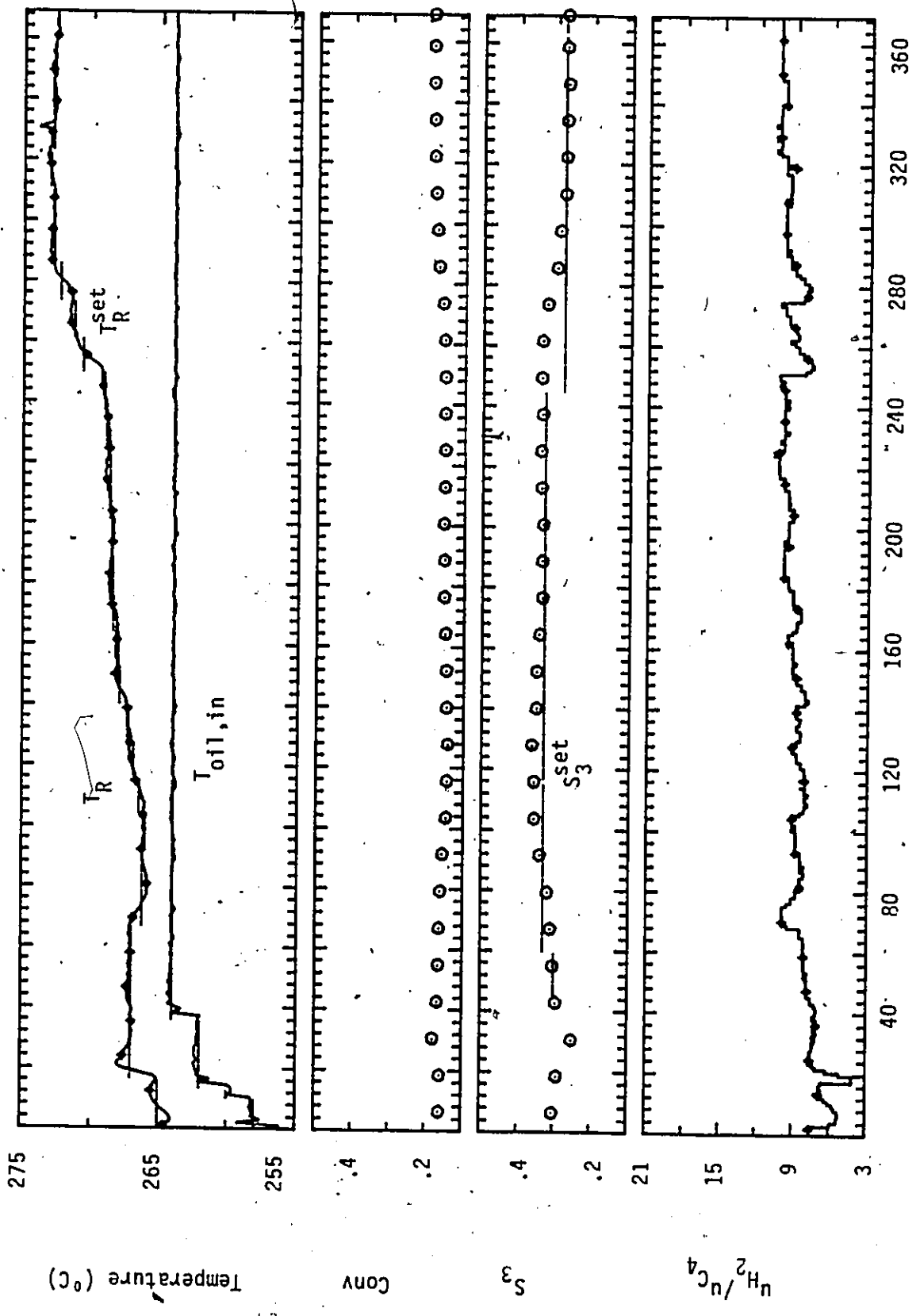
Figure 6.2   Dahlin + PI (Experimental)

the gas composition chromatograph analysis cycle, this controller was
designed (in Section 4.2) to incorporate dead time compensation by
specifying that the desired closed-loop response of the selectivity loop
resemble a 'first-order plus dead time process. The parameters, time
constant τ, gain K and the desired closed-loop time constant λ were
chosen to be 250 s, -0.22 and 500 s respectively   based on the simu-
lation results.

Figure 6.2 demonstrates that the performance of the control
system with the above controller parameters was satisfactory; S_3 moved
smoothly with some overshoot to the new setpoint .33. The reader is
reminded that the plotted S_3 responses in all the subsequent graphs
correspond to the time at which the chromatograph samples were taken;
the analysis information was known 360 s later. Thus when the change to
S_3^{set} was made from .3 to .33, the setpoint change would not be effective
until after the chromatograph sample had been analyzed. After the 360 s
analysis time, control action would then be taken based on the error
computed from the difference between the new setpoint and the previous
$S_3^{measured}$. The Dahlin controller calculated that the reactor temperature
should change by -0.82°C to meet the desired propane selectivity.

Figure 6.2 indicates that after about 120 control intervals, the
controller calls for a continual increase in reactor temperature to meet
the desired S_3 level. At the same time, the reactor feed ratio increased
continuously. The selectivity and conversion remain nearly constant.
The reason for this behaviour can be traced to a gradual change in
catalyst activity. The catalyst had been stored in the reactor for a
long period prior to this run. The reactivation period had probably been

too short and the catalyst was gaining activity during this reaction run. Furthermore, it must be remembered that the reactor together with the support structure has a relatively large thermal capacity which requires considerable time to be heated to operating temperature. As it reaches operating temperature, it represents less of a heat sink and thus the reactor operating conditions change gradually with time during this initial time. Note that the Dahlin controller was able to handle this nonstationary condition reasonably well. And when a stepdown in S_3^{set} was introduced, the propane selectivity moved smoothly right to the target resembling a first-order system as predicted by the Dahlin algorithm.

6.4.2 STR in Inner Loop for Reaction Temperature Control

The experimental runs for the STR in inner loop to control the reaction temperature without closing the outer selectivity loop are presented in this section. The highly exothermic nature of the reactions coupled with the large activation energies means that direct control of the reaction temperature, T_R, is necessary for safe and stable operation even though the propane selectivity is the ultimate economic control variable. Moreover, it is wise to tune for ξ, the constraining parameter, first, without the complication of the additional outer loop.

Model orders of $m = \ell = 1$ were used, based on an assumed or previously identified transfer function model for the process and the noise model. The choice of model orders was previously verified by simulation (Section 5.3.3).

Section 1: Minimum variance STR

For the run shown in Figure 6.3(a) and (b), the performance of

Figure 6.3a STR in Inner Loop (Experimental)

Figure 6.3b Controller Parameter Estimates, Controller Pole and Trace of P Matrix for Inner STR

the STR to control the reactor temperature in the inner loop was
evaluated. The initial parameters of the STR, $\underline{\theta}_0$: (1.840, -1.373,
1.333, -0.320) were calculated from the tuning parameters of the
PI controller, to ensure a very smooth transition from PI control
to STR control. As soon as the STR started at point A, the first
four sampling intervals were devoted to filling the VU and Y
vectors, but with the PI controller still operative. Since we were con-
fident that the initial guesses for the values of the STR parameters
were reasonably good, the initial conditions for the estimation algo-
rithm were $\underline{P}_0 = 1\underline{I}$, FLAM = 0.95 and $\xi = 0.0$. Here β_0 was allowed to
adapt.

It was found that when a setpoint change in T_R was introduced,
this minimum variance control called for excessively large variations
in the manipulated variable resulting in a bang-bang type of control
action on the feedratio controller. These excessive variations in the
butane flowrate would upset the level of propane selectivity and were
therefore unacceptable. Thus the inner STR was deactivated at point B
and the PI controller was allowed to take over.

Section 2: $\xi = 0.4$

In order to reduce the variations in the manipulated variable,
Clarke's [20] constrained minimum variance algorithm which minimizes the
performance index in Equation (4.3.16) was used. The inner STR was
initiated at point C for a second time with the initial conditions for
the estimation algorithm as $\underline{P}_0 = 1\underline{I}$, FLAM = 0.95 as previously in
Section 1 and with some basis from the simulation ξ was chosen to be 0.4.
The parameter, β_0, was fixed at a value of 1.33 (found from the simulation)

since it was felt that this value was a good guess and hence it was not necessary for it to adapt.

Four sampling periods were required to fill the VU and Y vectors. After this initial period, the controller parameter estimates (Figure 6.3b) started adapting (except β_0 which was fixed purposely). As soon as the first setpoint change to T_R from 266 to 268°C was introduced, the controller parameter estimates made immediate changes. As a piece of new information had come in, the sum of the diagonal elements of the P matrix (trace) which is proportional to the average variance of the controller parameter estimates was found to decrease instantaneously. Since no major new disturbances were entering the system between setpoint changes, the variances of the parameter estimates were seen to grow by a factor of 1/FLAM (FLAM being the discounting factor). We could observe this kind of trend for the rest of the STR runs.

After a few setpoint changes from 268 to 270 and then to 267°C, the controller had tuned itself to give steady control on the reaction temperature holding it to 267°C. However it was thought that the variations in the controlled variable, T_R, caused by the variations in the manipulated variable, u_{H_2}/u_{C_4}, were still too large in the initial transient. Other values for the parameter, ξ, were investigated.

At point D, it was found that the supply of hydrogen gas ran out and the butane gas supply was cut off by the safety device mentioned in Section 2.4.11. The system was momentarily under manual control. The reactor temperature was observed to decrease severely.

Sections 3 and 4 of Figure 6.3: $\xi = 0.8$ and $\xi = 1.6$

The inner STR was re-initiated again at point E with $\underline{P}_0 = 0.5 \underline{I}$

for a slower and smoother adapting of the controller parameters. The

other initial conditions were the same except for $\xi = 0.8$ and later $\xi = $

1.6 (at point F). This change is readily accomplished on-line by simply

changing the value of the constraining parameter ξ.

The controller parameters were found to converge to progressively

smaller values than before. The increase in ξ value effectively caused the

pole of the controller to move further inside the unit circle (Figure 6.3b)

and reduces the variability in the u_{H_2}/u_{C_4} gradually but at the expense

of increased variation in the reaction temperature. The controller

parameter also slowed down the response of the reaction temperature.

Since the variations found in propane selectivity for different ξ values

were roughly the same, it was decided to take the $\xi = 0.4$ setting with

the hope that the reaction temperature could be stabilized within the 360 s

analysis cycle time of the outer propane selectivity loop.

6.4.3 Dahlin + STR

The value of parameter, ξ, was then changed on-line to 0.4 and

two successive step down changes in T_R^{set} were introduced from 270 to 269

and then to 267°C (Figure 6.4a) in order for the STR to obtain new

infromation to tune its parameters. However, sustained oscillations were

observed this time. The T_R response to a decrease in setpoint change of

T_R was different from the last time under similar conditions. When the

reactor temperature reached 267°C, the S_3 was still at a low level of 0.2.

Another decrease of 2°C in T_R^{set} was intended in the subsequent setpoint

change to increase the propane selectivity level. In order to maintain a

driving force of 3°C difference for heat transfer across the wall, $T_{oil,in}$ was
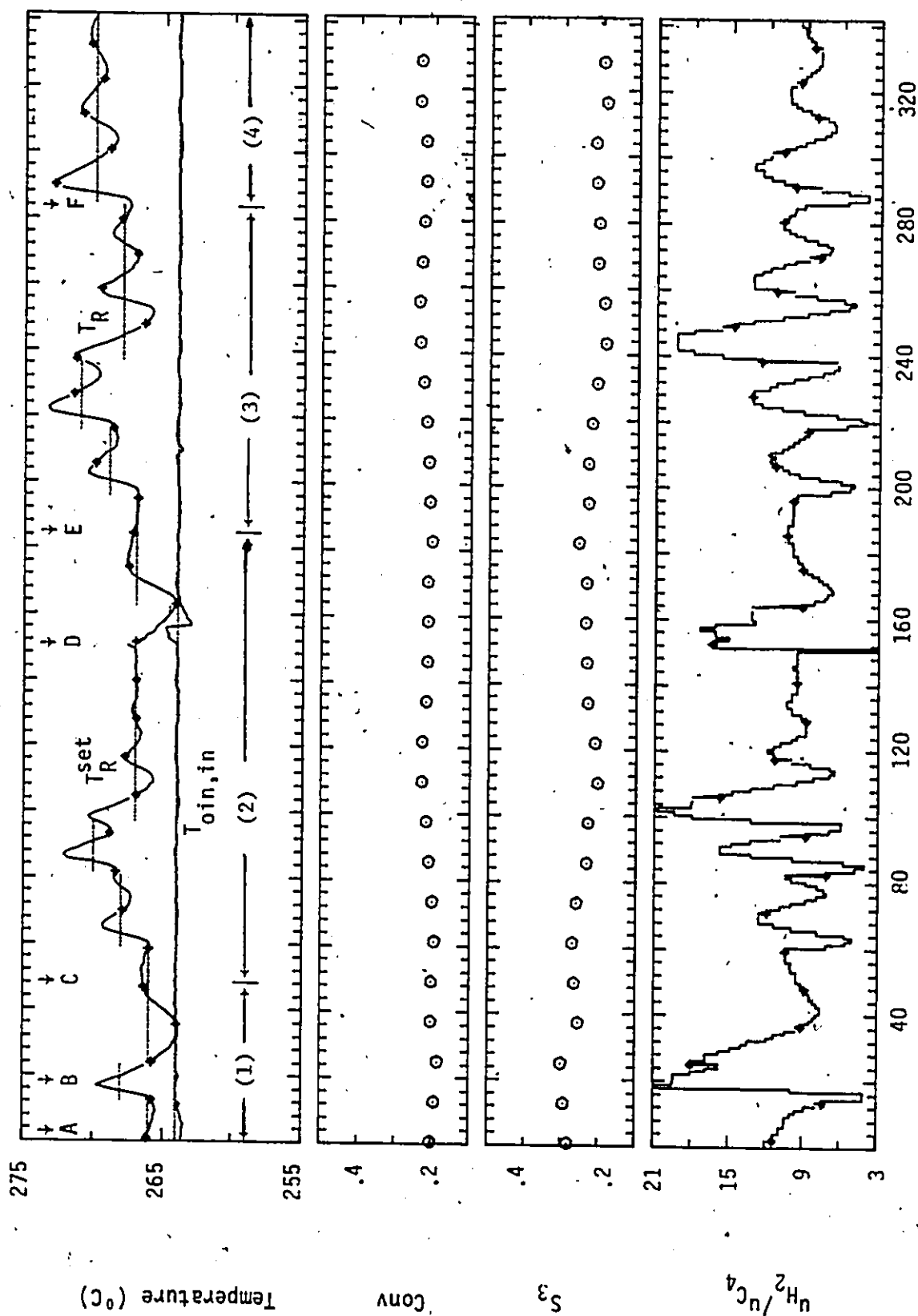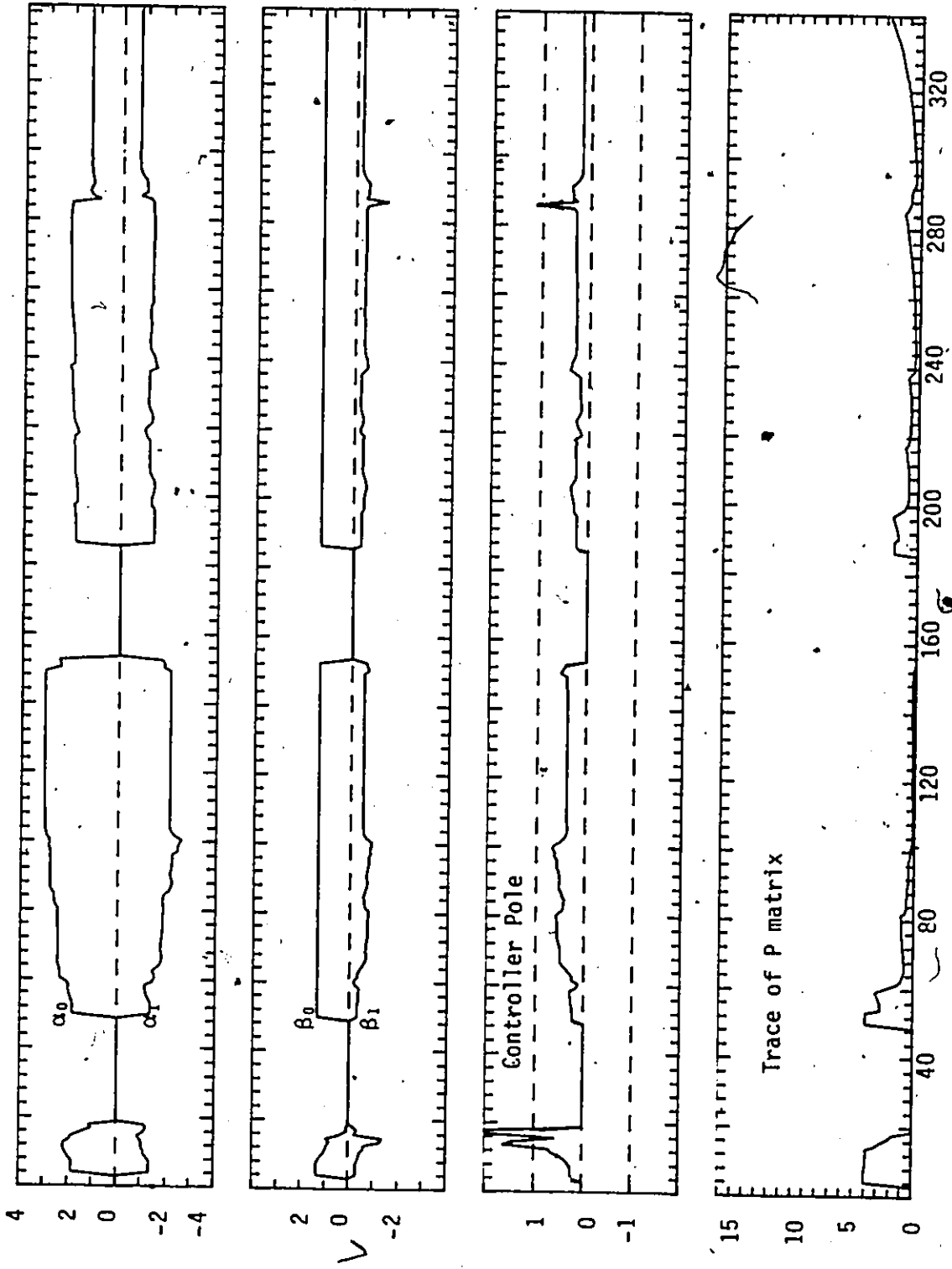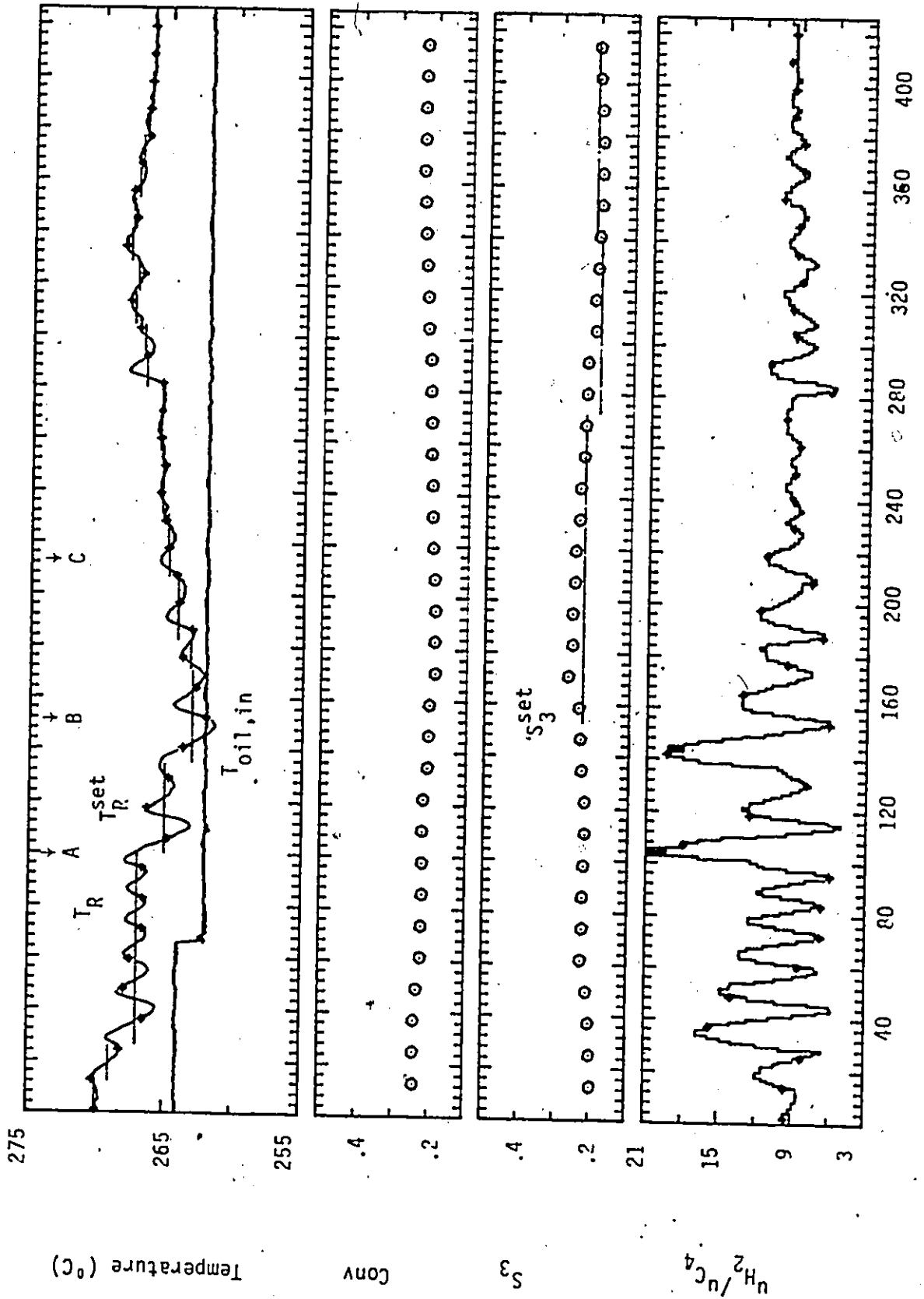
Figure 6.4a Dahlin + STR (Experimental)
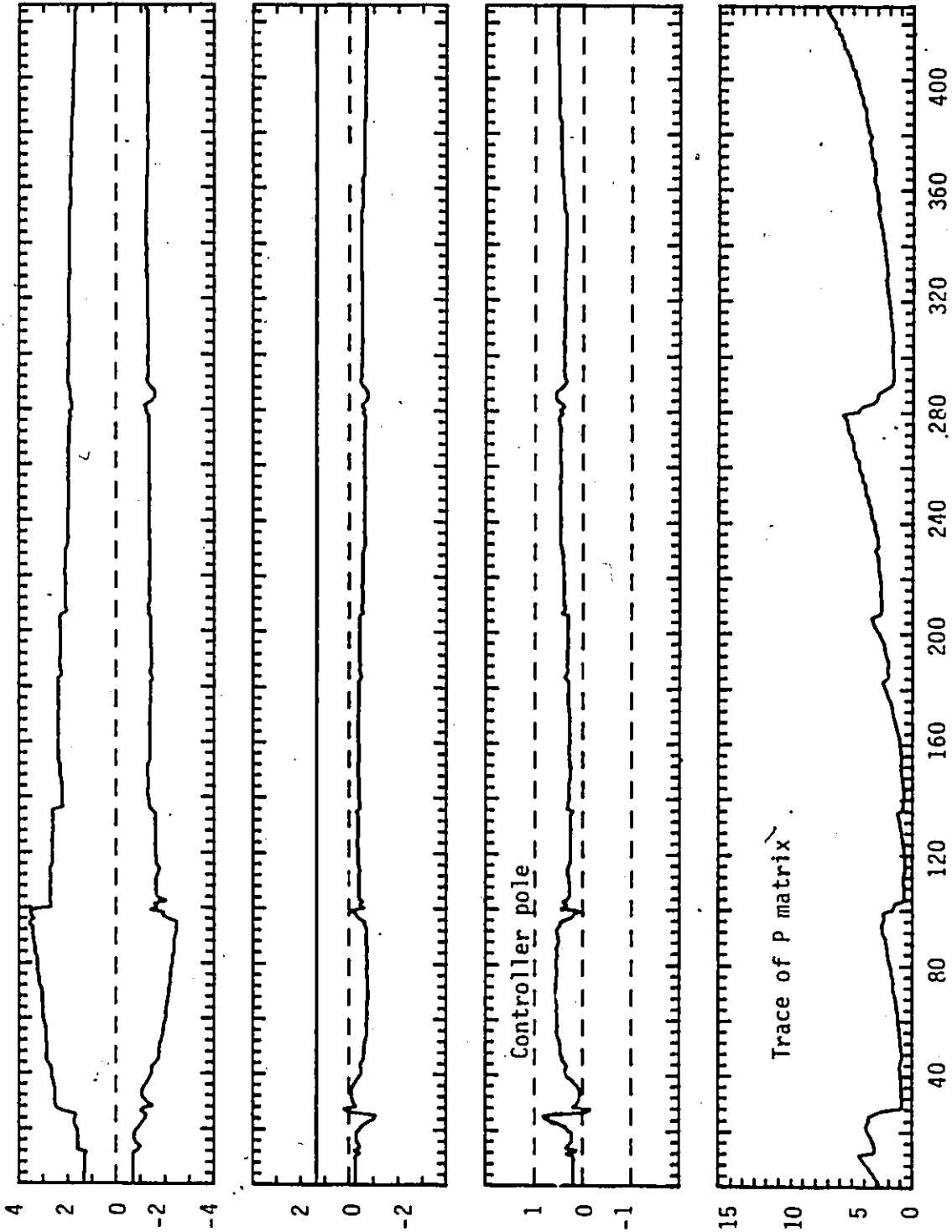
Number of control intervals, temperature loop (30 s)

Figure 6.4b Controller Parameter Estimates, Controller Pole and Trace of P Matrix for Inner STR

lowered from 264 to 262°C. The air-cooler responded instantaneously by opening wide the air valve and brought the $T_{oil,in}$ down to 262°C almost immediately. However this load change on the reactor wall forced the ratio controller for the feedrates to react in order to maintain the T_R at the desired setpoint. Unfortunately the temperature oscillations persisted.

At this point, the Dahlin controller on the propane selectivity was ready to be turned on. With this kind of sustained oscillations on T_R, it was expected to upset the level of S_3. Hence the constraining parameter ξ was backed off to a value of 0.8 at point A. Two more set-point changes of T_R were made in order to allow the STR to adapt. The Dahlin controller was activated at point B. There were some initial oscillations in S_3 due to the unsteady behaviour of T_R. After the controller parameters in Figure 6.4b had some abrupt adjustments at each setpoint change of T_R as requested by the Dahlin algorithm, they tuned themselves in by the STR and converge nicely bringing the T_R to target by the end of 360 s.

At point A, as soon as the first setpoint change for T_R from 267 to 265°C was introduced, the controller parameter estimates made an immediate adjustment, and the trace of the P matrix was found to decrease instantaneously again. At point C, the discounting factor FLAM was changed to 0.98 in order to have a relatively slow updating in the estimation algorithm.

The performance of the control system was evaluated for a few setpoint changes in S_3: 0.23 to 0.19 and then to 0.21. The propane selectivity was brought to the desired setpoint gradually each time according to an overdamped first-order behaviour as designed in the Dahlin

algorithm. This was facilitated by the inner STR which brought the T_R right onto the T_R^{set} as requested by the Dahlin controller at the end of 360 s.

In general, this control scheme performed satisfactorily. Given that the parameters used in the Dahlin algorithm gave rise to a very detuned controller, it is not surprising to see that it took a very long time (Approximately 45 minutes to 1 hour) for S_3 to reach the desired value. This is because the S_3 is very close to the setpoint, the error computed from the difference between S_3^{set} and $S_3^{measured}$ has a magnitude such as 0.01 that could only introduce a tiny fraction of a degree Centigrade change in T_R^{set}.

6.4.4 STR + STR

The last control scheme to be tested is the double STR configuration for both the temperature and selectivity control. There were difficulties in running the outer STR for the selectivity control and some potential problems are disclosed and discussed in turn below.

(1) Initial estimates for $\underline{\theta}_0$ and $\underline{P}_0$

As mentioned in Section 5.3.3, if $\underline{\theta}_0$ represents the best guess for $\underline{\theta}$ and $\underline{P}_0$ represents the uncertainty in $\underline{\theta}_0$, one can achieve very rapid updating when little prior knowledge is available (large values of $\underline{P}_0$ are used). On the other hand, very slow but smooth updating occurs when substantial prior knowledge on the parameters is available. However, the usual choice of $\underline{P}_0 = \sigma \underline{I}$ where σ is a constant giving rise to homogeneous values for the diagonal elements in the $\underline{P}_0$ matrix cannot be applied in this case because of the difference in the magnitude of the parameters in $\underline{\theta}_0$: (6.119, -1.444, 0.2, 0.103). Since the diagonal

elements of $\underline{P}_t$ represents $\text{var}(\Theta_{i,t})/\text{var}(\varepsilon_t)$, if the variances for 0.2 and 0.103 are of equal magnitude, the variance for −1.444 should be about 10 times as large and that for 6.119 about 30 times the magnitude.

(2) The constraining factor ξ

Figure 6.5 shows the experimental results for the evaluation of the double STR configuration. As usual there was in initial transient for the fluidized bed reactor to reach a thermal equilibrium. The inner STR was turned on first at point A with FLAM = 0.95, ξ = 0.8, $\underline{P}_0$ = 0.5$\underline{I}$, $\underline{\Theta}_0$ = (1.840, −1.373, 1.333, −0.320) as determined from the PI tuning parameters and β_0 was fixed. After the first few setpoint changes in T_R from 265 to 266°C, the controller parameter estimates started to tune themselves in. The STR led to an initial overshoot on T_R. On subsequent adjustments in the tuning parameters, T_R was brought to the setpoint value quickly.

At point B, the outer STR was activated with FLAM = 0.95 and ξ = 1. These parameters were chosen on the basis from the simulation and the plant experience with implementing the inner STR. The initial parameters for the outer STR, $\underline{\Theta}_0$: (6.119, −1.444, 0.2, 0.103), were calculated from the parameters of the Dahlin controller and the diagonal elements of $\underline{P}_0$: (7500, 2500, 250, 250) were scaled to the appropriate ratio as discussed in previous section. The initial four sampling intervals of the outer STR were used to fill VU and Y vectors; herefore, the Dahlin controller was operating during this stage.

The propane selectivity was controlled at 0.285 by the Dahlin controller. On the next setpoint change in S_3 to 0.23 the outer STR was effective and called for a large adjustment of T_R^{set} from 265.3 to 268.3°C.
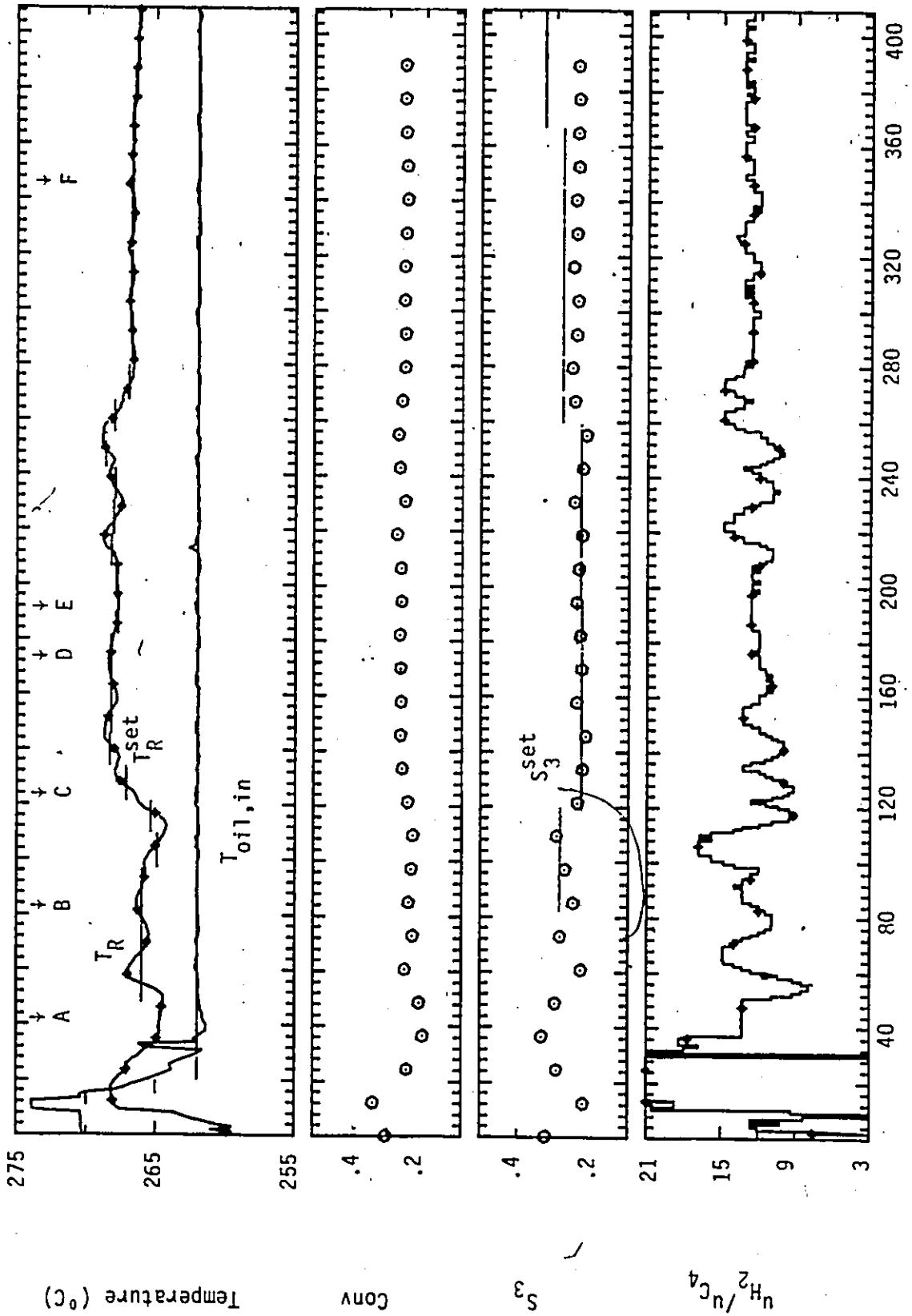
Figure 6.5a STR + STR (Experimental)
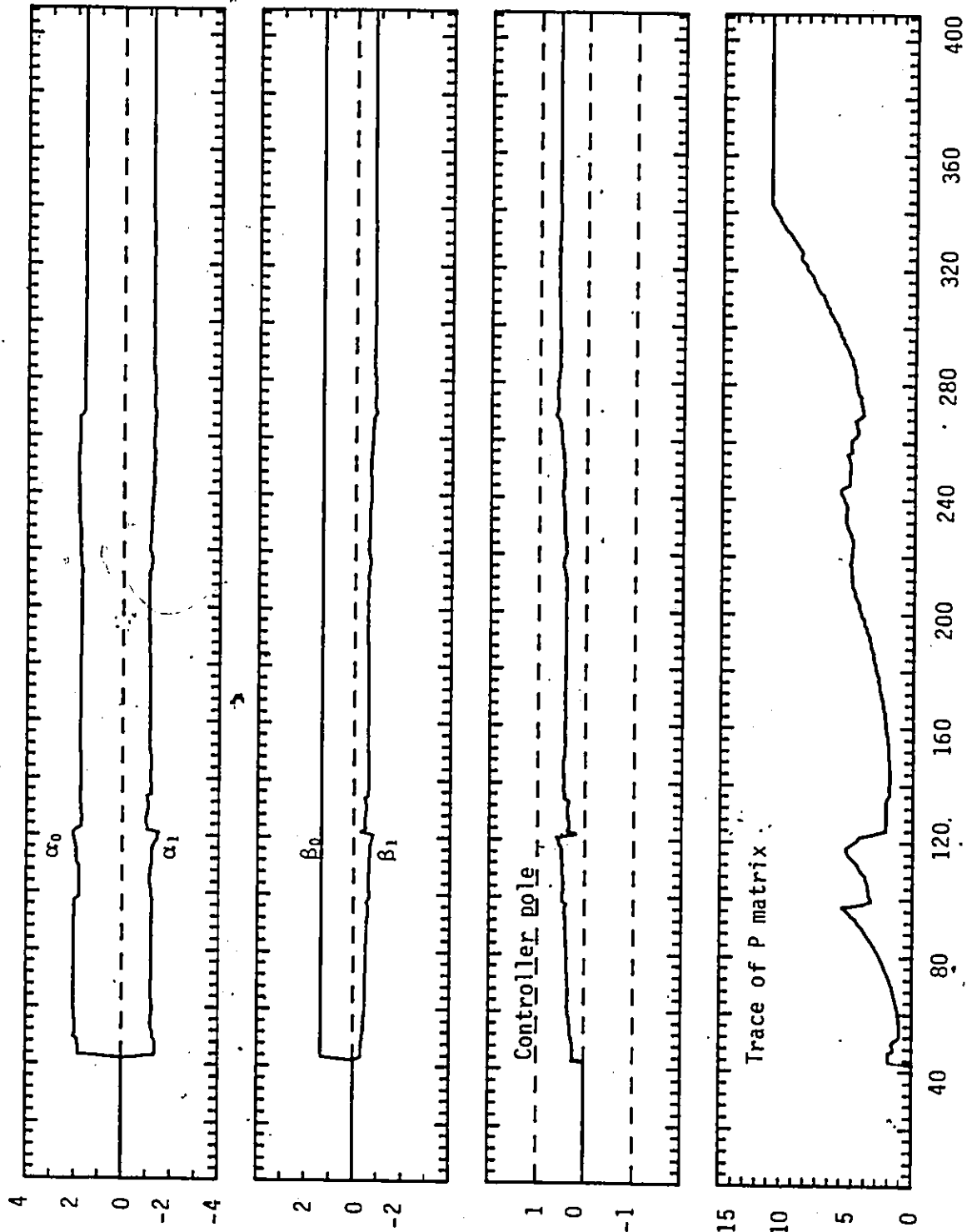
Figure 6.5b   Controller Parameter Estimates, Controller Pole and Trace of P Matrix for Inner STR
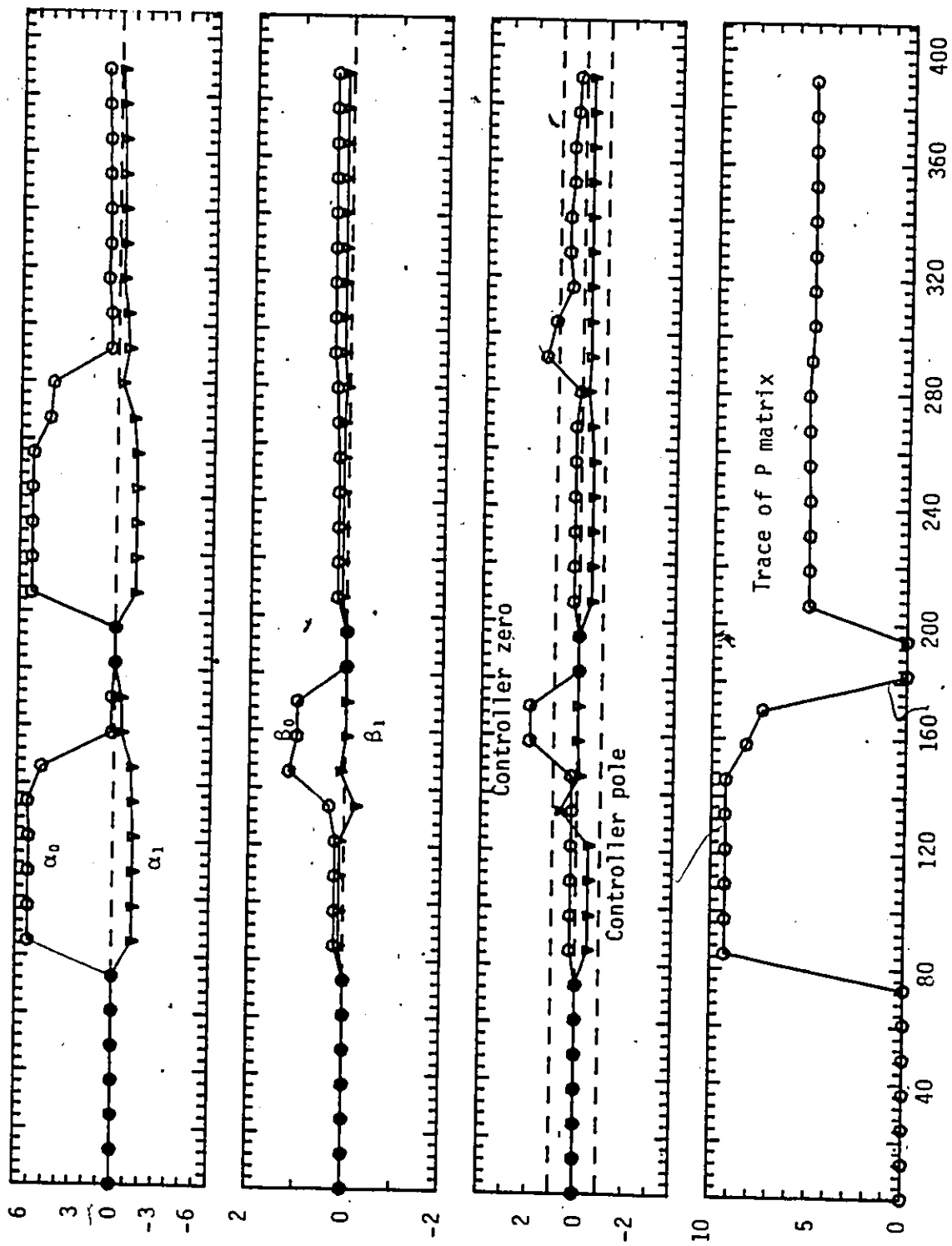
Figure 6.5c   Controller Parameter Estimates, Controller Roots and Trace of P Matrix for Outer STR

The inner STR brought the T_R right to the target by decreasing the set-point to the feedratio controller which responded accordingly. Hence the S_3 dropped to the desired level in the following sampling interval and remained around there for a few subsequent sampling intervals. So far the inner STR was performing extremely well and the controller parameters had converged, thus the discounting factor was changed to 0.98 on line for a relatively slow updating in the estimation algorithm at point C.

Later on at point D, it was detected that the zero of the outer STR moved outside the unit circle and remained there for two sampling periods. It was mistakenly thought that this might result in an unstable controller. The outer STR was immediately de-activated and the Dahlin controller took over for selectivity control. In fact there is·no problem with zero's of controller being outside unit circle. It is the pole, if being outside the unit circle, that will give stability problems.

After two sampling intervals, the S_3 was still maintained at a steady desired level and the T_R and u_{H_2}/u_{C_4} were reasonably constant, the outer STR was re-activated again at point E. The values of FLAM and ξ were the same as the previous values of 0.95 and 1.0 respectively. θ_0 was re-initialized to (6.119, -1.444, 0.2, 0.103) again. However there was a bug in the computer software so P_0 could not be re-initialized and took the values of those left behind from the outer STR that was last used: (88.3, 76.3, .078, .080). The ratios between these values were adequate.

Again for the first four sampling intervals the S_3 was still controlled by the Dahlin algorithm. When the outer STR became effective,

the controller parameters started to tune themselves and at the third
sampling interval α_0 was observed to decrease drastically as in the
previous case. Nevertheless, the gain of the controller remained at low
values for the rest of the experimental run. Despite the fact that two
consecutive setpoint changes in S_3 from 0.23 to 0.28 and then to 0.33
were made, the S_3 stayed at the same level and never moved closer to the
new setpoints except for the first two sampling periods after each set-
point changes was made. In fact after the change in S_3^{set} was introduced
from 0.23 to 0.28, the outer STR had only called for the first two
significant adjustments in T_R^{set}. The inner STR responded accordingly to
lower the T_R by calling for a change in u_{H_2}/u_{C_4}. Later on no appreciable
setpoint changes in T_R were requested by the outer STR and the reactor
temperature remained on the setpoint value, thus requiring little
adjustment in the feedratio.

Detailed analysis of the phenomenon has disclosed the following
reason for this observed behaviour. A value of 1.0 was assigned to ξ in
this experimental run. We can see that α_0 decreases significantly from
6.0 to 1.0 at that point where the trouble seems to arise. This means
that the gain was effectively reduced by six times as compared to the
Dahlin algorithm. Since the controller was designed to minimize the
performance index given by Equation (4.3.23)

$$\underset{T_R^{set}}{\text{Min}} \ E \sum_{j=t}^{t} [(S_3 - S_3^{set})^2_{j+1} + \xi \ \nabla \ (T_R^{set})^2_j]$$

that is minimizing a weighted sum of the variances of the output and
input of the controller. For a step change in S_3 from 0.23 to 0.28 and
then to 0.33, the variance of the output is of the magnitude of $(0.02)^2$

while the change in T_R^{set} can be of two to three degrees Centigrade having a variance of about $(0.5)^2$. If we put ξ as 1.0, the second term in the bracket of Equation (4.3.23) is about 600 times the first term. This implies that the controller was designed to minimize the variance in T_R^{set} rather than in the propane selectivity. It explains why this controller ignored the variance in S_3 but tuned the outer STR in such a way so as to maintain the T_R^{set} at a steady level. Obviously ξ would have to be of the order of 10^{-3} to obtain a reasonable STR.

Later on at point F, the estimation portion of the regulator was turned off for the inner STR because the trace of $\underline{P}$ matrix was observed to grow by a factor of 1/FLAM due to lack of information. Furthermore the controller parameters were believed to be well-tuned and converged at this stage. The trace of $\underline{P}$ matrix was then leveled off.

7. SUMMARY AND CONCLUSION

The main purpose of this research program was to determine the adequacy of conventional and adaptive multiloop cascade control on a pilot-plant fluidized bed involving an extremely non-linear complex chemical reaction. Three cascade control schemes were examined for temperature and selectivity control:

Control Scheme 1: a fixed proportional integral (PI) controller on the inner temperature loop and a Dahlin algorithm for the outer loop selectivity controller.

Control Scheme 2: an adaptive self-tuning regulator (STR) on the inner loop and a Dahlin controller for the outer loop.

Control Scheme 3: a double STR scheme for both the inner temperature and outer selectivity loops.

The use of self-tuning and adaptive controllers were considered in order to overcome the following challenging problems associated with the control of the fluidized bed reactor:

(1) Asymmetric dynamics: the time constants and gains depend upon the operating levels of T_R, T_{oil} and the feedrate ratio.

(2) Time varying parameter: the catalyst activity changes with time and the history of operation.

(3) Long measurement delay: the chromatograph takes 360 s to analyze a sample.

Based upon the mechanistic model equations describing the mass and energy balances of the system, an existing simulation [4] was modified to include the dynamic effects of the disengaging section above the

fluidized bed which was modelled as a perfectly mixed vessel and to enable the investigation of the different control schemes of interest. Extensive simulation studies were carried out. The conventional cascade control system, consisting of a PI controller for the reaction tempera- ture in the inner loop and Dahlin controller for the propane selectivity in the outer loop was improved by increasing the desired closed-loop time constant parameter, λ, in the controller. The performance of the Dahlin algorithm with $\lambda = 500$ s ($\tau = 250$ s) was satisfactory in the simulation results over a wide range of propane selectivity changes and even when the reactor system was subject to a load disturbance. The acceptable range of operation of the controller has thus been greatly extended, by effectively detuning the Dahlin controller. The well-behaved detuned Dahlin was further verified in the experimental run. The tuning para- meters for the PI controller, $K_p = 1.03$ and $K_I = 0.34$ were used at all times.

For control scheme 2 (with $\lambda = 500$, $\tau = 250$) for the Dahlin algorithm), the inner STR was first implemented with the following design parameters in the simulation:

1. model structure $m = \ell = 1$

2. discounting factor   FLAM = 0.98

3. constraining factor $\xi = 0.5$

4. initial parameter estimates $\underline{\theta} = 0$ for all parameters except for β_0 which was taken to be unity.

5. initial covariance matrix $\underline{P}_0 = 100\ \underline{I}$

This cascade control scheme in the simulation runs provided

adequate control when the system was subjected to the same range of propane selectivity changes and load disturbance.

Later, an actual reactor run was conducted using the same Dahlin controller while the STR has the following characteristics:

1. model structure $m = \ell = 1$

2. discounting factor   FLAM = 0.95 initially and 0.98 later afterwards

3. constraining factor $\xi = 0.8$

4. initial parameter estimates $\underline{\theta} = (1.840, -1.373, 1.333, -0.320)$ calculated from the PI tuning parameters

5. initial covariance matrix $\underline{P}_0 = 0.5 \; \underline{I}$.

The control scheme 2 was found to provide effective control and was able to better handle the control problems (1) and (2) mentioned earlier.

The double STR control configuration for both the temperature and selectivity control, i.e. the control scheme 3, was used to better account for all the control problems mentioned above. It should be noted that this control scheme was only tentatively tested by the simulation.

The inner STR had the same simulation tuning parameters as described above. The outer STR had the model structure of $m = \ell = 1$ and the same initial parameters for the estimation algorithm except for the $\underline{\theta}_0$ parameters which were (6., 1.4, .2, .1). These values were calculated from the Dahlin algorithm and $\underline{P}_0 = 10 \; \underline{I}$. The performance of the control scheme was found to be quite acceptable. Several unsuccessful attempts were made in the reaction runs. However, it is felt that the reasons for the failure were not a fault of the basic algorithm but of poor choice of parameters used in this implementation.

Based on the experience of implementing the STR on the temperature loop with the Dahlin controller on the outer selectivity loop in one case and a double STR on both loops in the other case, the conclusions concerning the practical considerations in using self-tuning regulators in this particular application can be summarized as follows:

(1) RLS Discounting Factor, FLAM

The discounting factor, FLAM, in the exponentially discounted least squares algorithm was found to be very useful in the tracking of the   parameters in time-varying processes. In this case, FLAM is set less than 1.0.

Starting off with a value of 0.95, FLAM was changed periodically on-line as follows: it should be increased when the parameters have nearly converged and decreased when known changes (for instance, in set point or in constraining factor ξ) are being made.

(2) Constraining Factor ξ

The numerical value of ξ was found to be different in the experimental runs than in the simulation work. The appropriate value for ξ has to be tuned on-line. A judicious choice for the value of ξ in the outer STR requires further investigation and is recommended to be of the order of 10^{-3}.

(3) Initial Choices of the Parameters $\underline{\theta}_0$ and $\underline{P}_0$

The initial estimates $\underline{\theta}_0$ were based on the tuning parameters of the PI controller in the case of inner STR and those of Dahlin controller in the case of outer STR. With this prior knowledge, small values for $\underline{P}_0$ were adequate for slow but smooth updating of the controller para-

meters. Bearing in mind the difference in the magnitude of the parameters

$\underline{\theta}$: (6.19, -1.444, 0.2, 0.103) in the outer STR, the initial estimates

$\underline{P}_0$ should be scaled accordingly. If not, poor control performance results.

(4) Deterministic Disturbances

The major disturbances to the inner (temperature) loop and the

outer (selectivity) loop were the measurement white noise and deterministic

step disturbances in the form of setpoint changes. The disturbances must

be frequent enough to excite the system so that the P matrix does not

become excessively large due to lack of information. The sum of the

diagonal elements of the P matrix (trace) which is proportional to the

average variance of the controller parameter estimates was found to grow

by a factor of 1/FLAM between setpoint changes. It decreased instan-

taneously as a piece of new information had come in. In this application,

it is advisable to implement the STR to allow tuning of the controller

over the periods when setpoint changes are introduced. As soon as the

controller parameters have converged, the estimation portion of the

regulator can be turned off when no major new disturbances are entering

the system.

7.1 Future Work

The simulation and experimental studies in this thesis gave not

only satisfactory results but also offered some insight into the control

of the fluidized bed reactor. However there are a number of areas that

require further investigation and these will be discussed as follows:

1. The double STR control configuration should provide a fruitful area

    of investigation by decreasing the value of ξ and supplying appropriate

    $\underline{P}_0$ values.

2. An obvious extension of the univariate STR is to multivariate STR to account for process interactions. A rather straight forward extension of the STR concept was proposed by Borisson [27]. However for the multivariable STR, a large number of parameters has to be identified. Unless some model reduction techniques are applied, this extension appears too cumbersome to use.

3. The on-line measurement of the product gas compositions via the gas chromatograph with an analysis cycle of 360 s is in fact too slow for a direct feedback control scheme. Some predictions of the exit conversion and product selections in between the sampling intervals are necessary. Some form of inferential control based on complex multivariable models of the reactor (see, for example, references [28], [15] and [29]) should provide better and more effective control of the fluidized bed reactor system.

REFERENCES

1. Shinskey, F.G., "Process-Control Systems", McGraw-Hill (1967).

2. Orlikas, A., Hoffman, T.W., Shaw, I.D. and P.M. Reilly, Can. J. Chem. Eng., 50: 628-636 (1972).

3. Shaw, I.D., Ph.D. Thesis, McMaster University, Hamilton, Ontario (1974).

4. McFarlane, R.M., M. Eng. Thesis, McMaster University, Hamilton, Ontario (1980).

5. Harris, T.H., "DGDAC Manual", Internal Report, Dept. of Chem. Eng., McMaster University, Hamilton, Ontario (1974).

6. Tremblay, J.P., Ph.D. Thesis, McMaster University, Hamilton, Ontario (1977).

7. Orlikas, A., M. Eng. Thesis, McMaster University, Hamilton, Ontario (1970).

8. Shaw, I.D., Hoffman, T.W. and P.M. Reilly, AIChE Symp. Ser., vol. 70, No. 141, 41-52 (1973)

9. Orcutt, J.C., Davidson, J.E. and R.L Pigford, Chem. Eng. Prog. Symp. Ser., No. 58, 38: 1-15 (1968).

10. Kato, K. and C.Y Wen, Chem. Eng. Sci., 24: 1351-1369 (1969).

11. Kobayashi, H., Arai, F. and T. Sunagawar, Chem. Eng. Tokyo, 29: 858 (1965).

12. Kjaer, J., "Thermodynamic Calculations on an Electronic Digital", Akademisk Forlag, Copenhagen (1963).

13. Bobrow, S., M.Eng. Thesis, McMaster University, Hamilton, Ontario (1969).

14. Bobrow, S., Johnson, A.I. and J.W. Ponton, "DYNSYS Manual", Dept. of Chem. Eng., McMaster University, Hamilton, Ontario (1970).

15. Jutan, A., MacGregor, J.F. and J.D. Wright, AIChE J, 23, No. 5: 742-750 (1977).

16. Marquardt, D.W., J. Soc. Ind. Appl. Math., 2:   (1963).

17. Dahlin, E.B., Instruments and Control Systems, 41: 77-83 (1968).

18. Astrom, K.H. and B. Wittenmark, Automatica, 9: 185-199 (1973).

19. Astrom, K.H., Borisson, U., Ljung, L. and B. Wittermakr, Automatica, 13: 457-476 (1977).

20. Clarke, D.W. and B.A. Fawthrop, Proc. IEE, 122: 929-934 (1975).

21. Boc, G.E.P. and G.M. Jenkins, "Time Series Analysis: Forecasting and Control", Holden-Day (1970).

22. Harris, T.J., M.Eng. Thesis, McMaster University, Hamilton, Ontario (1977).

23. Harris, T.J., MacGregor, J.F. and J.D. Wright, Technometrics, 22: 153-164 (1980).

24. Wilson, G.T., Ph.D. Thesis, University of Lancaster (1970).

25. Astrom, K.J., "Introduction to Stochastic Control Theory", Academic Press (1970).

26. Clarke, D.W. and R. Hastings-James, Proc. IEEE, 118, No. 10, 1503 (1971).

27. Borisson, U., Report 7513, Dept. of Automatic Control, Lund Institute of Technology (1975).

28. Jutan, A., Tremblay, J.P., MacGregor, J.F. and J.D. Wright, AIChE J, 23: 732-742 (1977).

29. Jutan, A., Wright, J.D. and J.F. MacGregor, AIChE J, 23: 751-758 (1977).

Section 3.3

A_c area for heat transfer between oil in heating/cooling coil and wall, m^2

A_w area for heat transfer between catalyst bed and wall, m^2

C concentration, mg mol/m^3

C_{pB} heat capacity of catalyst particles, J/(kg.K)

$\bar{C}_{pg}$ average molal heat capacity of gas, J/(kg mol.K)

C_{poil} heat capacity of oil, J/(kg.K)

C_{pw} effective heat capacity of wall, J/(kg.K)

d_b bubble diameter, m

d_p average particle diameter, m

F = 0.9, fraction of n-butane that reacts to form propane

g acceleration due to gravity, m/s^2

H height of bed at fluidization conditions, m

ΔH_j heat of reaction of the jth reaction, kJ/Kg mol

h_c effective heat transfer coefficient between oil and wall, J/(s.m^2.K)

h_w effective heat transfer coefficient between catalyst bed and wall, J/(s.m^2.K)

M_w mass of reactor wall, kg

n_o number of holes in perforated plate per unit areas, m^{-2}

N number of bubbles per unit volume of bed, m^{-3}

Q transfer rate, m^3/(s.bubble)

Q_{loss} heat loss from the wall, J/s

R gas law constant, m^3.Pa/(kg mol.K)

r_i rate of reaction of a component, kg mol/s

R_j rate of reaction of a component, kg mol/s

S	cross sectional area of bed, m^2
S	surface area of bubble, m^2
t	time, s
T	temperature, K

Subscripts for T:

oil,in	oil entering heating/cooling coil
oil,out	oil exiting heating/cooling coil
R	reactor catalyst bed
oil	average bulk temperature of oil in heating/cooling coil
w	reactor wall
u_b	bubble rise velocity, m/s^2
u_{mf}	superficial velocity at minimum fluidization, m/s
V	= SH, bed volume under fluidizing conditions, m^3
V_b	average bubble volume, m^3
V_e	volume of emulsion phase, m^3
V_o	total volumetric flowrate of inlet gas, m^3/s
W	weight of catalyst, kg
w_{oil}	mass flowrate of oil in heating/cooling circulating system, kg/s

Greek Letters:

ϵ	bed void fraction, dimensionless
$\bar{\rho}_g$	average molal density of gas, kg mol/m^3
ρ_p	average particle density, kg/m^3

Subscripts:

b   bubble phase

e   emulsion phase

o   feed

Section 4.3

$A(z^{-1})$ denominator of process dynamic transfer function (4.3.1)

a_t random shock

$\tilde{B}(z^{-1})$ numerator of process dynamic transfer function (4.3.1)

b   number of whole periods of delay

$C(z^{-1})$ polynomial in z^{-1}

d   order of the pole lying on unit circle of disturbance model (4.3.2)

$E\{\}$ mathematical expectation operator

FLAM   forgetting factor for discounted least squares (4.3.21)

$\underline{K}_t$ weighting vector for recursive least squares (4.3.10)

ℓ order of $\beta(z^{-1})$

m.   order of $\alpha(z^{-1})$

N_t disturbance affecting process output (4.3.3)

(p,d,q)   orders of polynomials in disturbance model

$\underline{P}_t$ weighting matrix for recursive least squares

t   time

U   manipulated variable or process inputs (mean corrected)

Y   controlled variable or process output (setpoint corrected)

z feedforward variable

z^{-1} backward shift operator

$\alpha(z^{-1})$ numerator of controller transfer function

$\beta(z^{-1})$ denominator of controller transfer function

ε_{t+b} b step ahead forecast error (4.3.6)

$\underline{\theta}_t$ vector of controller parameters to be estimated

$\theta(z^{-1})$ moving average term in disturbance model (4.3.2)

$\phi(z^{-1})$ autoregressive term in disturbance model (4.3.2)

Φ_t objective function for constrained control

$\delta(z^{-1})$ denominator of process dynamic transfer function (4.3.2)

ξ, ξ', ξ'' constraining weights

$\omega(z^{-1})$ numerator in process transfer function (4.3.2)

∇ difference operator $(1 - z^{-1})$

Superscripts:

$\hat{}$ estimate of the particular value

APPENDICES

A. Calibration Procedures

B. Illustration

C. Computer Program Listings

A.2.1 Calibration Procedure for the Flow System

A.2.1.1 n-butane flowrate

A wet-test meter was used to calibrate the flowrates of n-butane which ranged from .0045 m³/min (.15 s.c.f.m.) to .02 m³/min (.70 s.c.f.m.) for a total volumetric feedrate of .1 m³/min at S.T.P. when the ratio was constrained between 4 and 20. The zero and span on the butane ΔP transmitter was adjusted so that approximately 2 to 9.5 volts were produced respectively, across the dropping resistor on the output of the transmitter. At a suppling pressure of 239.2 kPa (20 p.s.i.g.) and a backpressure of 128.9 kPa (4 p.s.i.g.) on the rotameter, the calibration curve for the rotameter is shown in Figure A.2.1. A straight line fit to the calibration data in Figure A.2.2 gave the n-butane calibration equation for minicomputer software:

$$(u_{C_4})^2 = -.6233 + .15876 * (\text{ADC units})$$

where u_{C_4} was in s.c.f.m.

and   ADC units are 0-4095 computer units corresponding to 0-10 volts at the A/D input.

A.2.1.2 hydrogen flowrate

The flowrates of hydrogen ranged from .08 m/min (2.8 s.c.f.m.) to .095 m/min (3.34 s.c.f.m.) for the same total volumetric feedrate of .1 m/min at S.T.P. and the ratio being constrained between 4 and 20. Since these are high flowrates, nitrogen and a precision nozzle (Cox Instruments) was used and the results were corrected for hydrogen. The
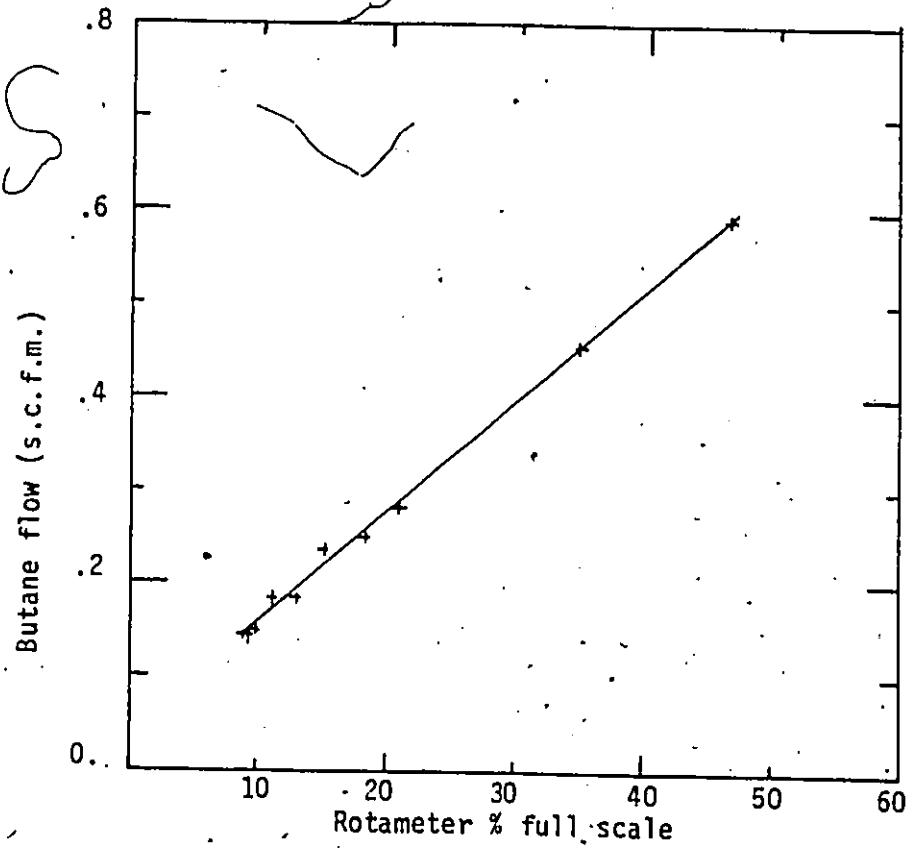
Figure A.2.1 Rotameter Calibration for n-butane Flow
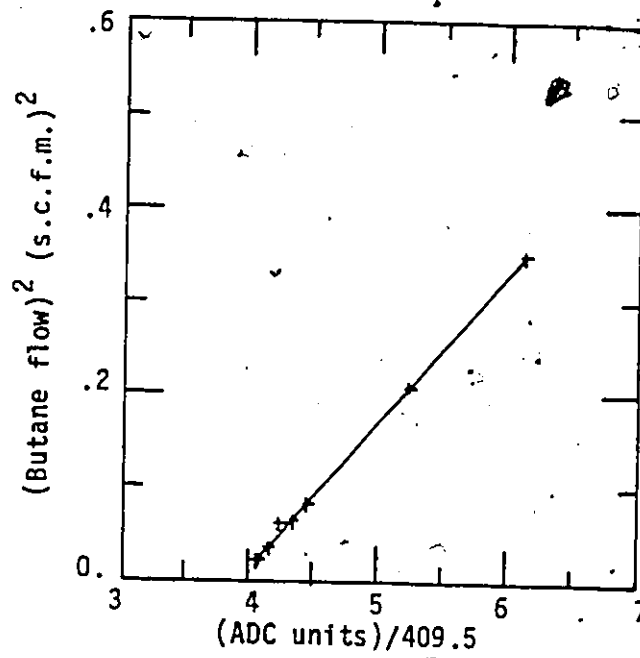
Figure A.2.2 Computer Calibration Plot for n-butane Flow

zero and span on the ΔP transmitter was again adjusted to produce approximately 2 to 9.5 volts respectively across the dropping resistor.

At a supplying pressure of 211.6 kPa (16 p.s.i.g.) and a back-pressure of 128.9 kPa (4 p.s.i.g.) on the rotameter, the rotameter calibration curve is shown in Figure A.2.3. The straight line fit to the calibration data in Figure A.2.4 gave the hydrogen calibration equation:

$$(u_{H_2})^2 = -6.1101489 + 3.1037964 * (ADC\ units)$$

where u_{H_2} was in s.c.f.m.
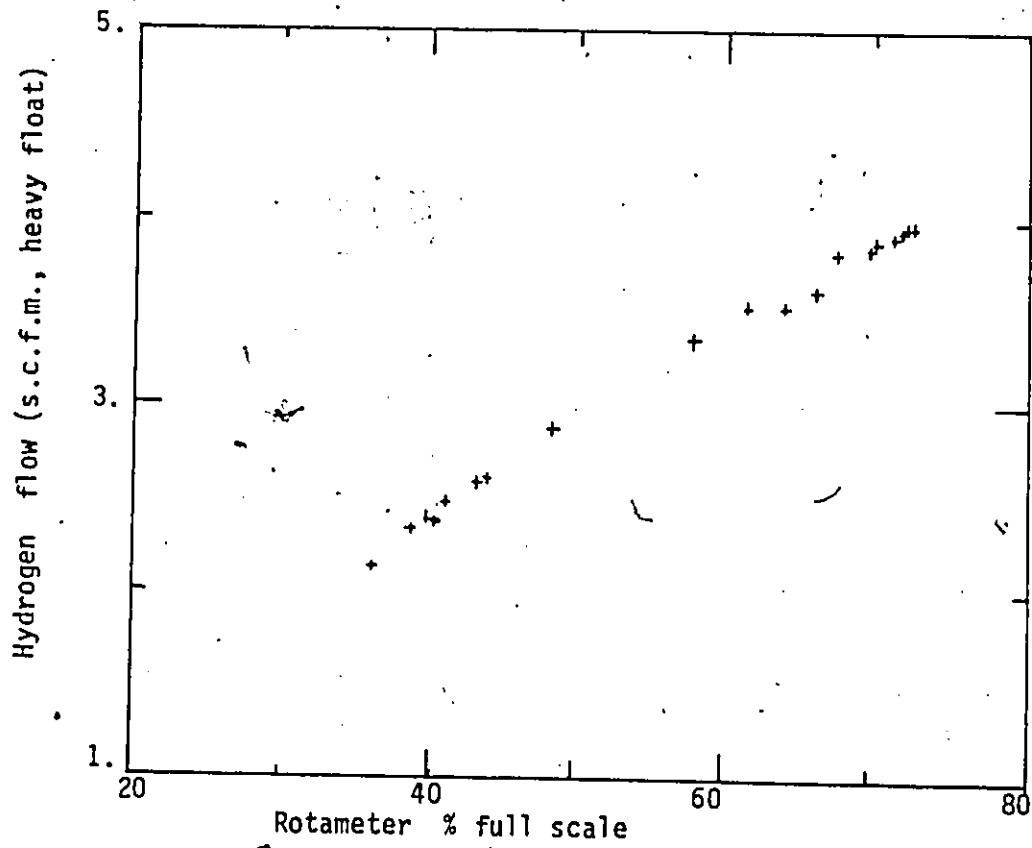
Figure A.2.3 Rotameter Calibration for Hydrogen Flow
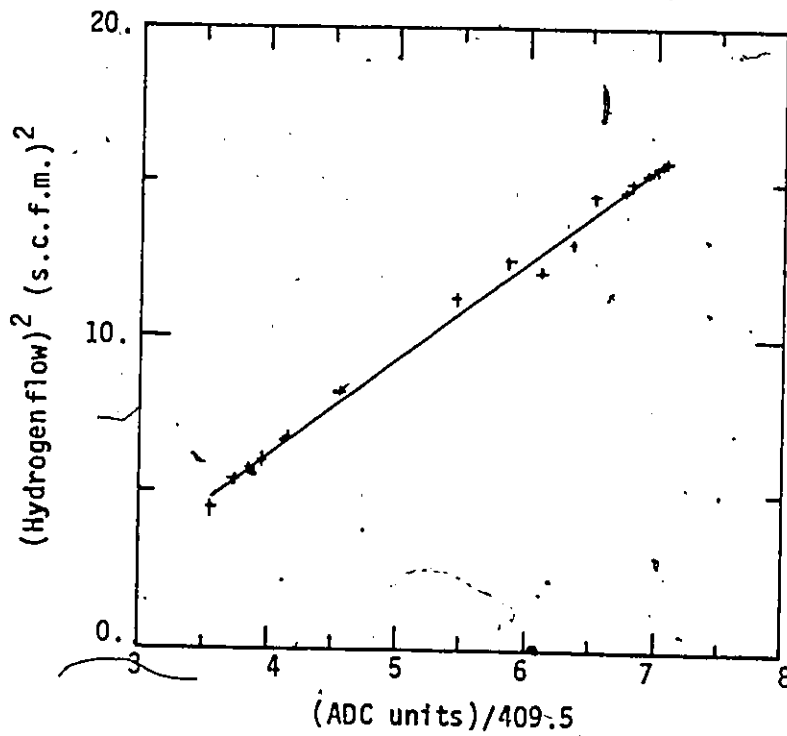
Figure A.2.4 Computer Calibration Plot for Hydrogen Flow

A.2.2 .The Beckman Model 6700 Gas Chromatograph

A.2.2.1 Settings of component boards in the programmer

The settings of the component boards used for the experimental study reported in Chapter 6 were as follows:

Component		C_1	C_2	C_3	C_4
Time	On	212	300	39	90
	Off	279	348	74	195
Component Function Switches	X1 range	OFF	ON	OFF	OFF
	X10 range	OFF	OFF	ON	ON
	auto zero	OFF	OFF	OFF	OFF
	polarity	OFF	OFF	OFF	OFF
	reverse	ON	ON	ON	ON
	hi/lo	LO	LO	LO	LO
Memory Select		6	5	4	3

A.2.2.2 Procedure for preparation of a calibration sample

The procedures for preparing a calibration mixture is as follows:

1. Vent bottle with 'BOTTLE VENT'

2. Close all 'A' valves (i.e. hydrogen, butane etc)

3. Ensure 'VACUUM TO ATMOSPHERE" and "VACUUM SOURCE' are closed

4. Turn on vacuum pump and slowly open "VACUUM SOURCE' until the vacuum
   is ~131.mm on left leg of Hg manometer.

5. Satrt adding gases

   a) butane

       - crack cylinder, pressure ≃ 20 p.s.i.g.

       - open main butane valve on packed bed front panel

       - quickly vent butane supply line by opening 'SUPPLY VENT'

       - add butane by opening 'A' valve for butane

       - close butane valve on front panel

   b) propane

       - crack cylinder, pressure ≃ 30 p.s.i.g.

       - vent line with 'SUPPLY VENT ' toggle

       - add desired amount by opening 'A' valve for propane

   c) ethane

       - same procedure as (b), but pressure ≃ 48 p.s.i.g.

   d) methane

       - same procedure as (b), but pressure ≃ 30 p.s.i.g.

   e) hydrogen

       - same procedure as (a)

6. Shut off all cylinders. Vent supply lines with 'VENT'

A.2.3 Calibration curves for different components

The calibration procedure for the gas chromatograph can be found 4 . The calibration data used to fit the calibration equation for methane, ethane, propane and butane are shown in Figures A.2.5, A.?.6, A.2.7 and A.2.8 respectively. The straight line fit to the data gave the calibration equation for each of the components:

$$X_{C_1} = -.12230 + .1633e\text{-}3 * (\text{ ADC units })$$

$$X_{C_2} = -.71312E\text{-}2 + .89712E\text{-}5 * (\text{ ADC units })$$

$$X_{C_3} = -.45635e\text{-}2 + .70969E\text{-}5 * (\text{ ADC units })$$

$$X_{C_4} = -.44743E\text{-}1 + .55301E\text{-}4 * (\text{ ADC units })$$

where   X is the absolute mole fraction of the component in the sample.
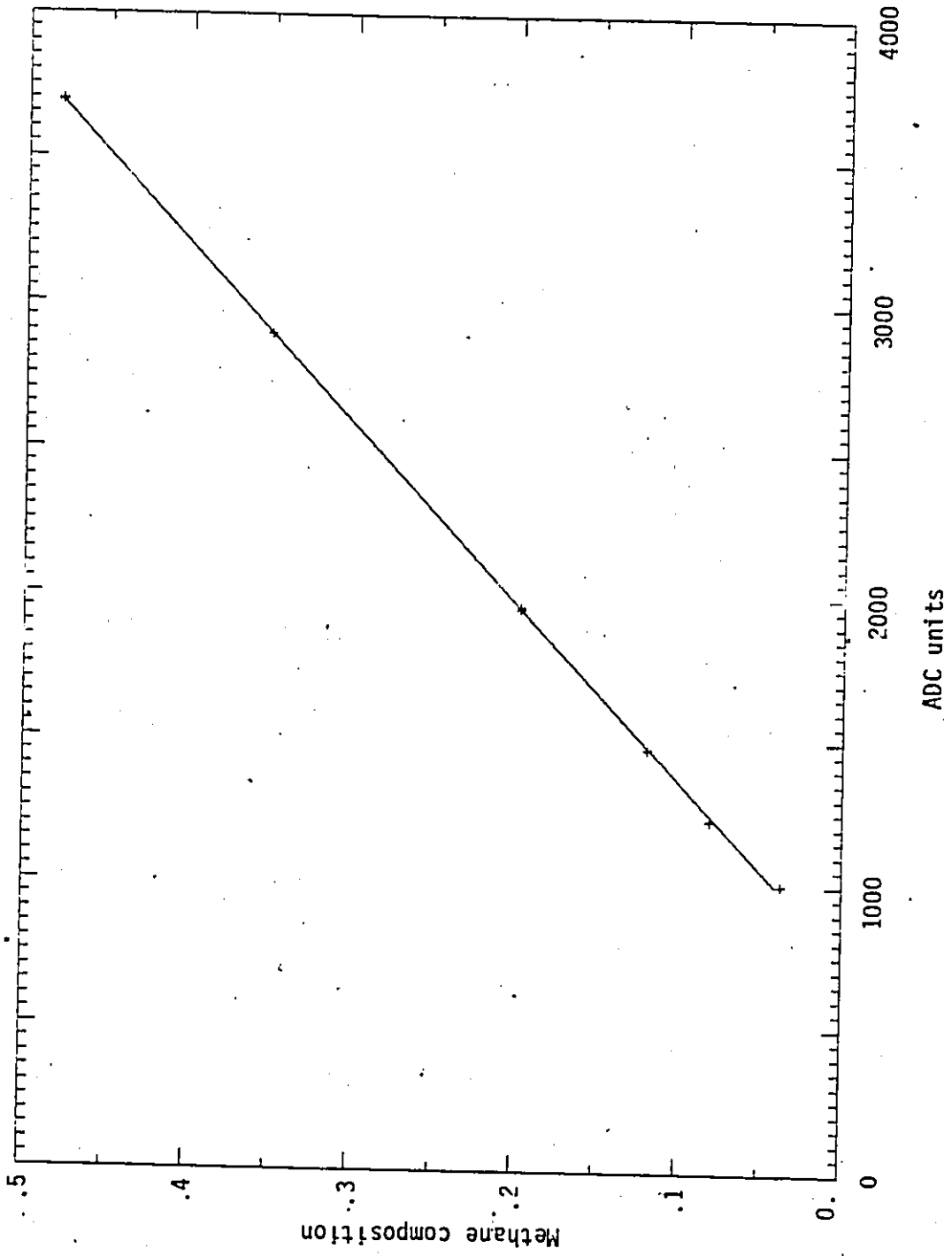
Figure A.2.5   Computer Calibrattion Plot for Methane Composition
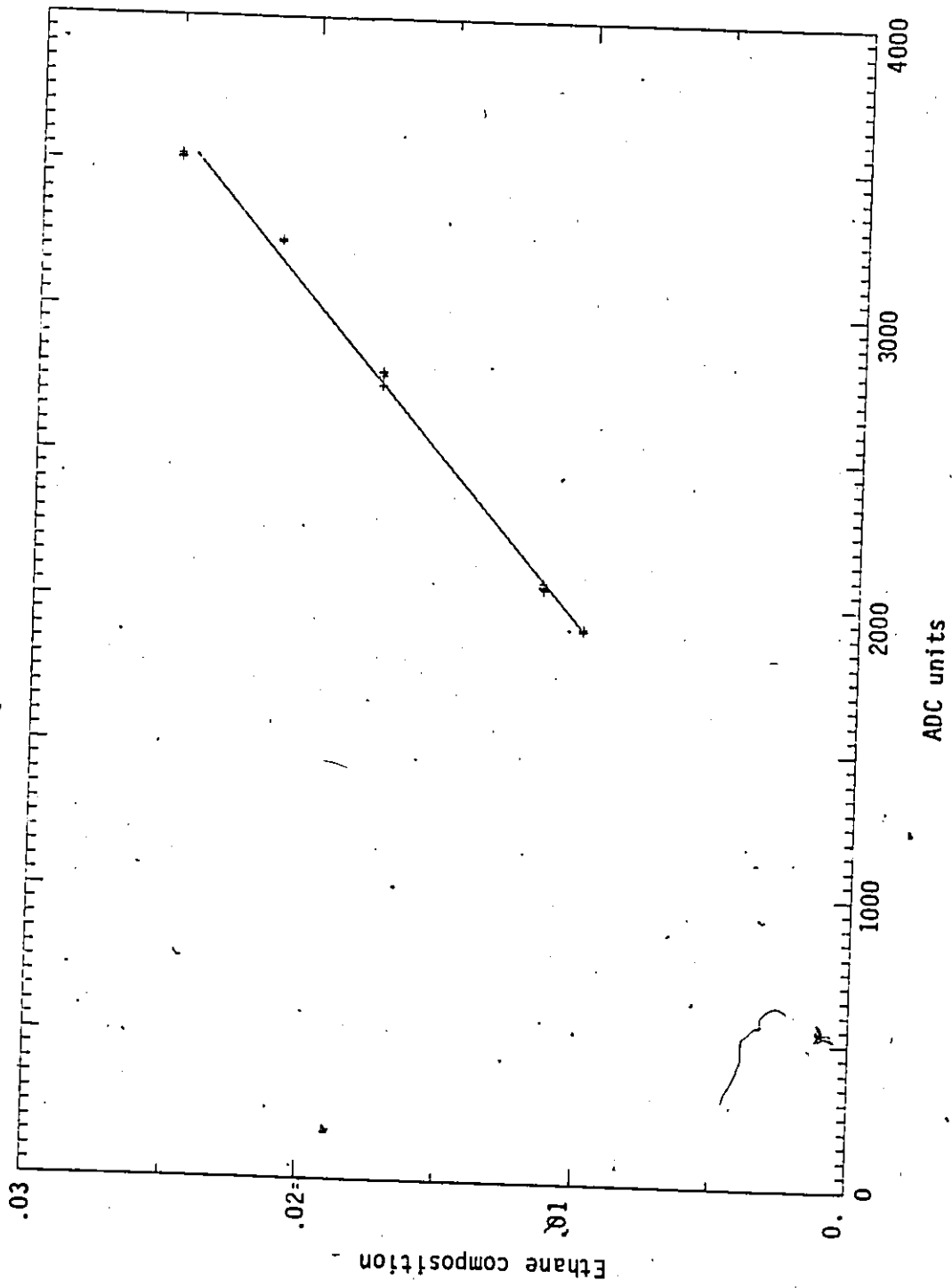
Figure A.2.6 Computer Calibration Plot for Ethane Composition
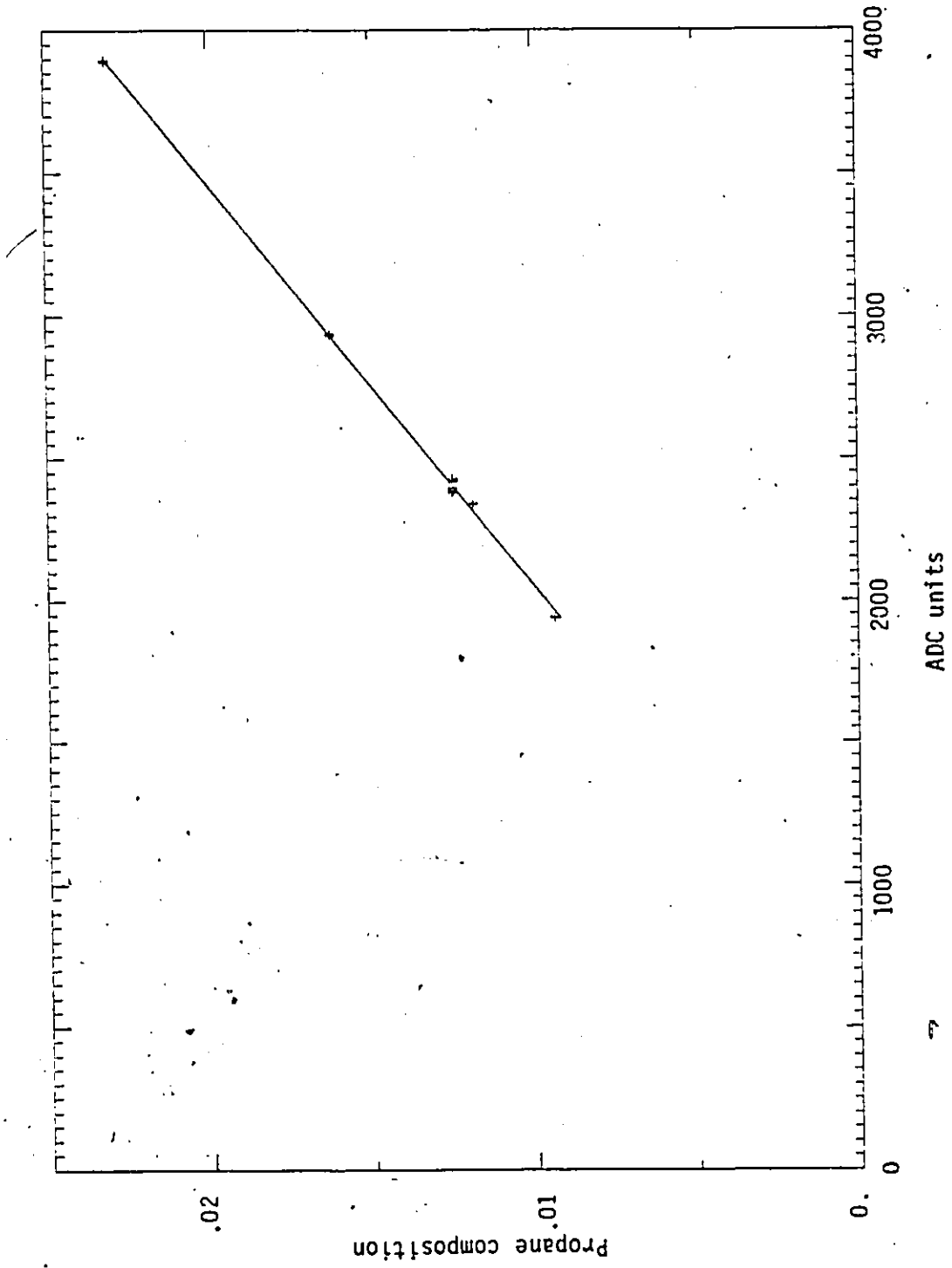
Figure A.2.7 Computer Calibration Plot for Propane Composition
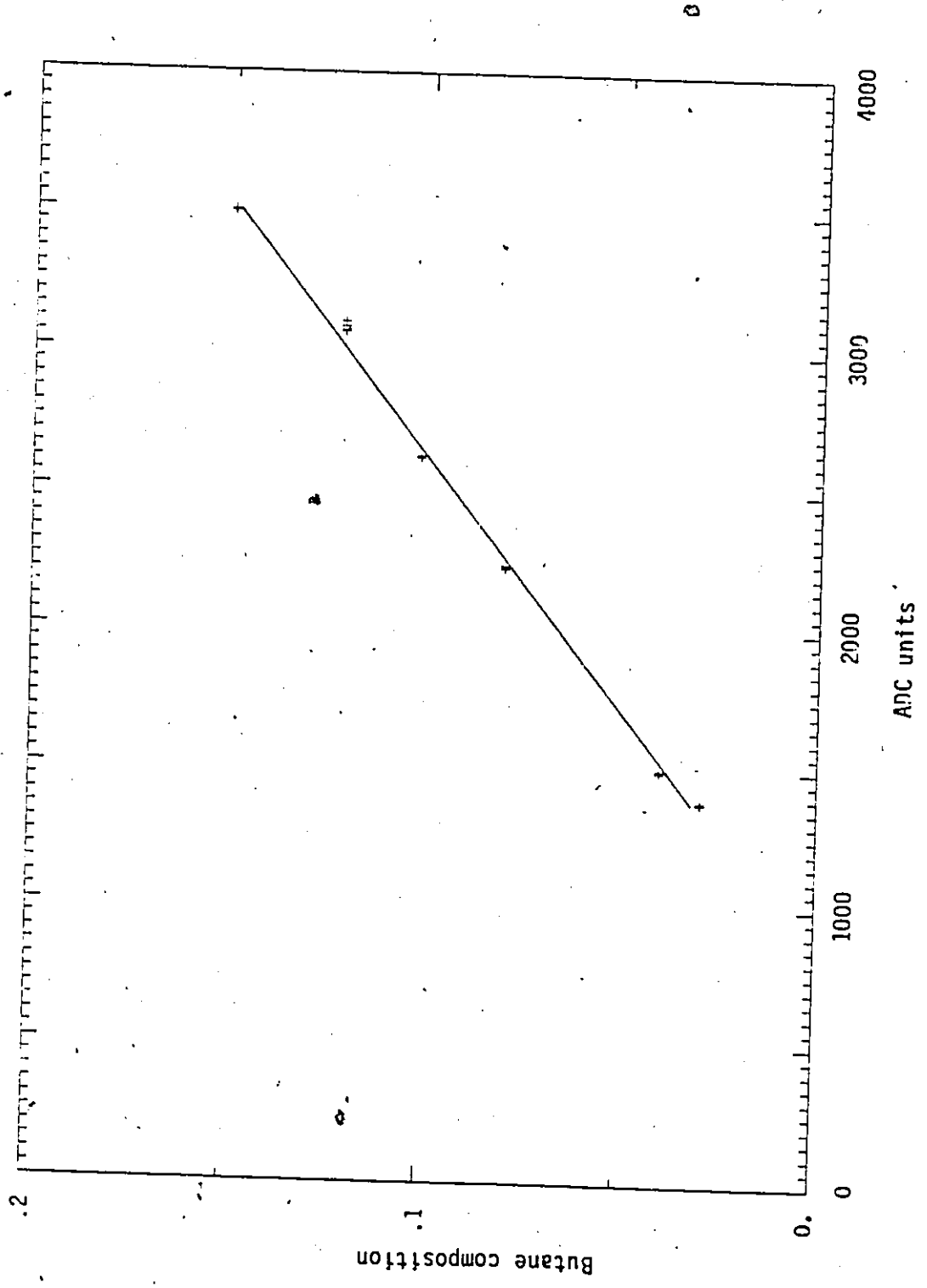
Figure A.2.8 Computer Calibration Plot for Butane Composition

B.4.1 To Compute the Structure of Constrained STR for Reaction Temperature Control in Inner Loop

From Equation (4.3.17), the term

$$N_{t+1} = \frac{1 - \theta z^{-1}}{1 - z^{-1}} a_{t+1} \qquad (B.4.1)$$

can be represented by the one step ahead forecast and the forecast error as in Equation (4.3.4)

$$\frac{1 - \theta z^{-1}}{1 - z^{-1}} a_{t+1} = \psi_1(z^{-1})a_{t+1} + \frac{T(z^{-1})}{1 - z^{-1}} a_t \qquad (B.4.2)$$

$\psi_1(z^{-1})$ and $T(z^{-1})$ can be found by equating the coefficients on left-hand-side and right-hand-side of Equation (B.4.2)

$$1 - \theta z^{-1} = 1(1 - z^{-1}) + T(z^{-1})z^{-1}$$
$$1 - \theta z^{-1} = 1 - z^{-1} + (1 - \theta)z^{-1}$$
$$\psi_1(z^{-1}) = 1 \qquad (B.4.3)$$
$$T(z^{-1}) = 1 - \theta \qquad (B.4.4)$$

The Equation (B.4.2) becomes

$$\frac{1 - \theta z^{-1}}{1 - z^{-1}} a_{t+1} = a_{t+1} + \frac{1 - \theta}{1 - z^{-1}} a_t \qquad (B.4.5)$$

Substituting Equation (B.4.5) into Equation (4.3.17) yields

$$Y_{t+1} = \frac{\omega_0}{1 - \delta z^{-1}} u_t + a_{t+1} + \frac{1 - \theta}{1 - z^{-1}} a_t \qquad (B.4.6)$$

The minimum variance controller can be derived by minimizing $E(Y_{t+1}^2)$.

Taking expectation of the square of Equation (B.4.6) gives

$$E(Y_{t+1}^2) = E\{\frac{\omega_0}{1 - \delta z^{-1}} U_t + \frac{1 - \theta}{1 - z^{-1}} a_t\}^2 + E\{a_{t+1}\}^2 +$$

$$2 E\{(\frac{\omega_0}{1 - \delta z^{-1}} U_t + \frac{a_t}{1 - z^{-1}})(a_{t+1})\} \qquad (B.4.7)$$

The third term on the right-hand-side of Equation (B.4.7) is equal to zero, thus Equation (B.4.7) becomes

$$E(Y_{t+1}^2) = E\{\frac{\omega_0}{1 - \delta z^{-1}} U_t + \frac{1 - \theta}{1 - z^{-1}} a_t\}^2 + E\{a_{t+1}\}^2 \qquad (B.4.8)$$

$E(Y_{t+1}^2)$ can be minimized by setting

$$\frac{\omega_0}{1 - \delta z^{-1}} U_t = \frac{1 - \theta}{1 - z^{-1}} a_t \qquad (B.4.9)$$

Thus

$$\nabla U_t = \frac{(1 - \delta z^{-1})(1 - \theta)}{\omega_0} a_t \qquad (B.4.10)$$

where $\nabla U_t = U_t - U_{t-1}$

Under this controller, $Y_{t+1} = a_{t+1}$ or $Y_t = a_t$. Substitute a_t into Equation (B.4.10) gives

$$\nabla U_t = \frac{(1 - \delta z^{-1})(1 - \theta)}{\omega_0} a_t \qquad (B.4.11)$$

By Equation (4.3.15) Clarke and Gawthrop [20] constrained STR will be of

the form

$$\nabla U_t = -\frac{(1 - \delta z^{-1})(1 - \theta)}{\omega_0 + \frac{\xi'}{\omega_0}(1 - \delta z^{-1})} \xi_t \qquad (B.4.12)$$

The controller thus has the structure

$$\beta_0 \nabla U_t = \beta_1 \nabla U_{t-1} + \alpha_0 Y_t + \alpha_1 Y_{t-1} \qquad (B.4.13)$$

C.3.1 Program Listing of Module HOLD01 : TYPE 8

```
      SUBROUTINE TYPE 8
      COMMON/CON/IG,KLOOP,NCOMP,NC5,DELT,NE,TIME(30),NS,NPR,TOLL,TOLU,
     +           EMAX,NPOL,TMAX,NCOUNT,JM,KJ,MPR,NGIM
      COMMON/MAT/MP(20,8),EP(20,5),S(2,500,20),EX(100)
      COMMON/UNIT/IM,NMP
      COMMON/PRED/S1,S2,S3,CON
      REAL MW(5)
      DIMENSION Y(10),X(5),DY(10)
      DATA MW/58.,44.,30.,16.,2./
C
C     REACTOR DISENGAGING SECTION MODULE
C     WRITTEN DEC 07, 80, SM YANG
C     PERFECTLY MIXED TANK
C
C     INITIAL CONCENTRATIONS IN THE DISENGAGING SECTION TAKE THE
C     VALUE OF THE CONC OF THE GAS LEAVING THE REACTION SECTION
C     OBTAINED AFTER THE FIRST PREDICTOR STEP
C
C     INFORMATION STREAM LIST
C
C     1   STREAM NO
C     2   FLAG
C     3   TOTAL FLOW
C     4   TEMP      DEG C
C     5
C     NAME THE STREAMS AND INFORMATION
C
      IN=MP(IM,3)
      IOUT=IABS(MP(IM,4))
      TO=S(IG,IN,4)-EP(IM,2)
C
C     DETERMINE VOLUMETRIC FLOW RATE IN
C     AMOLE = TOTAL # MOLES IN       MOLE/SEC
C     QIN   = VOLUMETRIC FLOWRATE IN     L/SEC
C
      AMOLE=0.
      DO 10 I=1,5
        II=I+5
   10 AMOLE=AMOLE+S(IG,IN,II)/MW(I)
      QIN=AMOLE*22.4
C
C     DETERMINE VOLUMETRIC FLOWRATE OUT
C
      QO=QIN*(TO+273.2)/273/S(IG,IN,5)
C
C     DETERMINE MASS HOLD-UP OF EACH COMPONENT IN THE VOLUME ON
C     CORRECTOR STEP
C
      INDEX=MP(IM,NMP+1)
      IF(IG.EO.1)GO TO 21
      DO 20 I=1,5
        II=I+5
   20 EX(INDEX+II-1)=S(IG,IN,II)*EP(IM,1)/QIN
C
   21 DO 30 I=1,5
   30 Y(I)=EX(INDEX+(IG-1)*5+I-1)
      DO 40 I=1,5
        II=I+5
   40 DY(I)=S(IG,IN,II)-QO*Y(I)/EP(IM,1)
C
C        CARRY OUT INTEGRATION VIA FUNCTION Y1
C
      DO 50 I=1,5
        II=I+5
```

```
      EX(INDEX+I-1)=Y1(1,EX(INDEX+II-1),DY(I),EX(INDEX+I-1))
      IF(IG.EQ.1)EX(INDEX+II-1)=EX(MP(IM,NMP+1)+I-1)
      Y(I)=EX(INDEX+I-1)
50 CONTINUE
C
C   FILLING IN OUTLET STREAMS
C
   DO 60 I=1,5
      II=I+5
60 S(IG,IOUT,II)=QO*Y(I)/EP(IM,1)
   S(IG,IOUT,11)=0.
   S(IG,IOUT,12)=0.
   S(IG,IOUT,4)=TO
   S(IG,IOUT,5)=1.
   S(IG,IOUT,2)=5.
C
C   CHECK IF SAMPLING STREAM IS NECESSARY
C
   IF(MP(IM,5).GE.0) GO TO 500
C
C   SET UP SAMPLING STREAM
C
   IOUT=IABS(MP(IM,5))
C
C   CALCULATE SELECTIVITY
C
   DO 70 I=1,4
      II=I+5
70 X(I)=S(IG,IOUT,I)/MW(I)
   FAC=.75*X(3)+.5*X(2)+.25*X(1)
   S1=X(1)/FAC
   S2=X(2)/FAC
   S3=X(3)/FAC
   CON=1./(X(4)/FAC+1)
500 RETURN
   END
```

C.3.2 Program Listing of KACT1

```
      PROGRAM KACT1(INPUT,OUTPUT,KXIOU,KXOOU,TAPE5=KXIOU,TAPE6=OJTPUT,
     +TAPE3=KXOOU)
      DIMENSION Y(75),TH(1),DIFF(1),SIGNS(1),SCRAT(250)
      DIMENSION XY(25,40)
      EXTERNAL MODEL
      COMMON/A/FLOW(25),T(25),FEED(5,9),NR
      DATA NPROB,NP/1,1/
      DATA NR,IOBS/3,9/
      DATA TH/5.3/
      DATA EPS1,EPS2/0.,1.E-3/
      DATA MIT,FLAM,FNU/15,.1,10./
      DATA DIFF,SIGNS/.01,1./

      REWIND 3
      REWIND 5

      P=1.1
C     READ AND VERIFY DATA
C
C
C     READ TEMPS AND FLOWS
C
      DO 105 I=1,IOBS
      READ(5,107)I1,I2,I3
      WRITE(3,107)I1,I2,I3
      READ(5,106)(XY(I,J),J=1,8)
      WRITE(3,106)(XY(I,J),J=1,8)
      READ(5,106)(XY(I,J),J=9,16)
      WRITE(3,106)(XY(I,J),J=9,16)
      READ(5,108)(XY(I,J),J=17,23)
      WRITE(3,108)(XY(I,J),J=17,23)
      READ(5,108)(XY(I,J),J=24,30)
      WRITE(3,108)(XY(I,J),J=24,30)

      TFEED=XY(I,16)+273.1
      C4SCFM=XY(I,18)
      SCFM=XY(I,19)
      FLOW(I)=SCFM*TFEED/(273.1*P)
      TR=XY(I,23)
      T(I)=TR*9./5.+32.1
      FEED(1,I)=0.
      FEED(2,I)=0.
      FEED(3,I)=0.
      FEED(4,I)=C4SCFM*P/SCFM
      FEED(5,I)=P-FEED(4,I)
105   CONTINUE
107   FORMAT(1X,3I4)
106   FORMAT(1X,8F9.2)
108   FORMAT(1X,7F9.3)
109   FORMAT(1X,I3,F6.0,16F7.2)
C
C     READ S3 AND CONVERSION DATA
C
      DO 501 I=1,IOBS
      READ(5,510)IM1,IM2,IM3
      WRITE(3,510)IM1,IM2,IM3
      READ(5,511)S1,S2,S3,CONV
      WRITE(3,511)S1,S2,S3,CONV
      XY(I,31)=S2
      XY(I,32)=S3
      XY(I,33)=CONV
      READ(5,511)X1,X2,X3,X4
      WRITE(3,511)X1,X2,X3,X4
      Y(3*I-2)=S2
      Y(3*I-1)=S3
```

```
      Y(3*I)=CONV
  501 CONTINUE
  510 FORMAT(1X,3I5)
  511 FORMAT(1X,4F10.5)
  502 CONTINUE


C     WRITE XY MATRIX
      WRITE(6,220)
      WRITE(3,220)
  220 FORMAT(//3X,"I",5X,"H2SCFM",4X,"C4SCFM",4X,"FLOW",8X,"TR",8X,
     +      "PC4",6X,"PH2",6X,"S2",6X,"S3",6X,"CONV"/)
      DO 505 I=1,IOBS
  505 WRITE(3,515)I,(XY(I,J),J=17,18),FLOW(I),T(I),FEED(4,I),FEED(5,I),
     +     (XY(I,J),J=31,33)
      WRITE(6,515)I,(XY(I,J),J=17,18),FLOW(I),T(I),(FEED(J,I),J=4,5),
     +     (XY(I,J),J=31,33)
  515 FORMAT(1X,I4,6F10.3,3F10.5)
      NOB=IOBS*NR
      CALL UWHAUS(NPROB,MODEL,NOB,Y,NP,TH,DIFF,SIGNS,EPS1,EPS2,MIT,FLAM
     +            FNU,SCRAT)
      STOP
      END

      SUBROUTINE MODEL(NPROB,TH,YPRED,NOB,NP)
      INTEGER P
      DIMENSION A(13),OUT(5)
      DIMENSION TH(NP),YPRED(NOB)
      COMMON/A/FLOW(25),T(25),FEED(5,9),NR
      A(1)=5.1E04
      A(2)=4.0E04
      A(3)=3.0E04
      A(4)=1.6E04
      A(5)=15.6604
      A(6)=10.6322
      A(7)=12.2229
      A(8)=6.8140
      A(9)=-2.155
      A(10)=-2.0753
      A(11)=2.6E04
      A(12)=4.5208
      A(13)=-2.2115
      A(5)=10.**A(5)
      A(6)=10.**A(6)
      A(7)=10.**A(7)
      A(8)=10.**A(8)
      A(12)=10.**A(12)
      HO=47.6
      XFAC=0.426
      GRAV = 980.0
      DBMAX = 10.0
      UMF = 0.77
      HN = 20.0
      RHOS = 0.957
      DP = 0.015

      IOBS=NOB/NR
      DO 500 I=1,IOBS

      U = FLOW(I)*1.46042
      TEMP = (T(I)-32.)*(5./9.) + 273.1
      UEMUL = UMF
      HMF = HO*1.043
      DO = 0.3261*(((U-UEMUL)*HN)**0.4)
      G1 = 1.0
```

```
      UX = U/G1
      HDBMAX = (DBMAX-DO)*UMF/(1.4*RHOS*DP*U)
      DBMEAN = DBMAX - 0.9
    2 HT = HMF*(1.0 + (U-UEMUL)/(0.711* SQRT(980.*DBMEAN)))
      DBSAVE = DBMEAN
      DBMEAN = ((DBMAX-DO)*0.5*HDBMAX + DBMAX*(HT-HDBMAX))/HT
      IF( ABS(DBSAVE-DBMEAN).GT.0.0001)GO TO 2
      Q = XFAC*11.0/DBMEAN
      X =-Q*HT/(0.711* SQRT(GRAV*DBMEAN))
      NH2 = 0
      NSW=1
      MSW = 1
      TOL=0.000001
      RTT=1.99*TEMP
      FAC = (1.0-0.557)/(1.0-0.449)
      RKB=TH(1)*FAC*A(5)* EXP(-A(1)/RTT)
      RKP1=TH(1)*FAC*A(6)* EXP(-A(2)/RTT)
      RKP2=A(7)* EXP(-A(3)/RTT)
      RKE2 = TH(1)*FAC*A(12)* EXP(-A(11)/RTT)
      RKE=A(8)* EXP(-A(4)/RTT)
      EXPX = EXP(X)
      GAM = (U*(1.0-(1.0-UEMUL/U)/EXPX))/(82.06*TEMP*HMF)
      P5 = FEED(5,I)
C
C
      REACTION KINETICS FOR EMULSION WHERE THE ONLY REACTION OCCURS
  800 Y2 = P5**A(9)
      P42 = (FEED(4,I)*GAM)/(GAM + RKB*Y2)
      RB = RKB*P42*Y2
      Z1=0.9*RB
      Z3 = RKP1*(P5**A(10))
      P32 = (Z1+FEED(3,I)*GAM*(1.0+RKP2))/(Z3+GAM*(1.0+RKP2))
      RP2=(Z1-Z3*P32)/(1.0+RKP2)
      Z4 = RKE2*(P5**A(13))
      P22 = (1.1*RB-RP2+(1.0+RKE)*GAM*FEED(2,I))/(Z4+(1.0+RKE)*GAM)
      RE2 = (1.1*RB-RP2-Z4*P22)/(1.0+RKE)
      P12=(4.0*RB-3.0*RP2-2.0*RE2)/GAM
      P52 = (FEED(5,I)*GAM - 3.0*RB + 2.0*RP2 + RE2)/GAM
C     SEARCH SO THAT GUESSED H2 WILL BE THE SAME AS THE CALCULATED H2
      PDIF=P5-P52
      IF(NSW.EQ.2) GO TO 703
      IF(PDIF.LE.0.0) GO TO 700
      MSW = 2
      PRT=P5
      P5 = P5 - 0.10
      DIFR=PDIF
      IF(P5.GE.0.0) GO TO 800
      P5 = 0.0001
      IF(NH2.EQ.0) GO TO 701
      P52 = 0.0001
      IPRINT = -999
      GO TO 704
  701 NH2 = 1
      GOTO800
  700 IF(MSW.EQ.1) WRITE(6,996) IPRINT,P5,P52,PDIF
      PLT=P5
      DIFL=PDIF
      NSW=2
      GO TO 750
  703 IF( ABS(PDIF).LT.TOL) GO TO 704
      IF( ABS(PDIF).LT. ABS(DIFR).OR. ABS(PDIF).LT. ABS(DIFL))GO TO 710
      WRITE(6,999) IPRINT,P5,P52,PLT,PRT,PDIF,DIFL,DIFR
  710 IF( ABS(DIFR).LT. ABS(DIFL)) GO TO 730
      IF(PLT.GT.P5) GO TO 715
      PRT = P5
      DIFR = PDIF
```

```
      GO TO 750
  715 PRT = PLT
      DIFR = DIFL
      PLT = P5
      DIFL = PDIF
      GO TO 750
  730 IF(PRT.LT.P5)   GO TO 735
      PLT = P5
      DIFL = PDIF
      GO TO 750
  735 PLT = PRT
      DIFL = DIFR
      PRT = P5
      DIFR = PDIF
  750 P5 = PLT - DIFL*(PRT-PLT)/(DIFR-DIFL)
      GOTO800
C
  704 PB1 = P12 + (FEED(1,I)-P12)/EXPX
      PB2 = P22 + (FEED(2,I)-P22)/EXPX
      PB3 = P32 + (FEED(3,I)-P32)/EXPX
      PB4 = P42 + (FEED(4,I)-P42)/EXPX
      PB5 = P52 + (FEED(5,I)-P52)/EXPX
      F1 = UEMUL/U
      F2 = (U-UEMUL)/U
      OUT(1)=F1*P12+PB1*F2
      OUT(2)=F1*P22+PB2*F2
      OUT(3)=F1*P32+PB3*F2
      OUT(4)=F1*P42+PB4*F2
      OUT(5)=F1*P52+PB5*F2
  380 IF(FEED(4,I) .EQ. 0.)GO TO 390
      F=FEED(4,I)
      DD=FEED(4,I) - OUT(4)
      S3=OUT(3)/DD
      S2=OUT(2)/DD
      GO TO 410
  390 IF(FEED(3,I) .EQ. 0.)GO TO 400
      F=FEED(3,I)
      DD=FEED(3,I) - OUT(3)
      S3=0.
      S2=OUT(2)/DD
      GO TO 410
  400 F=FEED(2,I)
      DD=FEED(2,I)-OUT(2)
      S3=0.
      S2=0.
  410 CONV=100.*DD/F
      S1=OUT(1)/DD
      EMULH2=P52

      YPRED(3*I-2)=S2
      YPRED(3*I-1)=S3
      YPRED(3*I)=CONV
  500 CONTINUE

  996 FORMAT(1X, 40HNEGATIVE ON FIRST STEP OF SEARCH FOR P52, 5X,I3,3F1
     .4)
  999 FORMAT( 1X, 45H THE ORCUTT SEARCH MAY BLOW UP FOR IPRINT =   ,I4,
     17E11.4)
      RETURN
      END
```

C.5.1 Program Listing of DASTFF2.

```
      PROGRAM DASTFF2(INPUT,OUTPUT,DATA,O235,TAPE5=DATA,TAPE6=OUTPUT
     1TAPE3=0235 )

****

      DIMENSION G(6,6),G2(6,6)
      DIMENSION US10(10),YS10(10),ZS10(10),P(6,6),THETA(10),PHI(10)
      DIMENSION US102(10),YS102(10),ZS102(10),P2(6,6),THETA2(10)
      DIMENSION PHI2(10)
      DIMENSION YTP(100),DUTP(100),Y2TP(100),DU2TP(100)
      DIMENSION AC(12),CC(12)
      DIMENSION VS3(1200)
      COMMON/PRED/S1,S2,S3,CON
      COMMON/MAT/MP(20,8),EP(20,5),S(2,50,20),EX(100)
      COMMON/AREA4/IFLAG

****

      REAL NT1,NT
      DATA THETA,THETA2/10*0.,6.,1.4,.2,.1,6*0./
      DATA NP,NP2/2*6/
      DATA IC,IP/0,0/
      DATA NT1/0./
      DATA K1,K2,KL,K2L/2*100,2*10/
      DATA KNT/0/

      DATA BO,RA0,RA1,RA2,RB1,BA1,BA2,BB/8*0./
      DATA B20,R2A0,R2A1,R2A2,R2B1,B2A1,B2A2,B2B/8*0./
C     MAIN PROGRAM TO SIMULATE RESPONSE FROM REACTION TEMP
C     TO RATIO OF HYDROGEN TO N-BUTANE FEEDRATES
C     NSTEP IS THE NUMBER OF INTEGRATION STEPS REQUIRED

      REWIND 5
      PRINT*,"ENTER NSTEP"
      READ*,NSTEP
      PRINT*,"NOISE TO BE ADDED ?"
      READ*,NOIZ
      PRINT*,"INNER TEMP CONTROLLER TO BE ACTIVATED ?"
      READ*,IT1
      PRINT*,"INNER STR TO BE ACTIVATED ?"
      READ*,IST
      IF(IST .NE. 1)GO TO 5
      PRINT*,"ENTER NA, NB & NC"
      READ*,NA,NB,NC
      PRINT*,"ENTER FLAM, ZETA, AETA"
      READ*,FLAM,ZETA,AETA
      IB=1
      NP=NA+NB+NC
*
*     INITIALIZING COVARIANCE MATRIX TO ZERO
*
      DO 19 IR=1,NP
      DO 19J=1,NP
      P(IR,J)=0.
   19 CONTINUE
*
*     INITIALIZING THETA, PHI VECTORS TO ZERO, P DIAGONAL
*     ELEMENTS TO 100.
*
      DO 29 IR=1,NP
      PHI(IR)=0.
      P(IR,IR)=100.
   29 CONTINUE
      THETA(NA+1)=1.
*
*     INITIALIZING US10 & YS10 TO ZERO
*
```

```
      DO 39 IR=1,10
      US10(IR)=0.
      YS10(IR)=0.
  39  CONTINUE

   5  PRINT*,"OUTER LOOP ACTIVATED? -- 1.DAHLIN  2.STR"
      READ*,IOP
      IF(IOP .NE. 2)GO TO 10
      PRINT*,"ENTER NA2, NB2 & NC2"
      READ*,NA2,NB2,NC2
      PRINT*,"ENTER FLAM2, ZETA2 & AETA2"
      READ*,FLAM2,ZETA2,AETA2
      PRINT*,"ENTER IB2"
      READ*,IB2
      NP2=NA2+NB2+NC2
      DO 219 IR=1,NP2
      DO 219 J=1,NP2
      P2(IR,J)=0.
 219  CONTINUE
      DO 229 IR=1,NP2
      PHI2(IR)=0.
      P2(IR,IR)=10.
      IF(IR .GT. NA2)P2(IR,IR)=1.
 229  CONTINUE
      THETA2(NA2+1)=.2
      DO 239 IR=1,10
      US102(IR)=0.
      YS102(IR)=0.
 239  CONTINUE


  10  NDELT=30

C     INFORM SUBROUTINE MODEL1 THAT A NEW INTEGRATION HAS BEEN INITI
      IFLAG=0
C     DEFINE INITIAL TR TW AND TOIL

      TR1=253.
      TW1=249.1
      TOIL1=247.1

C     DEFINE DESIRED TOTAL VOL FLOWRATE TO REACTOR

      SCFM=3.5

C     DEFINE VECTOR OF INPUTS , TFEED AND TOILIN.

      TFEED1=253.
      TFEED2=TFEED1
      TOILIN1=247.


C     DEFINE VECTOR OF DESIRED S3 SETPOINTS

      S3SET=.1

*
*****
*     CREATE VECTORS OF ERRORS FOR OBSERVED RESPONSES
*
      AM=0.
      SD1=.1
      SD2=.1
      SD3=.002
```

```
C        DEFINE THE FIRST 25 TR SETPOINTS WHICH WILL BE USED FOR THE INN
C        LOOP UNTIL THE S3 CONTROLLER TAKES OVER
*        TRSET=253.

         IF(IT1. EQ. 0)GO TO 1100
C        INITIALIVE PAST ERROR FOR TR-RATIO CONTROL.ER
         E2=0.
C        SET TR - RATIO PI PARAMETERS
         C1=1.03
         C2=0.34
C        DEFINE INITIAL FEED FLOWS FOR INTEGRATION STEP, UNTIL TR RATIO
C        CONTROLLER TAKES OVER
 1100    RATIO1=10.29
         C4SCFM1=SCFM/(RATIO1+1.)
         C4SCFM2=C4SCFM1
         H2SCFM1=SCFM-C4SCFM1
         H2SCFM2=H2SCFM1
****
         U=RATIO1
         USSP=RATIO1
*
.
         IF(IOP .EQ. 0)GO TO 1900
C        SET DAHLIN*S PARAMETERS

         EK=-.022
         T=360.
         TAU=250.
         ELAMBDA=500.
         A1=1.-EXP(-T/ELAMBDA)
         A2=EXP(-T/TAU)
         A3=EK*(1.-EXP(-T/TAU))
C        INITIALIZE PAST ERRORS FOR S3 CONTROLLER

         ERR2=0.
         TR2=253.
         TR3=253.
C        PROCEED WITH NSTEP-1 INTEGRATIONS, APPLYING CONTROL ACTION
C        AFTER EACH STEP
 1900    NUMB=NSTEP-1
         DO 2000 I=1,NUMB

C        DEFINE CURRENT AND ONE STEP AHEAD INPUTS
C        2 IS CURRENT TIME, 1 IS ONE STEP AHEAD
         TOILIN2=TOILIN1
           IF(I .GT. 252)TOILIN1=242.

C        INTEGRATE MODULES OVER ONE TIME INTERVAL
         CALL MODEL1(TR1,TW1,TOIL1,TFEED1,TFEED2,TOILIN1,TOILIN2,
        1H2SCFM1,H2SCFM2,C4SCFM1,C4SCFM2,TRP,TWP,TOILP)
```

```
*****         ADD NORMALLY DISTRIBUTED ERROR TO RESPONSES
*
*         IF(NOIZ .EQ. 0)GO TO 2010
*
          CALL GAUSS(13231,SD1,AM,ER1)
*         NT=.7*NT1+ER1
          TRP=TRP+ER1
*         NT1=NT
          CALL GAUSS(137,SD2,AM,ER2)
          TWP=TWP+ER2
          CALL GAUSS(1331,SD2,AM,ER3)
          TOILP=TOILP+ER3
          CALL GAUSS(1234567,SD3,AM,ER4)
          S3=S3+ER4
*
C         STORE THE PREDICTIONS IN THE APPROPRIATE PREDICTION VECTORS
C
 2010 VS3(I)=S3
C         *********************************************************
C
C         TAKE CONTROL ACTION
C
C         *********************************************************
C
C         DAHLIN'S ALGORITHM ON OUTER S3 LOOP
C
C         TEST IF THE 12TH TR-RATIO CONTROL ACTION IS COMING UP.  IF IT IS
C         NEW S3 DATA ARE AVAILABLE AND AN S3 CONTROL ACTION IS REQUIRED
*
*         IF(IOP .EQ. 0)GO TO 128
*
          IF(I .LT. 25)GO TO 128
          IF(I .LT. 30)S3SET=.32
          IF(IC .LT. 11)GO TO 128
          IC=-1
          IP=1
          IF(IOP .NE. 2)GO TO 1126
          Y2=VS3(I-12)
          IF(I .GT. 25)GO TO 1125
          U2=TRP
          USSP2=TRP
          YSP12=S3SET
          YSPM12=YSP12
 1125 YSPM2=AETA2*YSPM12+(1-AETA2)*YSP12
 1126 CONTINUE
          IF(I .GT. 30)S3SET=.25
          IF(I .GT. 80)S3SET=.32
          IF(I .GT. 130)S3SET=.36
          IF(I .GT. 190)S3SET=.40
          IF(IOP .EQ. 1)GO TO 2020
*
          YSP2=S3SET
          Z2=YSP2-YSP12
          IF(NC2 .EQ. 0)YSPM2=YSP2
*
          IF(I .LT. MP2)GO TO 1129
          CALL UYINCR(Y2,YSPM2,Z2,US102,YS102,ZS102)
          CALL FORM(PHI2,YS102(1+IB2),US102(1+IB2),ZS102(1+IB2),NA2,NB2,N
     +         NP2)
          OBFCN2=YS102(1)+ZETA2*US102(1+IB2)
```

```
      DO 11 J=1,NP2
        P2(J,3)=0.
        P2(3,J)=0.
   11 CONTINUE

      CALL RLS(OBFCN2,P2,PHI2,THETA2,FLAM2,NP2)

      IF(N2A .EQ. 2)B2A1=-THETA2(2)/THETA2(1)
      B20=THETA2(NA2+1)
      R2A0=THETA2(1)/B20
      R2A1=THETA2(2)/B20
      R2B1=THETA2(NA2+2)/B20
      IF(NA2 .NE. 3)GO TO 92
      R2A2=THETA2(3)/B20
      DISC2=R2A1*R2A1-4*R2A0*R2A2
      IF(DISC2 .LT. 0.)GO TO 72
        TWO REAL ROOTS
      R21=.5*(-R2A1+SQRT(DISC2))
      B2A1=SQRT(R21*R21)
      R22=.5*(-R2A1-SQRT(DISC2))
      B2A2=SQRT(R22*R22)
      GO TO 92
        IMAGINARY ROOT
        COMPUTE MAGNITUDE
   72 DISC2=SQRT(DISC2*DISC2)
      B2A1=.5*(SQRT(R2A1*R2A1+DISC2))
      B2A2=B2A1
   92 B2B=-THETA2(NA2+2)/B20

      CALL MD(P2,6,NP2,DET2,IDET2,G2)
      PRINT 1072,I,(P2(J,J),J=1,6),DET2,IDET2

   82 CALL FORM(PHI2,YS102(1),US102(1),ZS102(1),NA2,NB2,NC2,NP2)

      PRINT*,"KNT: ",KNT,DU2TP(KNT)

 1127 USSP2=U2
      YSP12=YSP2
      YSPM12=YSPM2

      TR1=U2
      IF(TR1 .LT. 250.)TR1=250.
      GO TO 128
 1129 CALL UYINCR(Y2,YSPM2,Z2,US102,YS102,ZS102)
      YSP12=YSP2
      YSPM12=YSPM2
 2020 ERR1=S3SET-VS3(I-12)
      TR1=(A1/A3)*(ERR1-A2*ERR2) + (1.-A1)*TR2  +   A1*TR3

      IF(TR1 .LT. 250.)TR1=250.

C     UPDATE FOR NEXT CONTROL ACTION

      ERR2=ERR1
      TR3=TR2
      TR2=TR1

  128 CONTINUE

      IF IST=1, IMPLEMENT S.T.R.

      IF(IST .NE. 1)GO TO 130
```

```
      Y=TRP
      IF(I .GT. 1) GO TO 125
      YSP1=TRSET
      YSPM1=YSP1
  125 YSPM=AETA*YSPM1+(1-AETA)*YSP1
      IF(IP .EQ. 1)GO TO 126
      YSP=TRSET
      Z=YSP-YSP1
      GO TO 127
  126 CONTINUE
      YSP=TR1
      Z=YSP-YSP1
  127 CONTINUE
*****
      IF(NC .EQ. 0)YSPM=YSP
*****
*

      IF(I .LT. NP)GO TO 129
      CALL UYINCR(Y,YSPM,Z,US10,YS10,ZS10)
      CALL FORM(PHI,YS10(1+IB),US10(1+IB),ZS10(1+IB),NA,NB,NC,NP)
      OBFCN=YS10(1)+ZETA*US10(1+IB)
      CALL RLS(OBFCN,P,PHI,THETA,FLAM,NP)

      IF(NA .EQ. 2)BA1=-THETA(2)/THETA(1)
      BO=THETA(NA+1)
      RA0=THETA(1)/BO
      RA1=THETA(2)/BO
      RB1=THETA(NA+2)/BO
      IF(NA .NE. 3)GO TO 9
      RA2=THETA(3)/BO
      DISC=RA1*RA1-4*RA0*RA2
      IF(DISC .LT. 0.)GO TO 7
      TWO REAL ROOTS
      R1=.5*(-RA1+SQRT(DISC))
      BA1=SQRT(R1*R1)
      R2=.5*(-RA1-SQRT(DISC))
      BA2=SQRT(R2*R2)
      GO TO 9
      IMAGINARY ROOT
      COMPUTE MAGNITUDE
    7 DISC=SQRT(DISC*DISC)
      BA1=.5*(SQRT(RA1*RA1+DISC))
      BA2=BA1
    9 BB=-THETA(NA+2)/BO
      IREM=MOD(I,10)
      IF (IREM .NE. 0) GO TO 8
      CALL MO(P,6,NP,DET,IDET,G)
      PRINT 107,I,(P(J,J),J=1,6),DET,IDET
    8 CALL FORM(PHI,YS10(1),US10(1),ZS10(1),NA,NB,NC,NP)
      CALL STRCL(U,USSP,THETA,PHI,NP,NA)
      US10(1)=U-USSP
   81 USSP=U
      YSP1=YSP
      YSPM1=YSPM

      PRINT 109,I,Y,U,US10(1),(THETA(J),J=1,NP),(PHI(J),J=1,NP)

      RATIO1=U
      GO TO 562
```

```
  129 CALL UYINCR(Y,YSPM,Z,US10,YS10,ZS10)
      YSP1=YSP
      YSPM1=YSPM
C     TR-RATIO CONTROLLER.
C     IF IP=0, S3CONTROLLER HAS NOT TAKEN ITS FIRST CONTROLA CTION
C     SO USE PREVIOUSLY SUPPLIED STARTING TR SETPOINTS
  130 IF(IT1 .EQ. 0)GO TO 562

      IF(IP .EQ. 1)GO TO 540
      E1=TRSET - TRP

      IF(E1 .LT. 4.)GO TO 542
      E1=4.
      TRSET=TRP+4.
  542 E1=-E1
      GO TO 560

  540 E1=TR1-TRP

      IF(E1.LT.4.0)GO TO 546
      E1=4.
      TR1=TRP+4.
  546 E1=-E1

  560 CONTINUE

      RATIO1=RATIO1 + C1*(E1-E2 + C2*E1)

C     BASED ON THIS NEW RATIO, SET C4 AND H2 FEEDRATES, SCFM
  562 IF(RATIO1 .LE. 4.)RATIO1=4.
      IF(RATIO1 .GE. 20.)RATIO1=20.

      C4SCFM1=SCFM/(RATIO1+1.)
      C4SCFM2=C4SCFM1
      H2SCFM1=SCFM-C4SCFM1
      H2SCFM2=H2SCFM1

C     UPDATE FOR NEXT CONTROL INTERVAL

      IF(IT1 .EQ. 0)GO TO 590
      E2=E1

C     RECORD NEW RATIO , C4SCFM AND H2SCFM FOR LATER PLOTTING

C     INCREMENT COUNTER FOR S3 LOOP

      IC=IC+1

C     IF S3 LOOP HAS TAKEN OVER SETTING TRSET, RECORD THESE FOR LATER
C     OUTPUT

      IF(IP .EQ. 0)GO TO 590
      TRSET=TR1

  590 CONTINUE

C     ********************************************************************
C     END OF CONTROL ACTION
```

```
C       ********************************************************************
 *
 *      TO CHANGE CATALYST ACTIVITY
 *
 *      IF(I .GT.  50)EP(1,2)=.9997476*EP(1,2)
 *      IF(I .GT. 1150)EP(1,2)=5.25
 *
        J=I+1
        F=I
        WRITE(3,108)I,TRP,TWP,TOILP,S3,
       1CON,RATIO1,TOILIN1
       +,TRSET,S3SET,EP(1,2)
        WRITE(3,1088)(THETA(K),K=1,4),BB,BA1,
       +(THETA2(K),K=1,4),B2B,B2A1
 *
 1234 CONTINUE
 2000 CONTINUE

C       THIS IS THE END OF NSTEP-1 INTEGRATIONS, OUTPUT TO LINE
C       PRINTER AND DISC


        WRITE(6,110)
  110 FORMAT(//2X,"I",3X,"TR",4X,"TW",4X,"TOIL",3X,"S1",3X,"S2",
       +3X,"S3",3X,"CON",2X,"C4",3X,"H2",1X,"RATIO",1X,"TOILIN",
       +1X,"TRSET",1X,"S2SET",2X,"A0",2X,"A1",2X,"B0",2X,
       +"B1",//)
 *
        TIME=0.

        TIME=I*NDELT
        J=I+1
        WRITE(6,108)I,TRP,TWP,TOILP,VS3(I),
       1CON,RATIO1,TOILIN1
       +,TRSET,S3SET,EP(1,2)
        WRITE(6,1088)(THETA(K),K=1,4),BB,BA1,
       +(THETA2(K),K=1,4),B2B,B2A1
 *
 *
 * 107 FORMAT(1X,I4,7E10.3,"E",I4)
 *1072 FORMAT(7X,I4,6E10.3,F10.3,"E",I4/)
  108 FORMAT(1X,I4,10F9.3)
 1088 FORMAT(1X,12F5.2)
  109 FORMAT(1X,I3,11F9.4)

 999    STOP
        END
        SUBROUTINE UYINCR(Y,YSPM,Z,US10,YS10,ZS10)
        DIMENSION US10(10),YS10(10),ZS10(10)
        DO 9 J=1,9
        I=11-J
        US10(I)=US10(I-1)
        YS10(I)=YS10(I-1)
        ZS10(I)=ZS10(I-1)
   9    CONTINUE
        US10(1)=0.0
        YS10(1)=-(Y-YSPM)
        ZS10(1)=Z
        RETURN
        END
        SUBROUTINE FORM(X,YS10,US10,ZS10,NA,NB,NC,NP)
        DIMENSION YS10(NA),US10(NB),ZS10(NC),X(NP)
        X(NP)=1.0
```

```
      DO 9 I=1,NA
      X(I)=YS10(I)
9     CONTINUE
      DO 19 I=1,NB
      X(NA+I)=US10(I)
19    CONTINUE
      DO 29 I=1,NC
      X(NA+NB+I)=ZS10(I)
29    CONTINUE
      RETURN
      END
      SUBROUTINE STRCL(U,USSP,THETA,X,NP,NA)
      DIMENSION X(NP),THETA(NP)
      SUM=0.
      DO 19 I=1,NP
      SUM=SUM+X(I)*THETA(I)
19    CONTINUE
      U = USSP-SUM/THETA(NA+1)
      RETURN
      END
      SUBROUTINE RLS(Y,P,PHI,THETA,FL,NP)
      DIMENSION P(6,6),PHI(NP),THETA(NP),S(10)
      REAL K(10)
      SUM=0.
      DO 9 I=1,NP
      DO 9 J=1,NP
      SUM=SUM+PHI(I)*PHI(J)*P(I,J)
9     CONTINUE
      DEN=SUM+FL
      ERRS=0.
      DO 19 I=1,NP
      SUM=0.
      DO 29 J=1,NP
      SUM=SUM+P(I,J)*PHI(J)
29    CONTINUE
      S(I)=SUM
      K(I)=SUM/DEN
      ERRS=ERRS+PHI(I)*THETA(I)
19    CONTINUE
      ERRS=Y-ERRS
      DO 5 I=1,NP
      DO 4 J=1,NP
      P(I,J)=(P(I,J)-S(I)*S(J)/DEN)/FL
4     CONTINUE
      THETA(I)=THETA(I)+K(I)*ERRS
5     CONTINUE
      RETURN
      END
      SUBROUTINE CRCORR(X,Y,CC,SDX,SDY,N,NL)
      DIMENSION X(N),Y(N),CC(1)
      SX = 0.
      SY = 0.
      SXX = 0.
      SYY = 0.
      DO 2 I=1,N
      SX = SX+X(I)
      SY = SY+Y(I)
      SXX = SXX+X(I)*X(I)
2     SYY = SYY+Y(I)*Y(I)
      TN = N
      SDX = SQRT((SXX-SX*SX/TN)/TN)
      SDY = SQRT((SYY-SY*SY/TN)/TN)
      NL1 = NL+1
      DO 3 K=1,NL1
      SXY = 0.
```

```
      NN = N-K+1
      DO 4 I=1,NN
      KK = I+K-1
   4  SXY = SXY+(X(I)-SX/TN)*(Y(KK)-SY/TN)
   3  CC(K) = (SXY/TN)/(SDX*SDY)
      RETURN
      END
      SUBROUTINE ACORR(Z,AC,SDZ,N,NL)
      DIMENSION Z(1),AC(1)
      NL1 = NL+1
      TN = N
      SZ = 0.
      DO 13 I=1,N
  13  SZ = SZ+Z(I)
      ZBAR = SZ/TN
      DO 10 JJ=1,NL1
      J = JJ-1
      SZZ = 0.
      NN = N-J
      DO 11 I=1,NN
  11  SZZ = SZZ+(Z(I)-ZBAR)*(Z(I+J)-ZBAR)
  10  AC(JJ) = SZZ/TN
      SDZ = SQRT(AC(1))
      VZ = AC(1)
      DO 12 J=1,NL
  12  AC(J) = AC(J+1)/VZ
      RETURN
      END
```

C.5.2 Program Listing of STPLT2

```
      PROGRAM STPLT2(INPUT,OUTPUT,0236,TAPE3=0236,TAPE6=OUTPUT)

      COMMON XY(400,23)
      COMMON/XYDLIM/XDMIN,XDMAX,YDMIN,YDMAX
      COMMON/PLTSPEC/IPEN,XLEN,YLEN,XOFF,YOFF

      REWIND 3

C     ENTER PARTICULARS
      PRINT*,"ENTER NSTEP"
      READ*,NSTEP
      NOB=NSTEP-1
      DELT=30

      PRINT*,"INNER STR PARAMETERS ?"
      READ*,IST
      IF(IST .NE. 1)GO TO 11
      PRINT*,"ENTER NA,NB"
      READ*,NA,NB

11    PRINT*,"OUTER STR PARAMETERS?"
      READ*,IOST
      IF(IOST .NE. 1)GO TO 21
      PRINT*,"ENTER N2A,N2B"
      READ*,N2A,N2B

*     READ AND VERIFY DATA

21    WRITE(6,110)
110   FORMAT(//2X,"I",3X,"TR",4X,"TH",4X,"TOIL",3X,"S1",3X,"S2",
     +3X,"S3",3X,"CON",2X,"C4",3X,"H2",3X,"RATIO",1X,"TOILIN",
     +3X,"TRSET",3X,"S3SET",3X,"A0",3X,"A1",3X,"B0",3X,
     +"B1",//)
      DO 105 I=1,NOB
      READ(3,108)(XY(I,J),J=1,11)
      F=I
      XY(I,1)=F
105   READ(3,1088)(XY(I,J),J=12,23)
      WRITE(6,109)(XY(I,J),J=1,11)
      WRITE(6,1088)(XY(I,J),J=12,23)
109   FORMAT(1X,F4.0,10F9.3)
108   FORMAT(1X,I4,10F9.3)
1088  FORMAT(1X,12F5.2)

*     START PRINTING ROUTINES


*     PLOT 7.RATIO,

      IPEN=3
      XDMIN=XY(1,1)
      XDMAX=241.
      YDMIN=4.
      YDMAX=20.

      XOFF=2.5
      XLEN=7.5
      YOFF=1.25
      YLEN=1.5


      CALL FRME
      CALL XTIC(20.,.0
      CALL XTIC(4.,.0
```

```
      CALL YTIC(4.,.08)
      CALL YTIC(2.,.05)

      CALL SPLOT(1,7,NOB)


C     PLOT 5.S3, 10.S3SET

      YOMIN=0.1
      YOMAX=0.5

      YOFF=2.875
      YLEN=1.

      CALL FRME
      CALL XTIC(20.,.08)
      CALL XTIC(4.,.05)
      CALL YTIC(.1,.05)

      CALL CPLOT(1,5,NOB)
      CALL DPLOT(1,10,NOB)
C     PLOT 6.CONV

      YOMIN=.2
      YOMAX=.6

      YOFF=4.
      YLEN=1.

      CALL FRME
      CALL XTIC(20.,.08)
      CALL XTIC(4.,.05)
      CALL YTIC(.1,.05)

      CALL CPLOT(1,6,NOB)
C     PLOT  2.TR, 4.TOIL, 9.TRSET, 11.TOILSP

      YOMAX=260.
      YOMIN=240.

      YLEN=1.875
      YOFF=5.125
      CALL FRME
      CALL XTIC(20.,.08)
      CALL XTIC(4.,.05)
      CALL YTIC(10.,.08)
      CALL YTIC(5.,.05)
      CALL CPLOT(1,2,NOB)
      CALL CPLOT(1,4,NOB)
      CALL DPLOT(1,9,NOB)

      CALL PLOT(12.,0.,-3)


C     PLOT INNER STR PARAMETER ESTIMATES

      IF(IST .NE. 1)GO TO 900
      YOMIN=-4.
      YOMAX=4.

      YLEN=1.85
```

```
      YOFF=5.2
      CALL PARPLT(1,12,13,NOB)

      YOFF=3.225
      YDMIN=-4.
      YDMAX=4.
      CALL PARPLT(1,14,15,NOB)

      YOFF=1.25
      YDMIN=-2.0
      YDMAX=2.0
      CALL PARPLT(1,16,17,NOB)
      CALL UNITTO(XY(1,1),1.,X1P,ZE)
      CALL UNITTO(XY(NOB,1),1.,X2P,ZE)
      CALL DASH(X1P,ZE,X2P,ZE,1)
      CALL UNITTO(XY(1,1),-1.,X1P,ZE)
      CALL UNITTO(XY(NOB,1),-1.,X2P,ZE)
      CALL DASH(X1P,ZE,X2P,ZE,1)

      CALL PLOT(12.,0.,-3)

C     PLOT OUTER STR PARAMETER ESTIMATES

  900 IF(IOST .NE. 1)GO TO 999
      YDMIN=-7.
      YDMAX=7.
      YLEN=1.85
      YOFF=5.2
      CALL PARPLT(1,18,19,NOB)
      CALL UNITTO(XY(1,1),0.,X1P,ZE)
      CALL UNITTO(XY(NOB,1),0.,X2P,ZE)
      CALL DASH(X1P,ZE,X2P,ZE,1)

      YOFF=3.225
      YDMIN=-2.
      YDMAX=2.
      CALL PARPLT(1,20,21,NOB)
      CALL UNITTO(XY(1,1),0.,X1P,ZE)
      CALL UNITTO(XY(NOB,1),0.,X2P,ZE)
      CALL DASH(X1P,ZE,X2P,ZE,1)

      YOFF=1.25
      YDMIN=-4.
      YDMAX=4.
      CALL PARPLT(1,22,23,NOB)
      CALL UNITTO(XY(1,1),0.,X1P,ZE)
      CALL UNITTO(XY(NOB,1),0.,X2P,ZE)
      CALL DASH(X1P,ZE,X2P,ZE,1)
      CALL UNITTO(XY(1,1),1.,X1P,ZE)
      CALL UNITTO(XY(NOB,1),1.,X2P,ZE)
      CALL DASH(X1P,ZE,X2P,ZE,1)
      CALL UNITTO(XY(1,1),-1.,X1P,ZE)
      CALL UNITTO(XY(NOB,1),-1.,X2P,ZE)
      CALL DASH(X1P,ZE,X2P,ZE,1)

      CALL PLOT(12.,0.,-3)

C     END ALL PLOTTING

  999 CALL PLOT(0.,0.,999)
      STOP
      END

C     SUBROUTINES
```

```
      SUBROUTINE FRME
      COMMON/XYDLIM/XDMIN,XDMAX,YDMIN,YDMAX
      COMMON/PLTSPEC/IPEN,XLEN,YLEN,XOFF,YOFF

      CALL NEWPEN(4)

      XSCALE=(XDMAX-XDMIN)/XLEN
      YSCALE=(YDMAX-YDMIN)/YLEN
      XORG=XDMIN-XOFF*XSCALE
      YORG=YDMIN-YOFF*YSCALE
      XMIN=XORG
      YMIN=YORG
      XMAX=XDMAX+3.
      YMAX=YDMAX+3.
      CALL PLTIN(XSCALE,YSCALE,XORG,YORG,XMIN,XMAX,YMIN,YMAX)
      CALL FRAME
      CALL NEWPEN(2)
      RETURN
      END
      SUBROUTINE CPLOT(ITM,IJ,NOB)
      CONTINUOUS CURVE
      COMMON XY(400,23)
      COMMON/XYDLIM/XDMIN,XDMAX,YDMIN,YDMAX
      COMMON/PLTSPEC/IPEN,XLEN,YLEN,XOFF,YOFF
C     MOVE PEN TO FIRST DATA POINT,PEN UP

      CALL PLOTT(XY(1,ITM),XY(1,IJ),3)
      CALL NEWPEN(IPEN)

      J=25
      DO 63 I=1,NOB
      IF(IJ .NE. 2 .AND. IJ .NE. 5)GO TO 63
      IF(I .NE. J)GO TO 63
      J=J+12
      CALL UNITTO(XY(I,ITM),XY(I,IJ),XC,YC)
      CALL GRAF(XC,YC,.08,11)
   63 CALL PLOTT(XY(I,ITM),XY(I,IJ),2)
      RETURN
      END
      SUBROUTINE DPLOT(ITM,IJ,NOB)
      DOTTED CURVE
      COMMON XY(400,23)
      COMMON/XYDLIM/XDMIN,XDMAX,YDMIN,YDMAX
      COMMON/PLTSPEC/IPEN,XLEN,YLEN,XOFF,YOFF
      DO 64 I=1,NOB
      IF(IJ .LT. 25)GO TO 63
      CALL UNITTO(XY(I,ITM),XY(I,IJ),XC,YC)
      CALL GRAF(XC,YC,.08,11)
   63 CALL PLOTT(XY(I,ITM),XY(I,IJ),3)
      CALL NEWPEN(4)
   64 CALL PLOTT(XY(I,ITM),XY(I,IJ),2)
      RETURN
      END
      SUBROUTINE GPLOT(ITM,IJ,IS3,CODE)
      CALL SUBROUTINE GRAF
      COMMON XY(400,23)
      COMMON/XYDLIM/XDMIN,XDMAX,YDMIN,YDMAX
      COMMON/PLTSPEC/IPEN,XLEN,YLEN,XOFF,YOFF
      J=25
      DO 67 I=1,IS3
      IF(I .NE. J)GO TO 67
      J=J+12
      CALL UNITTO(XY(I,ITM),XY(I,IJ),XC,YC)
      CALL GRAF(XC,YC,.08,CODE)
```

```
   67 CONTINUE
      RETURN
      END
      SUBROUTINE SPLOT(ITM,IJ,NOB)
      ZERO HOLD CURVE
      COMMON XY(400,23)
      COMMON/XYDLIM/XDMIN,XDMAX,YDMIN,YDMAX
      COMMON/PLTSPEC/IPEN,XLEN,YLEN,XOFF,YOFF
      CALL PLOTT(XY(1,ITM),XY(1,IJ),3)

      J=25
      DO 72 I=2,NOB
      IF(I .NE. J)GO TO 71
      J=J+12
      CALL UNITTO(XY(I,ITM),XY(I-1,IJ),XC,YC)
      CALL GRAF(XC,YC,.08,11)
   71 CALL PLOTT(XY(I,ITM),XY(I-1,IJ),2)
   72 CALL PLOTT(XY(I,ITM),XY(I,IJ),2)
      RETURN
      END
      SUBROUTINE PARPLT(ITM,MA,NA,NOB)
      COMMON XY(400,23)
      COMMON/XYDLIM/XDMIN,XDMAX,YDMIN,YDMAX
      COMMON/PLTSPEC/IPEN,XLEN,YLEN,XOFF,YOFF
      CALL FRME
      CALL XTIC(20.,.08)
      CALL XTIC(4.,.05)
      CALL YTIC(1.,.05)
      CALL UNITTO(XY(1,1),0.,X1P,ZE)
      CALL UNITTO(XY(NOB,1),0.,X2P,ZE)
      CALL DASH(X1P,ZE,X2P,ZE,1)
      DO 10 I=MA,NA
      IF(I .LT. 18)GO TO 8
      CALL GPLOT(ITM,I,NOB,I-MA+1)
    8 CALL CPLOT(ITM,I,NOB)
   10 CONTINUE
      RETURN
      END
      SUBROUTINE XTIC(XINTVL,TICLEN)
      COMMON/XYDLIM/XDMIN,XDMAX,YDMIN,YDMAX
      COMMON/PLTSPEC/IPEN,XLEN,YLEN,XOFF,YOFF
      NTICS=((XDMAX-XDMIN)/XINTVL+.5)+1
      XD=XDMIN
      YD=YDMIN
      DO 20 I=1,NTICS
      XD=XDMIN+FLOAT(I-1)*XINTVL
      CALL UNITTO(XD,YD,XP,YP)
      CALL PLOT(XP,YP,3)
      CALL PLOT(XP,YP+TICLEN,2)
      CALL PLOT(XP,YP+YLEN,3)
      CALL PLOT(XP,YLEN+YP-TICLEN,2)
   20 CONTINUE
      RETURN
      END
      SUBROUTINE YTIC(YINTVL,TICLEN)
      COMMON/XYDLIM/XDMIN,XDMAX,YDMIN,YDMAX
      COMMON/PLTSPEC/IPEN,XLEN,YLEN,XOFF
      NTICS=((YDMAX-YDMIN)/YINTVL+.5)+1
      XD=XDMIN
      YD=YDMIN
      DO 20 I=1,NTICS
      YD=YDMIN+FLOAT(I-1)*YINTVL
      CALL UNITTO(XD,YD,XP,YP)
      CALL PLOT(XP,YP,3)
      CALL PLOT(XP+TICLEN,YP,2)
```

```
      CALL PLOT(XP+XLEN,YP,3)
      CALL PLOT(XP+XLEN-TICLEN,YP,2)
20    CONTINUE
      RETURN
      END
      SUBROUTINE XTLAB(XINTVL,HEIGHT)
      COMMON/XYDLIM/XDMIN,XDMAX,YDMIN,YDMAX
      NLABS=((XDMAX-XDMIN)/XINTVL+.5)+1
      YD=YDMIN
      XD=XDMIN
      CALL UNITTO(XD,YD,XP,YP)
      YPP=YP-1.5*HEIGHT
      DO 100 I=1,NLABS
      XD=XDMIN+FLOAT(I-1)*XINTVL
      CALL UNITTO(XD,YD,XP,YP)
      XP=XP-(.5*HEIGHT)
      ENCODE(2,20,ICH) XD
      CALL LETTER(1,HEIGHT,0.,XP,YPP,ICH)
100   CONTINUE
20    FORMAT(F2.0)
      RETURN
      END
      SUBROUTINE YTLAB(YINTVL,HEIGHT)
      COMMON/XYDLIM/XDMIN,XDMAX,YDMIN,YDMAX
      NLABS=((YDMAX-YDMIN)/YINTVL+.5)+1
      XD=XDMIN
      YD=YDMIN
      CALL UNITTO(XD,YD,XP,YP)
      XPP=XP-1.5*HEIGHT
      DO 100 I=1,NLABS
      YD=YDMIN+FLOAT(I-1)*YINTVL
      CALL UNITTO(XD,YD,XP,YP)
      YP=YP-.5*HEIGHT
      ENCODE(2,20,ICH) YD
      CALL LETTER(1,HEIGHT,0.,XPP,YP,ICH)
100   CONTINUE
20    FORMAT(F2.0)
      RETURN
      END
      SUBROUTINE FRAME
      COMMON/XYDLIM/XDMIN,XDMAX,YDMIN,YDMAX
      CALL PLOTT(XDMIN,YDMIN,3)
      CALL PLOTT(XDMAX,YDMIN,2)
      CALL PLOTT(XDMAX,YDMAX,2)
      CALL PLOTT(XDMIN,YDMAX,2)
      CALL PLOTT(XDMIN,YDMIN,2)
      RETURN
      END
      SUBROUTINE PLOTT(XD,YD,N)
      CALL UNITTO(XD,YD,XP,YP)
      CALL PLOT(XP,YP,N)
      RETURN
      END
```